Catalysis Today 420 (2023) 114180

Contents lists available at ScienceDirect

Catalysis Today

journal homepage: www.elsevier.com/locate/cattod

Challenges in unconventional catalysis☆

Annemie Bogaerts [a], Gabriele Centi [b,*], Volker Hessel [c,d], Evgeny Rebrov [d]

[a] Research group PLASMANT, Department of Chemistry, University of Antwerp, BE-2610 Wilrijk, Antwerp, Belgium
[b] Department ChiBioFarAm, University of Messina, ERIC aisbl and CASPE/INSTM, Messina 98166, Italy
[c] School of Chemical Engineering and Advanced Materials, The University of Adelaide, Adelaide, SA 5005, Australia and School of Engineering, University of Warwick, Library Rd, Coventry CV4 7AL, England, UK
[d] School of Engineering, University of Warwick, Coventry CV4 7AL, UK and Department of Chemical Engineering and Chemistry, Eindhoven University of Technology, P. O. Box 513, 5600 MB Eindhoven, the Netherlands

ARTICLE INFO

Keywords:
Plasma catalysis
Plasmonic catalysis
Electrical field
Microfluidic reactor
Process intensification

ABSTRACT

Catalysis science and technology increased efforts recently to progress beyond conventional "thermal" catalysis and face the challenges of net-zero emissions and electrification of production. Nevertheless, a better gaps and opportunities analysis is necessary. This review analyses four emerging areas of unconventional or less-conventional catalysis which share the common aspect of using directly renewable energy sources: (i) plasma catalysis, (ii) catalysis for flow chemistry and process intensification, (iii) application of electromagnetic (EM) fields to modulate catalytic activity and (iv) nanoscale generation at the catalyst interface of a strong local EM by plasmonic effect. Plasma catalysis has demonstrated synergistic effects, where the outcome is higher than the sum of both processes alone. Still, the underlying mechanisms are complex, and synergy is not always obtained. There is a crucial need for a better understanding to (i) design catalysts tailored to the plasma environment, (ii) design plasma reactors with optimal transport of plasma species to the catalyst surface, and (iii) tune the plasma conditions so they work in optimal synergy with the catalyst. Microfluidic reactors (flow chemistry) is another emerging sector leading to the intensification of catalytic syntheses, particularly in organic chemistry. New unconventional catalysts must be designed to exploit in full the novel possibilities. With a focus on (a) continuous-flow photocatalysis, (b) electrochemical flow catalysis, (c) microwave flow catalysis and (d) ultrasound flow activation, a series of examples are discussed, with also indications on scale-up and process industrialisation. The third area discussed regards the effect on catalytic performances of applying oriented EM fields spanning several orders of magnitude. Under well-defined conditions, gas breakdown and, in some cases, plasma formation generates activated gas phase species. The EM field-driven chemical conversion processes depend further on structured electric/magnetic catalysts, which shape the EM field in strength and direction. Different effects influencing chemical conversion have been reported, including reduced activation energy, surface charging, hot spot generation, and selective local heating. The last topic discussed is complementary to the third, focusing on the possibility of tuning the photo- and electro-catalytic properties by creating a strong localised electrical field with a plasmonic effect. The novel possibilities of hot carriers generated by the plasmonic effect are also discussed. This review thus aims to stimulate the reader to make new, creative catalysis to address the challenges of reaching a carbon-neutral world.

1. Introduction

Heterogeneous catalysis played a decisive role in establishing the current processes for refinery and petrochemistry in the last decades, besides its crucial role in several environmental protection technologies [1–5]. At the same, the advances in the precise control of the synthesis of catalytic nanomaterials and the understanding of the reaction mechanism using both theoretical approaches and in-situ/*operando* methods have drastically improved the possibility of catalysts-tailored design and control of their performances [6–12].

The transition to an electrifying production based on renewable

☆ This joint manuscript was prepared from the four PIs of the ERC Synergy Project SCOPE (Surface-COnfined fast-modulated Plasma for process and Energy intensification in small molecules conversion, project ID 810182) which promoted the UCRA 2022 conference

* Corresponding author.
E-mail address: centi@unime.it (G. Centi).

https://doi.org/10.1016/j.cattod.2023.114180
Received 1 February 2023; Received in revised form 18 April 2023; Accepted 7 May 2023
Available online 8 May 2023

Nomenclature

ANN−GA	artificial neural network−genetic algorithm.
APGD	atmospheric pressure glow discharge.
CER	chlorine evolution reaction.
CO_2RR	electrocatalytic reduction of CO_2.
DC	direct current.
DBD	dielectric barrier discharge.
DFT	density functional theory.
DRIFTS	diffuse reflectance infrared Fourier transform spectroscopy.
DRM	dry reforming of methane.
EM	electromagnetic (field).
EPOC	electrochemical promotion of catalysis.
E-R	Eley–Rideal.
ER	electroreforming.
GA	gliding arc.
GC	gas chromatography.
HC	hot carrier.
HEL FlowCAT	trickle bed reactor for meso-flow transformations.
HER	hydrogen evolution reactions.
HMF	hydroxymethylfurfural.
L-H	Langmuir–Hinshelwood.
LSPR	localized surface plasmon resonance.
IR	infrared.
YSZ	yttria-stabilized-zirconia.
KSI	ketosteroid isomerase (enzyme).
ML	machine learning.
MS	mass spectrometry.
MW	microwave.
NEMCA	non-faradaic electrochemical modification of catalytic activity.
NP	nano particles.
OTEM	optically coupled transmission electron microscopy.
OZ439	antimalarial drug candidate.
PCEC	protonic ceramic electrolysis cells.
SMB	simulated moving-bed.
SPR	surface plasmon resonance.
SQ	Shockley–Queisser.
SRM	steam reforming of methane.
STF	solar-to-fuel.
TDDFT	time-dependent density-functional theory.
TOF	turnover frequency.
TPD	temperature-programmed desorption.
TRL	technology readiness level.
VOC	volatile organic compounds.
WGS	water gas shift.

energy sources and the progressive substitution of the dependence on fossil resources has introduced new grand challenges in process and catalyst design [13–18], only partially present in converting biomass feedstock rather than fossil fuels.

1.1. Unconventional catalysis to electrify production

Electrification of chemical processes requires catalysts that can operate directly with renewable energy sources. Electro-, photo- and plasma catalysis are the three main classes of these novel catalytic technologies. Even if they have been used for decades at a lab scale, they have received an exponential increase in interest in recent years for the above motivations [18], with an increasing push in scaling up these technologies to realise new process solutions. Although electro-, photo- and plasma catalysis are conceptually different, they share many similarities in the mechanism of action, for example, in the conversion of CO_2 [19]. The common aspect is that highly reactive charged species [20] are generated on the catalyst by (i) application of an electrical potential (electrocatalysis [21–29], eventually with a photo-active element integrated into the device, e.g., photoelectro-catalysis); (ii) photo-induced charge separation or insitu photogenerated electrical current (photo-catalysis) [30–36]; and (iii) interaction with the catalyst surface of the excited species and radicals generated in the gas phase by non-thermal plasma (plasma catalysis) [37–43].

The path of transformation and control of the reactivity and selectivity highly depend on these in-situ generated "highly-reactive" species, which control to avoid side reactions, is the common aspect of the three catalytic technologies. At the same time, the catalyst may be dynamically changed on the surface when these "highly-reactive" species are generated [44].

In parallel, introducing these electro-, photo- and plasma catalysis processes on a commercial scale and the novel possibility for a distributed production of chemicals and process intensification [45–50] offered by these technologies create new challenges in reactor design [45,51–59] and a push towards the development of unconventional, potentially disruptive catalysts [60–64]. There are thus strong relations between the concepts of unconventional catalysis, reaction environments and reactor design, and the need to intensify and accelerate the exploration of these possibilities to meet the challenges for electrification of the chemical industry and new models of sustainable production, minimising the use of fossil fuels.

Over the last year, publications and reviews on electro-, photo- and plasma catalysis increased exponentially. Still, the reactions investigated are restricted to the conversion of small molecules (CO_2, N_2, H_2O, CH_4) and few biomass intermediates, with little effort in exploring novel creative solutions, materials and approaches to overcoming the limits of current methods.

1.2. Scope and limitations

This review aims to foster research interest in unconventional catalysis. We selected to cover four complementary topics. The first two sections regard plasma catalysis and microfluidic reactors, which are consolidated research areas, although still considered unconventional because they are out of the mainstream. Two other areas are examples of mostly unexplored areas (the effect of a strong electrical field external or generated at the nanoscale catalyst level by plasmonic effect, respectively), which can be breakthrough directions. Altogether, they provide a unitary message of how to foster research on unconventional catalysis, even if the discussion on each topic maintains its specificity related to the different aspects addressed. It should be remarked that each section does not aim to provide a systematic review but only to introduce the background information to understand the relevance of new approaches for catalysis.

These four topics share the common objective of fostering the reader's creativity to study unconventional catalysis combined with renewable energy [13,14,65,66]. Although all the possibilities of unconventional catalysis cannot be discussed here, we believe this review provides enough food for thought to guide readers, especially the younger ones, in making new, creative catalysis. Addressing the challenges of reaching a carbon-neutral world requires this creative effort.

2. Plasma catalysis

2.1. Background

In plasma catalysis, a catalyst is combined with plasma, a (partially) ionised gas consisting of electrons, ions, radicals, excited species, and neutral molecules. This reactive cocktail of species makes plasma interesting for many applications in sustainable chemistry, such as CO_2 and CH_4 conversion and N_2 fixation (e.g.,[40,42,67–71]), because the high reactivity allows thermodynamically or kinetically complex reactions to proceed at mild conditions, e.g., atmospheric pressure and (near) room temperature. Moreover, plasma operates by applying electricity and can be quickly switched on/off, so it is very suitable to be combined with fluctuating renewable electricity and, thus, for electrification of chemical reactions [14,71]. Nevertheless, due to the high reactivity of plasma, it cannot selectively produce targeted compounds. Therefore, the combination of plasma with catalysts seems an ideal marriage, where plasma creates the reactivity, thereby lowering the energy barrier of the catalytic reactions, and the catalyst can provide the required selectivity.

Plasma-catalyst synergy has indeed been reported, i.e., the performance of plasma catalysis is larger than the sum of the performance in plasma and catalysis alone. Fig. 1 gives an example for CO_2 and CH_4 conversion [42,72]. However, this synergy is not always observed or is sometimes misinterpreted. The catalysts are typically selected based on the analogy with similar conventional heterogeneous catalysis reactions. Still, the optimal thermal catalysts are not necessarily optimal in plasma catalysis because of other reaction paths, as discussed below.

Plasma catalysis can operate in two modes, i.e., in-plasma catalysis (single-stage), where the catalyst is placed inside the plasma, and post-plasma catalysis (two-stage), where the catalyst is placed after the plasma. Most work has been done with in-plasma catalysis, using dielectric barrier discharge (DBD) plasmas operating at or slightly above room temperature. In this case, catalysts are typically coated on dielectric beads, or catalyst powders are pelletised, and these beads or pellets (with dimensions of typically 1–2 mm) fill the discharge gap. Hence, the reactive, short-lived plasma species can directly contact the catalyst surface, fully exploiting the possible synergy between plasma and catalysis. On the other hand, in-plasma catalysis is not possible in some other plasma types that are very promising for sustainable chemistry because of their better energy efficiency than DBD. Examples are gliding arc (GA), microwave (MW), atmospheric pressure glow discharge (APGD) and nanosecond (ns) pulsed plasmas. They cannot accommodate catalysts inside the plasma because they are characterised by too high temperatures (typically several thousands of Kelvin). However, in these so-called warm plasmas, the catalyst can be placed post-plasma and activated by the hot gas flowing out of the plasma reactor. Thus, other catalysts should be used depending on the operation mode. While for post-plasma catalysis, thermal catalysts could be suitable, in-plasma catalysis should use materials other than typical thermal catalysts, i.e., they should be tailored to the plasma composition to result in synergy (see further).

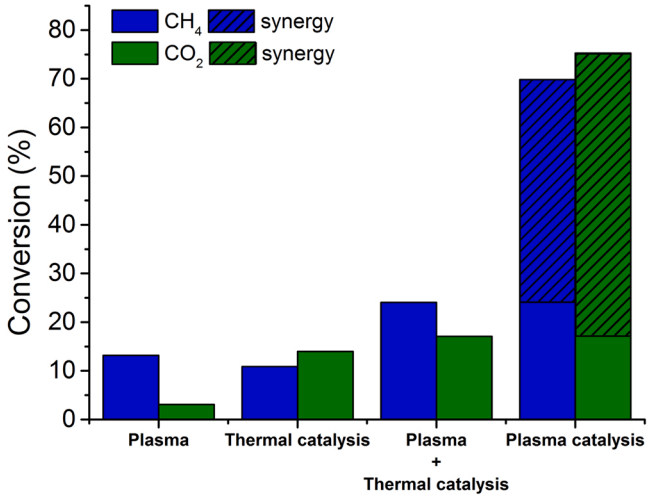

Fig. 1. Typical example of synergy in plasma catalysis: the CO_2 and CH_4 conversion in plasma catalysis are higher than the sum of the conversions in plasma and catalysis alone.
Reproduced from [42] with permission from the Royal Society of Chemistry, based on data from [72]. Copyright RCS, 2017.

2.2. State of the art

Plasma technologies are already applied in the area of gas cleaning and conversion [73], to remove low concentrations of volatile organic compounds (VOC), particulate matter and NO_x (e.g., [37,41,43,74–77]). In sustainable chemistry, plasma catalysis plays a more specific role, and we limit discussion to this lower technology readiness level (TRL) area. Examples include CO_2 splitting, CO_2 hydrogenation, dry reforming or partial oxidation of CH_4 to produce syngas, higher hydrocarbons or oxygenates, as well as NH_3 synthesis from N_2 and H_2 (see more details below and, e.g., [40,42,67–71]). These applications still face several challenges, such as the need for higher energy efficiency, product yield and selectivity, as well as the need to design better catalysts tailored to the plasma composition, as mentioned above. This requires thorough insight into the underlying mechanisms of plasma-catalyst interaction, which are still far from understood (e.g., [41,43,78–80]).

CO_2 splitting. Much research has been carried out on CO_2 splitting. The focus is not on targeting selected products but on how the catalyst affects the plasma and, thus, the CO_2 conversion and energy efficiency in DBD plasma. It is demonstrated that even the dielectric beads (catalyst supports) significantly affect the plasma (e.g., [81,82]). The dielectric constant plays an important role, as it causes polarization of the beads, and thus electric field enhancements at the contact points, which enhances the electron energy and affects the electron impact ionisation, excitation and dissociation reactions in the plasma [83,84]. However, the dielectric constant is not the only parameter affecting the plasma because the trends in performance do not precisely follow the dielectric constant [81]. Hence, the underlying mechanisms are more complex. It was also demonstrated that a metallic foam electrode in a DBD plasma could significantly enhance CO_2 conversion and energy efficiency [85]. Hence, plasma-catalytic CO_2 splitting is a valuable model reaction to understand better the effect of placing catalysts, or even just the supports or different metal electrodes, inside the plasma.

CO_2 hydrogenation. Plasma-catalytic CO_2 hydrogenation is also gaining increasing interest, and depending on the catalyst, either CO (reverse water-gas-shift reaction), CH_4 (methanation), or CH_3OH (methanol) can be formed. Especially CH_3OH formation is interesting. In thermal catalysis, the reaction proceeds via the adsorption of CO_2 to produce adsorbed formate (HCOO) or CO intermediates, followed by stepwise hydrogenation into CH_3OH. The reaction is exothermic and is therefore favoured by low temperatures. However, the latter limits the catalyst activation, so temperatures of 200–350 °C (and pressures of 17–100 bar) are used in practice. Plasma catalysis allows the reaction to proceed at low temperatures and atmospheric pressure. Wang et al. [86] applied a DBD reactor packed with Cu/Al_2O_3 catalyst, operating at 30 °C and 1 bar, and reported a CO_2 conversion of 21%, i.e., comparable to thermal catalysis. The low temperature was maintained by a liquid-water ground electrode, which favoured CH_3OH formation.

CH_4 conversion. For plasma-catalytic dry reforming of methane (DRM), it appears more difficult to selectively produce targeted products due to the many species formed. We believe more systematic research is also needed to understand better how the catalyst (or the dielectric support) affects the plasma [87]. Typically, the main products are the syngas components (CO/H_2) [88], but the direct production of

oxygenates or higher hydrocarbons is also possible [89]. Wang et al. [89] studied the combined conversion of CO_2 and CH_4, as well as the selectivity of gaseous and liquid products, for catalyst alone, plasma alone, and plasma + catalyst, using different catalyst materials, in a DBD reactor at 30 ^{o}C and atmospheric pressure. The Cu/Al_2O_3 catalyst alone yielded no conversion at this low temperature. Adding a catalyst to the plasma resulted in a slightly lower conversion of CO_2 and CH_4 than in plasma alone, attributed to the change in discharge behaviour. The total selectivity of gaseous products (mainly H_2, CO and C_2H_6) and liquid products (primarily acetic acid, methanol and ethanol, and some fractions of acetone) was similar for plasma alone and plasma catalysis. Still, plasma catalysis showed the potential to tune the distribution of the different liquid products. Indeed, the Cu/Al_2O_3 catalyst could enhance the selectivity of acetic acid to 40%.

Furthermore, formaldehyde was not detected in the case of plasma alone and only formed when using Pt/Al_2O_3 or Au/Al_2O_3 catalysts [89]. However, the total fraction of liquids was only around 1%. This stresses the crucial need for a better understanding of the optimal catalysts for directly converting CO_2 and CH_4 into value-added oxygenates with higher selectivity.

Nevertheless, this example illustrates that DBDs are promising for plasma catalysis, despite their lower energy efficiency than so-called warm plasmas [42], as they allow the integration of catalysts directly inside the plasma region, in contrast to the warm plasmas mentioned above. If catalysts can be designed to produce selectively oxygenates (or higher hydrocarbons), the lower energy efficiency will be more competitive with other (non-plasma) conversion technologies, as the one-step production of these value-added chemicals avoids using additional Fisher-Tropsch or methanol synthesis downstream processes. For instance, Biswas et al. [90] recently reported oxygenate production by combining plasma conversion of CO_2 and ethane. Two other successful examples of plasma catalysis in DBD were recently reported by Yi et al., i.e. for NH_3 reforming of CH_4 over Cu-based catalysts, producing HCN and H_2 at a reduced temperature [91], and for the selective oxidation of CH_4 to CH_3OH [92].

Kim et al. [93] and Mehta et al. [94] discussed the critical role of the reactor temperature in CH_4 conversion. At low temperatures, for which $\Delta G > 0$, CH_4 conversion proceeds inside the plasma, irrespective of the presence or absence of packing or catalyst, while at high temperatures, for which $\Delta G < 0$, plasma alone or plasma with non-catalytic packing seems to be quite inactive, but the combination of plasma and catalyst leads to improved conversion compared to thermal catalysis [93]. Indeed, bond breaking in the plasma is required for thermodynamically uphill reactions, and the plasma-driven conversion is initiated by electron impact dissociation of CO_2 and CH_4. In addition, standard catalysts will not be effective for thermodynamically uphill reactions because they are active for both forward and backward reactions. This explains why packing the reactor with a catalyst or support does not necessarily yield CO_2 and CH_4 conversion improvements. The changes observed may be attributed to the packing effects on the discharge characteristics [94]. Hence, there is a need to design catalysts for which plasma activation can promote forward CH_4 and CO_2 conversion reactions without promoting the reverse. For thermodynamically downhill reactions, vibrationally excited molecules can enhance the reaction rates in the presence of a suitable catalyst due to the energy barrier reduction. Indeed, vibrationally excited CH_4 produced in plasma can dissociate more easily at a catalyst surface. This was demonstrated for CH_4 conversion at elevated temperatures in a plasma with Ni catalyst, where the apparent activation energy for CH_4 activation was reported to drop significantly under plasma stimulation [95,96].

Another aspect for which plasma catalysis can be beneficial is to avoid coking and coke-related deactivation. Indeed, coke deposits typically block catalyst pores and deactivate active sites. Metal catalysts can sinter at high reaction temperatures, necessary for highly endothermic reactions, resulting in a lower active surface area. Plasma catalysis can overcome these problems by operating at lower temperatures, minimising the issues of sintering and coking, and providing alternative regeneration strategies where the plasma can remove the coke deposits [97].

An interesting example of successful post-plasma catalysis is presented by Delikonstantis et al. [98]. The authors used an ns-pulsed plasma for CH_4 conversion, which mainly yielded C_2H_2. However, because C_2H_4 is a higher-value compound, they placed a catalyst post-plasma for the further C_2H_2-to-C_2H_4 conversion. A Pd/Al_2O_3 catalyst resulted in higher C_2H_4 selectivities than plasma alone or an Au/TiO_2 catalyst. The Pd-based catalyst resulted in the hydrogenation of the C_2H_2 formed in the plasma towards C_2H_4, with an overall C_2H_4 yield of 25.7% per pass. This two-step process was carried out in a single reactor, and besides the applied plasma power, no extra heat or H_2 input was needed because both were provided by CH_4 cracking in the plasma zone. Furthermore, a life cycle assessment revealed that the two-step process gave a lower carbon footprint than the one-step process and was more environmentally sustainable than other peer processes (i.e. thermally driven and bio-based) when using natural gas [99].

NH_3 synthesis. This is a simple reaction, ideally suited to study the fundamental mechanisms (see section (c) below). Most work has been performed in DBD plasmas, which are the simplest type of plasma catalysis reactors, although not preferable for energy efficiency. Many different catalysts were used in literature, including various metals and bimetallic catalysts, on various supports, such as Al_2O_3, MgO, SiO_2, and $BaTiO_3$, as well as carbon-based materials, and in various forms, including powders, pellets and spheres (see [100–102] for details). Fig. 2 presents an overview of the energy yield vs obtained NH_3 concentration from various papers in the literature using different plasma types. The best results reported were an NH_3 yield of up to 9% [101] and an energy cost of down to 1.5 MJ per mole NH_3 produced [100], but these record values were not obtained in the same study or identical conditions. Generally, energy costs below 20 MJ/mol have only been reported for very low yields (<<1%). When compared with typical values for the Haber–Bosch process, i.e., 15% NH_3 yield and 0.4 MJ/mol energy cost (at least for small-scale production, compatible with renewable energy sources: ~10 tons/day) [100], the energy cost of plasma catalysis would have to be significantly reduced to be adopted in industry, even allowing for the decreasing cost of renewable energy.

Moreover, energy costs reported for plasma catalysis typically do not consider losses in the power supply, which can be even 50%. These losses should also be accounted for to allow a fair comparison. Fig. 2 does not present the energy cost but the energy yield (g-NH_3/kWh). However, this figure also illustrates that none of the existing plasma catalysis reports are already competitive. The target (large green sphere), as defined by Rouwenhorst et al. [70], is an alternative for small-scale ammonia synthesis.

The picture looks different for NH_3 obtained from plasma-based NOx production, as demonstrated by Hollevoet et al. [100,102]. Indeed, the authors proposed placing a lean-NOx trap after a plasma reactor producing NO_x for the further reduction into NH_3, i.e., the so-called PNOCRA process (plasma-NO_x and catalytic reduction to ammonia). As demonstrated in the review with techno-economic analysis by Rouwenhorst et al. [69], NO_x production by plasma can proceed at a lower energy cost. This is especially true in warm plasmas, due to the higher temperature, important for the thermal Zeldovich mechanism for NO production, and (in some cases) a vibrational-translational non-equilibrium, further enhancing the efficiency of the Zeldovich mechanism. Since this overview by Rouwenhorst et al. [69], even better NO_x yield, production rate and energy cost were obtained in atmospheric pressure GA and MW plasmas [103,104]. A record-low energy cost of 0.42 MJ/mol NOx was reported in a pulsed plasma jet, albeit at a low NOx concentration of 240 ppm [105]. However, this low NOx concentration was no problem for the PNOCRA process because the lean-NOx trap is adopted from automotive technology and can easily convert low NOx concentrations into concentrated NH_3. Hollevoet et al. [102] reported an overall energy cost of only 2.1 MJ/mol NH_3 at ammonia

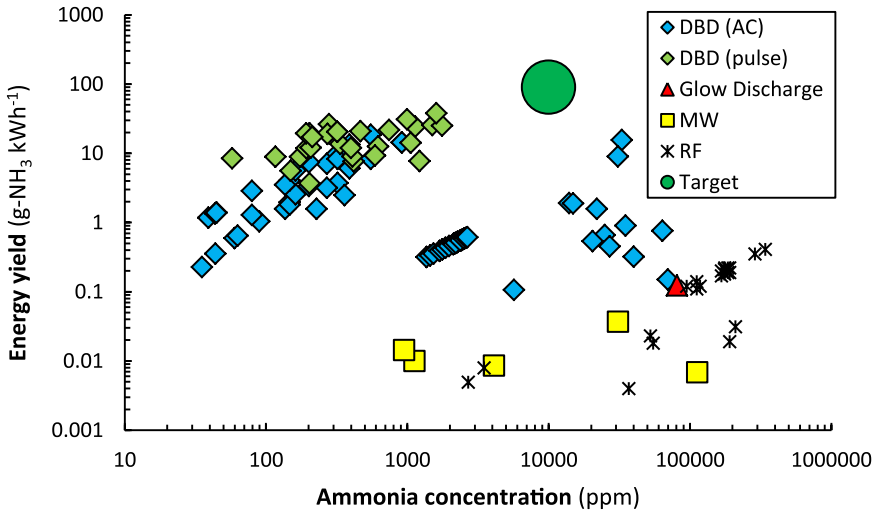

Fig. 2. Reported energy yield vs. NH_3 concentration for different plasma (catalysis) studies collected from literature, in comparison with the alternative for small-scale NH_3 synthesis (defined here as "target").
(a) Reproduced from [70] with permission from the Royal Society of Chemistry. Copyright RCS, 2020.

concentration above 1%, making PNOCRA the least energy-consuming small-scale NH_3 production process at mild conditions demonstrated so far.

Note that various other concepts have been developed recently, based on integrating plasma N_2 fixation to NO_x, with some catalytic and/or electrochemical reduction to NH_3 (e.g., [106–110]). For instance, Sharma et al. [110] also demonstrated NH_3 production from N_2 and H_2O using a plasma-activated proton-conducting solid oxide electrolyser. In this innovative concept, hydrogen species produced by water oxidation over the anode are transported through the proton-conducting membrane to the cathode, reacting with the plasma-activated nitrogen toward NH_3.

2.3. Challenges

Plasma catalysis has potential application in the classical or more innovative configurations discussed above. Still, more research is needed to obtain the necessary insights, certainly for in-plasma catalysis, i.e., how the catalyst influences the plasma, and vice versa, how the plasma (components) affect the catalyst performance. The underlying mechanisms are indeed very complex, as illustrated in Fig. 3. This insight is crucial to synthesising the ideal, cost-effective, highly active, stable catalysts tailored to the plasma environment. Insights from thermal catalysis are undoubtedly helpful, but other processes will come into play, such as the interaction of plasma-produced radicals and (vibrationally or electronically) excited molecules with the catalyst surface, and might even be dominant. Because of the similarities with electro- and photo-catalysis, insights from these domains are also crucial, although again, conditions are different, and insights cannot be directly translated.

A paradigm shift. Most research was trial-and-error based, where thermal catalysts were placed inside the plasma, hoping to see synergy. However, there is a paradigm shift in the concept of plasma catalysis compared to thermal catalysis, which is still mostly overlooked. Indeed, while in thermal catalysis, reactants chemisorb and undergo surface-mediated reactions to form the products, the plasma already provides external activation in plasma catalysis. Hence, the question arises: how can the catalyst optimally interact with the various reactive plasma species (i.e., radicals, excited molecules, charged species, etc.) without simply quenching them? Logically, radicals will recombine into stable molecules at the catalyst surface. This is no problem if it happens to the desired products, but it likely goes back to the reactants, reducing the plasma performance and energy efficiency. In addition, more insights are needed into how the catalyst can exploit other plasma components,

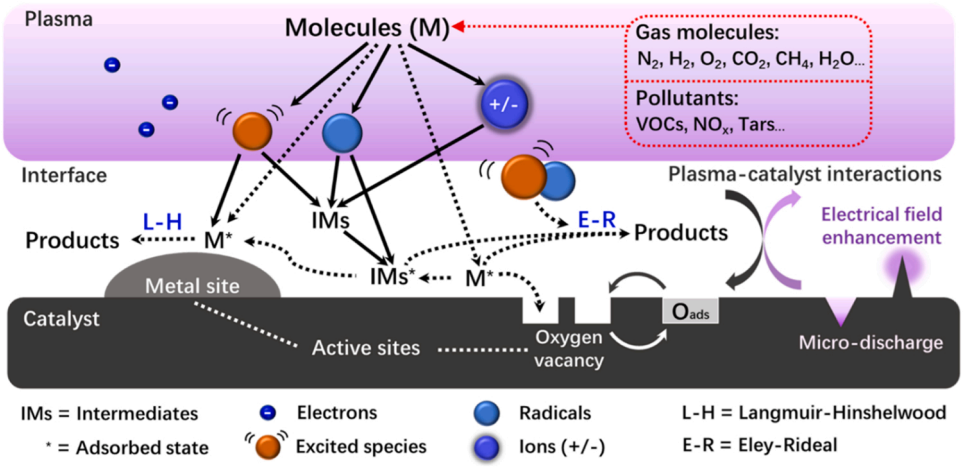

Fig. 3. Schematic overview of the main processes occurring with in-plasma catalysis.
Reproduced from [41] with permission. Copyright IOPScience

such as the electric field and surface charging. Furthermore, the plasma can also transform the catalyst structurally or compositionally during operation, which must also be accounted for.

Promoting plasma catalysis synergy. Vice versa, the plasma conditions should be optimised to promote the synergy with the catalyst. In this respect, the reduced electric field (i.e., the ratio of the electric field over gas number density) is a crucial parameter, as it affects the electron energy and, thus, the plasma chemistry. We believe that vibrationally (or electronically) excited molecules should be promoted in the plasma, rather than radicals, because the excited molecules would reduce the dissociation energy barrier at the catalyst surface, thus enhancing the catalytic reactions. In contrast, radicals would instead be quenched at the catalyst surface and can recombine back into the reactants. However, most DBD plasmas operate at high values of a reduced electric field, mainly producing radicals rather than vibrationally excited molecules. Nevertheless, if the plasma conditions (i.e., primarily the reduced electric field) could be tuned to produce vibrationally (or electronically) excited species selectively, we hypothesise there is more chance for plasma-catalyst synergy.

Optimizing plasma-catalyst interaction. Moreover, when designing an optimal catalyst, one should not only consider the chemical composition, but the first and necessary condition is also to have sufficient contact between the plasma and catalyst. Otherwise, chemical reactions happen inside the plasma, and the catalyst has no real contribution. This might be the case in some plasma catalysis studies, where no beneficial effect is observed. Hence, plasma reactors must be designed to optimize the transport of species generated in the plasma to the catalyst surface. This could be realised using specific support shapes, like honeycombs, three-dimensional fibre-deposition (3DFD) structures, or smaller gaps between the catalyst beads in a packed bed. However, the gaps should still be large enough for plasma streamers to propagate. More research is needed in this direction as well.

Plasma inside the catalyst. Another crucial research question in plasma catalysis is whether plasma streamers can penetrate catalyst pores and what is the minimum pore size. Computer modelling revealed that the Debye length defines the minimum pore size. The latter depends on the electron density and temperature in the plasma streamer. At typical DBD conditions used for plasma catalysis, it is 500 nm or more [111,112]. This has significant consequences for plasma catalysis because if the pore size is smaller, like for typical catalytic supports (e.g., zeolites), plasma streamers will thus not be able to penetrate inside the pores. If catalyst nanoparticles were deposited inside the pores of these supports, they would not be reached by the plasma streamers. Note that plasma species might still be able to diffuse into the pores, but their concentration will also drop deeper inside the pores, depending on their lifetime. This insight is also crucial for applying the appropriate catalyst synthesis methods: it might be more beneficial to use a synthesis method that only deposits the catalyst particles at the outside surface of the beads so they will all be in contact with the plasma.

2.4. How to overcome the challenges and create new opportunities

The holy grail in plasma catalysis is to design the optimal catalyst tailored to the plasma conditions and tune the plasma conditions to let them work in optimal synergy with the catalyst. Designing the optimal catalyst should focus on shaping (allowing sufficient contact between plasma components and catalyst surface) and composition/structure.

Catalyst screening and machine learning. One option to find the optimal catalyst is through catalyst screening, which may provide valuable guidelines and design trends. Machine learning (ML) based on catalyst screening could be helpful here to train a model for catalyst optimisation. However, this requires sufficient experimental data to be available, which is typically not yet the case. This explains why ML is not yet well-established in plasma catalysis, in contrast to thermal catalysis [113]. We know only a few examples in literature [114–117].

Besides catalyst screening and ML, designing dedicated plasma catalysts should also be possible based on a thorough understanding of the plasma-catalytic mechanisms. This understanding can be obtained from experiments and modelling (ideally, a combination of both).

***In-situ* catalyst surface characterization.** More and more labs are developing in-situ surface characterisation for plasma catalysis. Many catalyst characterisation methods (such as X-ray diffraction, X-ray photoelectron spectroscopy, O_2 chemisorption, SEM, TEM, etc.) are difficult for in-situ characterisation during direct plasma exposure. While these methods are still very useful before and after plasma catalysis to check, e.g., structural changes caused by plasma exposure, in-situ surface characterisation is much more valuable to obtain deeper insights into the plasma–catalyst interactions during plasma operation [41,73]. However, the molecules detected by infrared (IR) are those which accumulate on the surface and are not necessarily the most reactive species.

Most work is done with diffuse reflectance infrared Fourier transform spectroscopy (DRIFTS) [118–122], which is also commonly applied in thermal catalysis. Transmission IR can be used and has some advantages, such as easier quantitative studies, less temperature dependence, no grain size dependence and smaller temperature gradients in the catalyst material [123]. Transmission IR cells have been developed for a low-pressure glow discharge plasma [124] and, more recently, also for a DBD at atmospheric pressure under continuous flow [125,126]. Ideally, if in-situ IR cells can be coupled to gas chromatography (GC) or mass spectrometry (MS) at the gas outlet, this will enable *operando* studies, i.e. measuring the plasma-catalytic performance together with the surface characterisation [125,127]. However, operation under plasma conditions requires that the electrodes of the plasma reactor are spatially separated from any metallic parts of the spectrometer, which yields large dead volumes in most IR cells so that measured conversions are typically low [126]. This makes in-situ *operando* plasma catalysis studies not yet very straightforward.

Besides in-situ IR, temperature-programmed desorption (TPD) can also be used to identify species adsorbed on a catalyst surface. It was recently used to investigate CO_2 hydrogenation in DBD with Co and Cu catalysts [128]. In addition, the authors used GC and MS to monitor the gas-phase composition. By pre-treating the surface with isotopically labelled CO_2, the exchange of atoms between gas and surface could be tracked. Isotopic labelling was also applied by Navascués et al. [129] to elucidate the chemical mechanisms in $NH_3/D_2/N_2$ in a packed bed DBD. Furthermore, X-rays-based methods are also gaining interest for in-situ structural analysis of catalysts because of the brightness of synchrotron radiation (e.g., [130]). Finally, in-situ measurement of the catalyst surface temperature in a DBD plasma provides valuable insights, although such measurements are also quite challenging [122,126,130].

Chemical kinetics modelling. Complementary to experiments, modelling is also helpful in gaining deeper insights into the underlying mechanisms. Chemical kinetics (or microkinetic) modelling is applied to study chemical pathways in the plasma or at the catalyst surface.

(a) Opportunities for NH_3 synthesis. Based on a chemical kinetics model for plasma-catalytic NH_3 synthesis in a DBD reactor, van 't Veer et al. [131] investigated the central pathways in the plasma and at the catalyst surface. Electron impact dissociation of N_2 and H_2 inside the plasma creates N and H atoms, which can recombine into NH radicals. The latter adsorb on the catalyst surface, and upon hydrogenation, this leads to the formation and desorption of NH_3. DBD plasmas consist of microdischarge filaments, and the model could distinguish between the processes occurring inside the microdischarges and in between them (so-called afterglows). The model also revealed that most of the NH_3 is produced between the microdischarges, while during the microdischarges, the NH_3 is dissociated by electron collisions. Fig. 4 provides a schematic overview of the pathways predicted by the model (a) during and (b) in between the microdischarges.

Such modelling insights are very useful, as they can guide experimental work. Indeed, based on the above model predictions that NH_3 is decomposed inside the plasma filaments, Rouwenhorst et al. [132] used

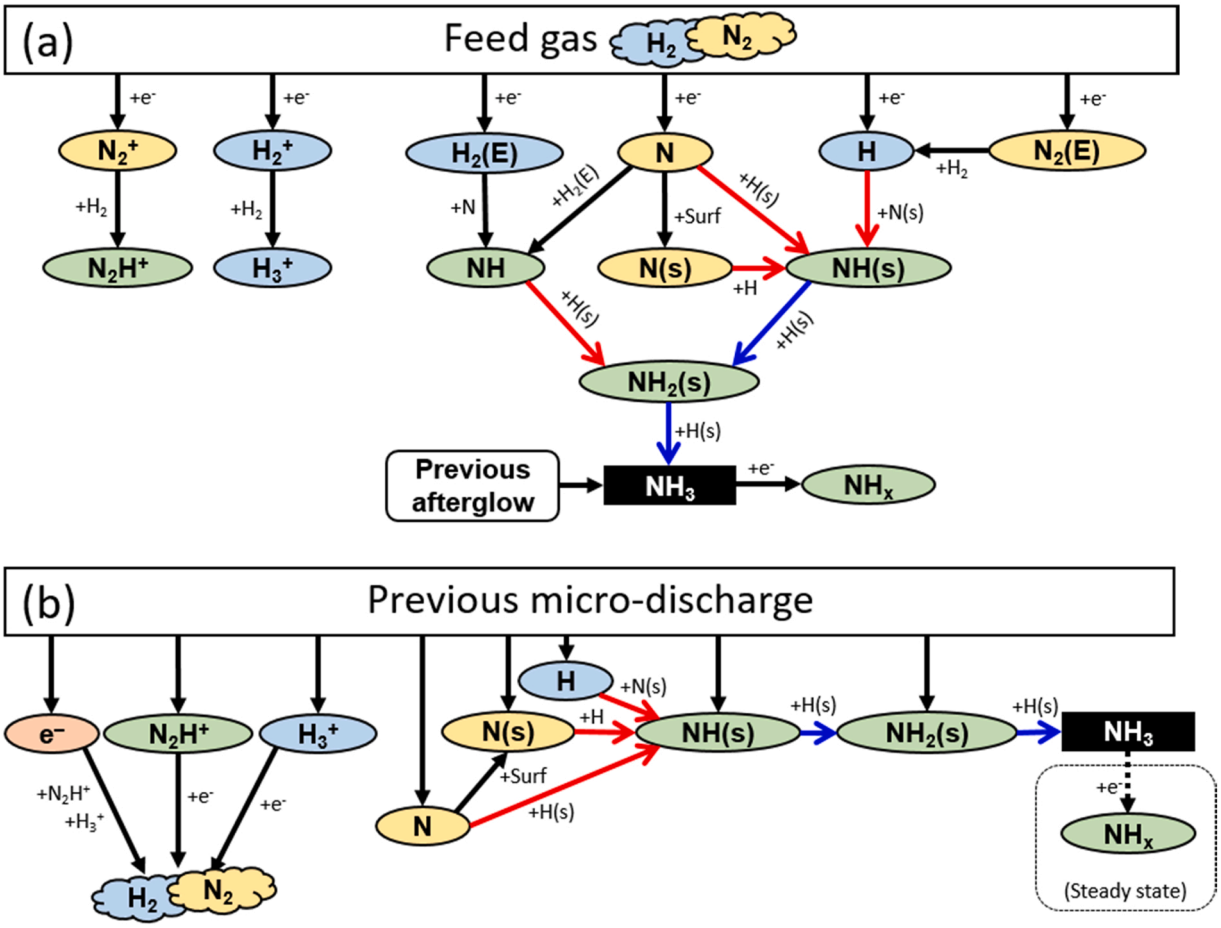

Fig. 4. Reaction pathways predicted by plasma and surface chemical kinetics modelling, leading to NH_3 synthesis in a DBD plasma with catalyst, during the microdischarges (a) and in between them (i.e. so-called afterglows) (b). Both Eley-Rideal (E-R) and Languir-Hinshelwood (L-H) reaction steps occur, as indicated by red and blue arrows, respectively. (a) During the micro-discharges, reactive species are created by electron impact collisions with the feed gas, and they give rise to NH_3 formation. At the same time, NH_3 is also dissociated upon collision with electrons. (b) In the subsequent afterglows, the reactive species created during the microdischarges react further into NH_3 via several E-R and L-H reactions.
Reprinted with permission from [131]. Copyright (2020) American Chemical Society.

an adsorbent (zeolite 4 A) for in-situ NH_3 removal from the plasma phase to avoid such decomposition, followed by desorption after plasma turn-off. The NH_3 yield with in-situ NH_3 removal was improved by a factor of two compared to without an adsorbent. Such in-situ product removal will be of interest to other applications to avoid product decomposition in the plasma phase.

A similar approach of so-called "shielding protection" was reported by Wang et al. [133], who used mesoporous MCM-41. The Ni catalyst active sites were deposited on the external surface of MCM-41 to enhance plasma−catalyst interactions, and thus NH_3 production (up to above 5% NH_3), and the desorbed NH_3 could diffuse into the mesopores of MCM-41. Because plasma could not be created inside these mesopores (because they were smaller than the Debye length; see discussion in section 2.3 above [111,134]), the NH_3 was shielded from decomposition in the plasma. These are two excellent examples of rational design of catalysts based on detailed insights into the mechanisms, as obtained from modelling [131].

Li et al. [135,136] presented a similar (but opposite) innovative concept for combined plasma-based CO_2 capture and utilisation. The authors used a DBD plasma reactor packed with hydrotalcite pellets as a solid sorbent. The plasma could instantly desorb the CO_2 from the hydrotalcite surface. A single pass CO_2 conversion of up to 67% was achieved. The authors also discussed the possibility of periodic operation of multiple reactors (in parallel and series) for continuous CO_2 capture and conversion [135].

While the above chemical kinetics model of van 't Veer et al. [131] mainly focused on plasma chemistry, detailed surface microkinetic models for plasma catalysis can also give valuable insights into the desired catalyst materials. Mehta et al. [137] demonstrated by microkinetic modelling that plasma-produced vibrationally excited N_2 molecules have a higher reactivity at a catalyst surface due to the lower dissociation barriers at the surface. In this way, catalysts that bind nitrogen relatively weakly can become strongly active, thereby overcoming the typical scaling relations in thermal catalysis. This shifts the peak of the 'volcano curve' away from Fe-based catalysts (as used in the Haber–Bosch process) and drastically improves the NH_3 synthesis rate on these catalyst materials that are kinetically limited by N_2 dissociation. In addition, their model revealed that due to the non-thermal plasma excitation, the NH_3 yield could exceed equilibrium limits [138]. The same group showed experimentally that higher gas and surface temperatures would increase the NH_3 yield and energy efficiency. Thus, they indicate a separate control of the gas and surface temperature [139].

Engelmann et al. [140] developed a more extended microkinetic model to investigate the effect of radical reactions on the plasma-catalytic NH_3 synthesis, besides the effect of N_2 vibrational excitation. They applied their model to a wide range of catalyst materials, demonstrating that when radical adsorption and ER reactions determine the reaction pathways, besides the more common LH reactions that are dominant in thermal catalysis, the NH_3 synthesis

becomes virtually independent of the catalyst material, resulting in rather flat volcano plots. Various experimental data confirm these model predictions (e.g., [141]), indicating that in most common (DBD) plasma-catalytic conditions, radical adsorption and ER reactions indeed dictate the plasma-catalytic NH_3 synthesis mechanisms. This can explain why plasma-catalyst synergy is often not very pronounced in experiments because the plasma reactivity is already very high due to the radicals created. Recently, Ndayirinde et al. [142] investigated various bi- and trimetallic catalysts and demonstrated that these do not yield large variations in NH_3 production. Moreover, the observed variations were correlated to changes in the physical characteristics of the plasma, suggesting that the catalysts have limited surface chemical-catalytic effects but rather act as plasma modifiers. This aspect is still largely underestimated up to now. Still, we believe more attention should be paid to how the catalyst materials affect the plasma behaviour in searching for optimal catalysts.

In parallel with the insights from microkinetic modelling, Rouwenhorst et al. [143] reported that NH_3 synthesis in DBD plasma with catalysts can be classified into four possible mechanisms, i.e., (i) plasma-phase NH_3 synthesis, (ii) surface-enhanced plasma-driven NH_3 synthesis, (iii) plasma-enhanced semi-catalytic NH_3 synthesis, and (iv) plasma-enhanced catalytic NH_3 synthesis, depending on whether dissociation of both N_2 and H_2, only N_2, or neither N_2 and H_2 occurs in the plasma. The authors concluded that plasma should promote N_2 and H_2 dissociation on the catalytic surface by exciting the molecules and not dissociating them in the plasma for better energy efficiency. This is, however, only possible in low-power DBD plasmas. This indicates that the plasma conditions (mainly the reduced electric field) should be tuned to maximise vibrational excitation for more efficient NH_3 synthesis. However, the NH_3 yield will be low at low power, so a compromise may be needed to optimise the NH_3 yield and energy cost.

(b) Opportunities for CH_4 and CO_2 conversion. In another microkinetic model, Engelmann et al. [144] demonstrated for the non-oxidative coupling of CH_4 that the optimal catalyst material depends on (i) the desired products and (ii) the plasma conditions. Specifically, plasma conditions that mainly give rise to vibrational excitation of CH_4 yield enhanced C_2H_4 formation on most catalysts (e.g., Pt, Rh, Pd and Cu). In contrast, the more noble catalysts (like Ag) promote C_2H_6 formation. On the other hand, plasma conditions that favour radical formation (as is the case for most DBD plasma conditions) mainly yield C_2H_4 formation on all catalysts [144]. Furthermore, a microkinetic model for plasma-catalytic CO_2 hydrogenation on a Cu(111) surface revealed that plasma-generated radicals and intermediates could enhance the CH_3OH production rate by 6–7 orders of magnitude compared to thermal catalysis [145]. Likewise, the plasma-generated radicals and intermediates could significantly improve the oxygenated product yields in the case of plasma-catalytic oxidative coupling of CH_4 [146]. Such chemical kinetic models can generally elucidate how various plasma species affect the catalyst surface chemistry. This can guide the tuning of the plasma composition to target the formation of desired products.

(c) Avoiding post-plasma recombination. The last example where insights from modelling and experiments are very useful to improve the plasma conversion performance relates to the recombination of products after the plasma. Modelling and experiments of CO_2 plasmas have demonstrated that large (supra-equilibrium) conversion is possible inside the plasma. Still, it drops beyond the plasma due to the recombination of the reaction products [147,148]. This problem can be overcome by fast quenching, i.e., rapid cooling after the plasma, as demonstrated for NO_x production in a GA plasma [149] and for CO_2 conversion in an MW plasma, reaching excellent conversion and energy efficiency, even at conditions close to atmospheric pressure [150,151].

Another promising solution to this post-plasma recombination problem is removing one of the reaction products so that recombination cannot happen anymore. This was recently demonstrated by Delikonstantis et al. [152] with plasma-assisted chemical looping, indicating that plasma with post-plasma scavenging (chemical looping) materials can significantly overcome chemical equilibrium limits. Furthermore, Xu et al. [153] suggested that the O atoms produced by CO_2 splitting can also be efficiently harvested and used as a waste-free terminal oxidant to oxidise alkenes to epoxides, hence providing extra added value, besides preventing the recombination with CO back into CO_2.

Finally, a similar principle of oxygen scavenging was demonstrated by several authors for a post-plasma carbon bed [154–156], where the produced O and O_2 from CO_2 conversion react with the carbon atoms, thereby reducing the problem of recombination with CO. In addition, when the temperature at the carbon bed is sufficiently high, the unconverted CO_2 can also react with the carbon atoms, giving rise to the reverse Boudouard reaction and producing more CO. Such a post-plasma carbon bed was demonstrated to enhance the overall CO_2 conversion and energy efficiency by a factor of two while producing up to three times more CO, and removing nearly all O_2 from the product mix, thus significantly reducing separation costs [156].

Although more research is needed to demonstrate the long-term improved performance, these examples show that post-plasma catalysis, or placing materials after the plasma, can lead to much better performance.

3. Unconventional catalysis in flow chemistry

3.1. Background

Exploring unconventional catalysis in microfluidic reactors means learning from conventional catalysis in flow chemistry. Microreactor chemical processing is called flow chemistry if taken from the viewpoint of chemistry [157,158]. Microfluidic reactors comprise continuous-flow reaction pathways of different fabrication histories, including microfabricated devices, items from commercial small-scale analytical instruments (e.g. capillaries and connectors from high-pressure liquid chromatography, HPLC) and assemblies within mini-scale continuous--flow devices creating microfluidic conducts (e.g. mini-packed bed reactors, solid particle assembly in a mini-scale tube) [159].

Microreactors, as one name for all those, with their flow chemistry, can conduct chemical reactions within a short time scale, which should reasonably not be longer than one hour [160–162].

3.2. State of the art - flow catalysis concepts with "conventional catalysis"

While hardly owned, catalysis concepts have been reported in microreactors, as the chemical mechanism is believed to be unchanged in flow chemistry, microreactors, and flow chemistry, with their advanced processing opportunities, promoted excellent catalyst studies, both for heterogeneous and homogenous catalysis as follows.

One example of a heterogeneous stereoselective catalytic reaction using achiral substrates was part of the continuous-flow multistep synthesis of the antidepressant drug (S)-rolipram [163]. Catalysts and reactants were deposited on a polymeric solid carrier, meaning the reaction operated like an ion exchanger. The quality of the reaction was so high that no interim operation, e.g. purification or solvent switch, was required. Reactions were done in three steps with a strongly varying temperature profile, from 75 to 0–120 °C. Enantiomerically pure (S)-rolipram was crystallized with a total yield of 50% at a productivity of 1 g/d.

An example of an advanced flow chemistry study using homogenous catalysis is the Michael addition between diethylmalonate and p-chloro-β-nitrostyrene using a Takemoto bifunctional thiourea catalyst in the Chemtrix Labtrix platform. The product was achieved with 98% conversion and 85% enantiomeric excess. The catalyst rated 9000 h^{-1} mol productivity divided by mol catalyst [164]. The same flow catalysis approach was used to synthesise a precursor of anticonvulsant and antiepileptic drug (S)-Pregabalin [165].

3.3. Challenges

The challenge for flow chemistry catalysis is to learn from a renaissance of emerging catalysis science with three noteworthy characteristics: (1) catalyst placement into microchannel by coating and immobilization (e.g. on beads): (2) catalyst performance in highly accelerated reaction conditions; and (3) revisit of electric and electromagnetic-induced catalysis, which matches miniaturised processing.

Catalyst placement. Concerning the catalyst placement, the fast mass transfer, facilitated by short internal dimensions, allows coating on the walls of microchannels, or generally micro conduits [166]. That can be done up to a pilot-scale, close to chemical production (on a pharmaceutical scale) [167]. Heterogeneous flow catalysis uses beads in a small tube to form a packed bed [168]. Catalyst immobilization techniques used for flow catalysis include covalent support, self-support, adsorption, H-bonding, ionic interaction, and nonconventional media [169]. Flow biocatalysis studies pioneered catalyst (enzyme) immobilization on a heterogeneous support, typically a polymer (resin) [170]. Flow biocatalysis was used to synthesise 5-hydroxymethylfurfural (HMF) from glucose against a biomass process, with cellulose providing glucose [171]. The product was obtained in three steps via enzymatic isomerization of glucose, arylboronic acid-mediated fructose complexation, and dehydration to HMF. Glucose isomerase was immobilized on polymeric support to allow recycling. An innovative multiphase flow contact increased the yield of a biocatalytic reaction [172].

Highly accelerated processing. Highly intensified process schemes have been postulated and identified for microreactors to enhance the reaction rate to a time scale which suits flow chemistry and allows them to gain their typical benefits. This has been termed "novel process windows", including high-temperature, high-pressure, designer solvent processing [173–175]. Novel process windows adapt to process intensification, which aims at process integration and process simplicity among integrated processes.

Electric and electromagnetically activated catalysis. We will detail this point in the following. Electric catalysis is given by electrochemical and plasma flow chemistry, with plasma chemistry reported in this manuscript. Electromagnetic activation and catalysis use photo-, microwave- and ultrasound-induced flow chemistry.

3.4. How to overcome the challenges and create new opportunities

The challenges of electric and electromagnetically activated catalysis in flow are explained in the example of photo flow chemistry and revisited later for other approaches.

Photocatalysis intensification and characteristics. Intensification can have various assets of expression, including reaction acceleration, higher selectivities, reliability for scaling-out, safe use of hazardous intermediates, less waste production, exploration of new reactions, and use of online analytical process control [176]. Photocatalytic transformations in continuous-flow reactors allow wide and versatile use in process chemistry, including organic synthesis, pharmaceutical manufacturing, advanced materials, and wastewater purification [177].

Flow chemistry automation can help to develop and perform complex catalytic processing, as demonstrated for the multistep synthesis of the antimalarial drug candidate OZ439 with several in-line purifications and process-analysis units. A machine-assisted protocol was used for the continuous-flow synthesis of OZ439 [178]. The first step in the three-step synthesis is the continuous flow hydrogenation of dihydroxybiphenyl on a HEL FlowCAT platform run in trickle bed operation using a Pd/C catalyst [179].

Visible light-mediated photocatalysis is an emerging field in organic synthesis, e.g., using sunlight instead of energy-consuming UV light from LED technology for photo flow catalysis [180–182]. Photocatalysis has genuine advantages regarding incorporating a wide range of functional groups, biocompatibility, site-specific selectivity, and process simplicity [183].

Photo flow chemistry can, in the extreme, lead to rigorous process simplicity, i.e. in chemical protocols omitting a catalyst and using abundant sources to replace today's fossil chemicals. A continuous-flow catalyst-free hydrogenation protocol of ortho-methyl phenyl ketones was achieved by taking hydrogen out of water [184].

Multiphase processing capability is key to making complex molecules. Photoflow catalysis is often done under multi-phase conditions for which microreactor operation is advantageous by photon- and mass-transfer enhancement [177].

Advanced heating for photocatalysis. Photoflow catalysis and modern heating techniques can mutually benefit. The multistep continuous flow synthesis of olanzapine was propelled by inductive heating to reduce reaction times and increase process efficiency significantly. The Buchwald–Hartwig coupling of an aryl iodide and aminothiazole yielded 88%, using a palladium catalyst and Xantphos ligand [185].

(a) Opportunities by photo flow catalysis. Continuous-flow photocatalysis [174] in microreactors benefits from the high penetration of light in the microchannel, as do also microwaves. The typical microchannel dimensions match the physics of light penetration, determined by Lambert-Beer law. This allows operating at a much higher concentration than usual, finally even omitting solvents and working with pure reactants, pushing limits of productivity. As an example of solvent-free operation, the in situ formation of bromine, in the absence of a solvent, was accomplished in flow for the photochemical bromination of benzylic functionalities, with complete conversion within 15 s. The process mass index, the ratio of all process mass to the products as a measure of waste production, decreased from 13.3 to 4.3 [186].

Many photosensitizers and photocatalysts have been developed [187]; see Fig. 5. Photochemical sensitization is key to success for photocatalytic transformations and is closely related to photocatalysis [188]. Photosensitization can involve energy transfer, hydrogen abstraction, or electron transfer. Photocatalysis is employed mainly for noble metal-catalysis in organic chemistry [189].

Dual catalysis strategies employ photosensitising and other catalytic functions in photochemical flow synthesis (e.g. phase transfer) [187]. As another example, symbiosis of photoredox-mediated hydrogen atom transfer and transition-metal catalysis generates activated C–H bonds with low dissociation energies [190]. The enantioselective α-hydroxylation of β-dicarbonyl compounds was conducted in a dual catalyst system, including a phase transfer catalyst for chirality transfer and another catalyst for singlet oxygen formation. Yields up to 96% and good enantioselectivities up to 90% enantiomeric excess were achieved, at a massive reduction in reaction time, from 24 h in batch to 55 min in flow conditions [191].

Heterogeneous photocatalysts for flow chemistry Homogeneous transition metal complexes are widely established as photocatalysts because of their photophysics, offering a range of electrochemical redox potential while being photostable. On the flip side, these photocatalysts are toxic, often need synthesis rather than to be commercially available, and are critical transition metal elements as supply and costs. Heterogeneous photocatalysts provide an alternative to the 'one-way use' of homogeneous catalysts, which demands separation and purification by fixing the catalyst to support. Heterogeneous catalysts, however, are generally less efficient. This is primarily due to their presence as a separate phase which causes mass transport issues and adds needs on adsorption onto a solid surface. Flow chemistry can at least remove the first bottleneck and boost the overall reaction system by significantly penetrating photons to the reaction volume and catalyst [192]. This opens the potential for sustainability, also seen from the viewpoint of green chemistry [193,194].

Real-word applications. Oxidations represent powerful photosensitized transformations that must be conducted in multi-phase mode when introducing molecular oxygen as a gaseous reactant to create (singlet) radicals as reactive species. Often pure oxygen is used, which

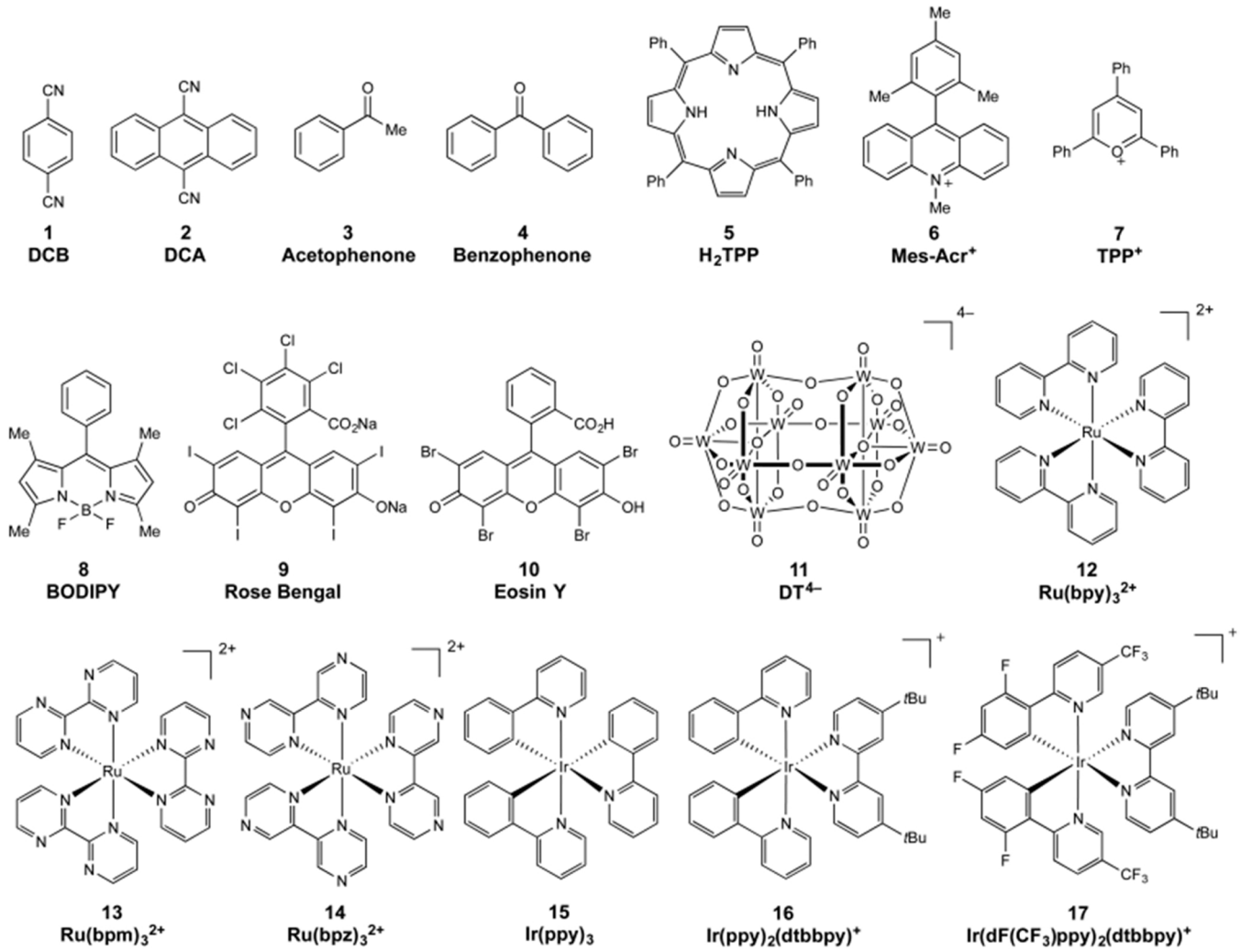

Fig. 5. Common photocatalysts.
Reproduced with permission from [188]. Copyright ACS, 2016.

creates an issue of process safety. Photo flow microreactors can foster the in-situ provision of singlet oxygen and allow the safe processing of potentially explosive mixtures with pure oxygen as well as the efficient interface transfer to the liquid phase, using gas-liquid segmented (Taylor) flow. This was utilized for the photocatalytic flow synthesis of artemisinin, an ingredient of anti-malaria drugs [195]; see Fig. 6. The

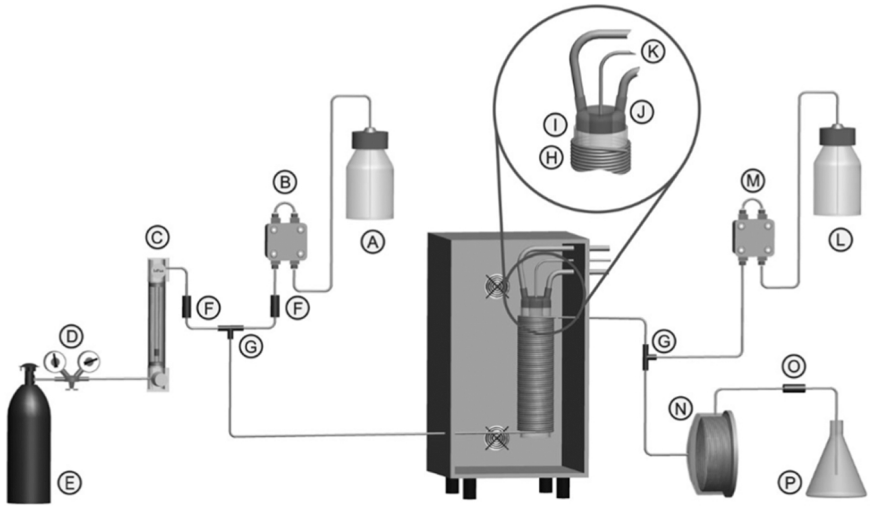

Fig. 6. Experimental setup for the photocatalytic flow synthesis of artemisinin.
Reproduced with permission from [195]; see there for details on the components of the setup. Copyright Wiley-VCH, 2012.

photosensitizer 9,10-dicyanoanthracene replaced meso-tetrapheny lporphyrin, because of higher quantum yield and improved photostability. This process was scaled-up to the industrial size [196]. Sanofi Company transferred the process in 2014 in Italy to a production scale at a capacity of up to 60 t/a, nearly reported to be 33% of the world demand per year [197].

A sustainable variant of the artemisinin process was developed with a renewable biomaterial reactant and a bio photocatalyst [198]. A crude extract of *Artemisia annua* leaves was used as a natural resource. Natural chlorophylls in the extract demonstrated their capability as a sensitizer for singlet oxygen formation, with strong light absorption in the visible range that allowed the use of LED arrays. 5 min of irradiation resulted in a 88% yield of the hydroperoxide intermediate, which was on the spot converted by Hock cleavage and oxidation via a second flow synthesis. Artemisinin was achieved in 64% yield, with almost as good performance as for the above-reported flow synthesis with pure reactants and synthetic catalysts, 69% yield.

Photopolymerizations are relevant for making macromolecules, and photo flow chemistry can aid in precision polymer design. Continuous-flow chemistry uses photocaged dienes as a supramolecular matrix for monodisperse macromolecular synthesis. Sequence-defined linear chains with eight repeating units were achieved using protecting groups and a two-stage flow process [199]; see Fig. 7. Photo flow synthesis was also used for reversible deactivation radical polymerization [200].

The hydrodechlorination of chlorophenols in wastewater was facilitated in flow mode. A palladium/carbon nanotube-nickel foam catalyst released hydrogen from formic acid. The catalytic could be recovered [201].

Scale-up to production scale and commercial supply. Numbering-up, a common microreactor scale-up concept, has been demonstrated for the scale-up of gas-liquid photocatalytic reactions, using only commercially available components for the flow chemistry setup. The flow distribution displayed a standard deviation of less than 5% [202].

Continuous-flow photo equipment is commercially available; suppliers are Vapourtec Ltd., FutureChemistry Holding BV, Creaflow, Peschl Ultra-violetGmbH, and Corning Inc. Kilogram scale flow reactors have been reported [203].

Emerging trend – Photobiocatalysis. The visible-light photochemistry and biocatalysis symbiosis allow synthesis under mild conditions [204,205]. Applications on co-factors regeneration were reported together with new challenges such as photoenzymes, tandem and concurrent photobiocatalysis [206].

(b) Opportunities in electrochemical flow catalysis. Electrochemical microreactors combine thin-layer cell technology and microstructuring techniques. Unique is to tune synthetic redox chemistry, with electrons as traceless reagents. This circumvents using hazardous and toxic agents as an environmentally friendly solution. Sustainable electricity, from solar and wind energy, is utilized. This offers an opportunity to produce chemicals locally and diminish hazardous chemicals' transport and storage.

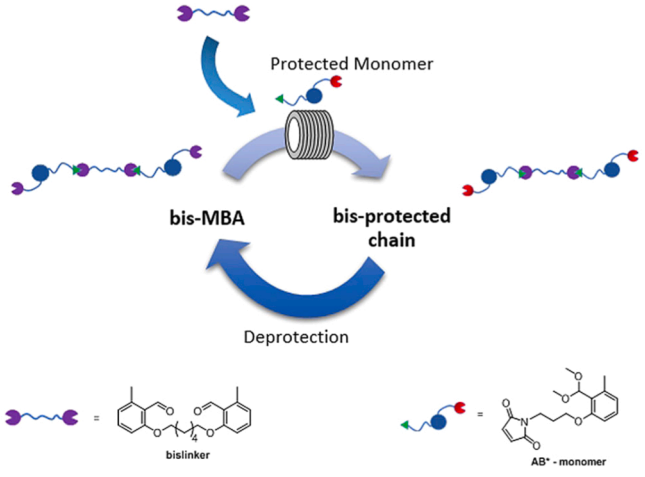

Fig. 7. Two-step sequential process to grow linearmacromolecular chains in a sequence-defined fashion.
Reproduced with permission from [199]. Copyright Wiley-VCH, 2019.

Typically, an electrochemical microreactor is assembled in a miniaturized plate-to-plate electrode configuration with parallel microchannels [207]. Mass and heat transport engineering determine the performance of electrochemical flow reactors and need re-investigation and require speciality reactor design [208], leading to novel reactor solutions, such as a coaxial travelling microwave multichannel reactor [209]. A more extendible and versatile electrochemical design comprises layered independent cell modules. An electrochemical multi-cell reactor with 75 parallel microchannels was operated using divided or combined microcells in bipolar or monopolar mode [210]. Combined electro-organic synthesis/simulated moving-bed (SMB)-purification was tested for the multi-cell microreactors.

Process intensification and simplification. Electrochemical flow chemistry allows high conversion at room temperature, e.g. a nearly quantitative conversion of 4-methoxytoluene to 4-methoxybenzaldehyde at a selectivity of 98% [207]. A crucial advantage is to reduce the concentration of conducting salt, essentially down to zero [211].

Electrochemistry is a powerful method for generating reactive intermediates, such as organic cations [212]. Those highly active intermediates can be instantly contacted with a stable molecule for reaction (in situ method) or, without a reaction partner, produced stand-alone for accumulation, a "pool"; see Fig. 8. A reaction with another molecule follows the latter case. The first case is chosen when the active species are short-lived. Microreactors, with their short mixing and fluid transfer times, are ideal for handling transient species, with more flexibility towards the instantaneous and pool modes.

Essential for scale-up is integrating small interelectrode gaps in the productive electrochemical systems at pilot and industrial scales [213].

(c) Opportunities in microwave flow catalysis. Microwaves allow catalyst heating with control over the temperature rise, avoiding hot spots and settling precisely elevated temperature, as demonstrated for palladium-loaded polymer/carrier composites in a catalytic microreactor [214]. This leads to process intensification to accelerate the catalytic reaction rate. Vice versa, microwaves improve the catalyst. Thin catalyst films provide uniformity of microwave absorption in the microchannels [215]. Microprocessing in continuous-flow reactors overcomes the limits of microwave penetration depth [216].

Microwave modes and catalyst variation. Selective catalyst heating for improved catalytic activity was made by microwave-assisted flow synthesis of the Ullmann etherification of phenol and 4-chloropyridine, using copper as catalyst [217] and single or multimode microwave heating; see Fig. 9. The surface of the copper nanocatalyst plays a crucial role in process simplicity, allowing stable chloropyridine salts and unactivated phenol [218]. Cu/ZnO wall-coated and Cu/TiO_2 fixed-bed flow reactors showed higher yields than a batch reactor operated with microwave es. Multimode microwave heating in continuous flow exceeded the performance of copper catalysts in conventional reactors. $CuZn/TiO_2$ catalyst shows a twofold yield increase over the Cu/TiO_2 catalyst due to the activation of the zinc by oxidation. A comparison of single- and multimode microwaves exhibited a threefold yield increase for single-mode microwaves. A proper definition of the nanocatalyst can prevent high thermal overshooting. Catalyst deactivation and leaching were observed at longer process times.

Superheated processing. Metal film-coated capillary microreactors under microwave heating allow for achieving temperatures much above the solvent temperature, which accelerates chemical reactions [219]. Superheated microwave processing was demonstrated for continuous S (N)Ar reaction flow. Diaryl ethers were generated at 195 °C and 25 bar, at a reaction time of 60 s, much faster than a stopped-flow microwave

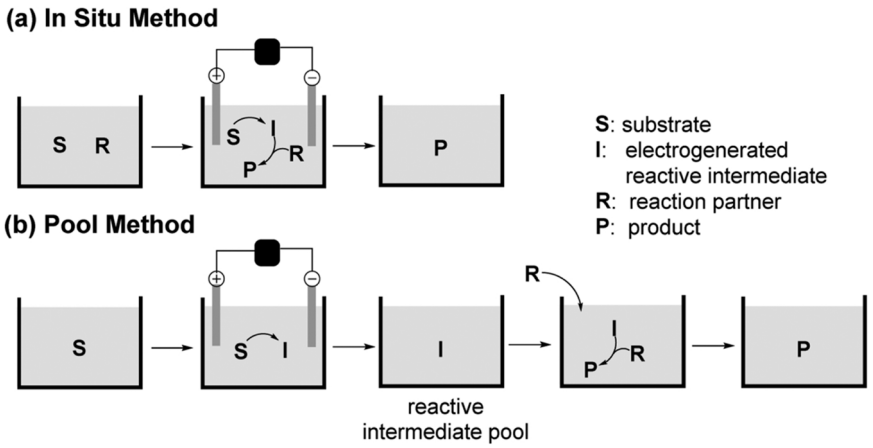

Fig. 8. In Situ Method and Pool Method for the electrochemical generation of reactive intermediates.
Reproduced with permission from [212].Copyright ACS, 2018.

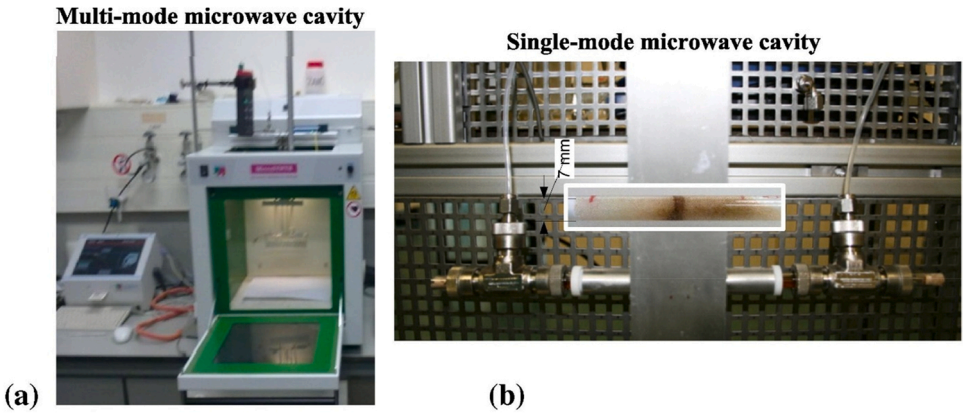

Fig. 9. Two types of microwave activation for flow-chemistry. (a) coiled fixed-bed reactor in a multi-mode microwave system; (b) tubular fixed-bed reactor in a single-mode microwave system.
Reproduced with permission from [217]. Copyright Elsevier, 2012.

reactor, needing tens of minutes [216].

The continuous-flow aqueous Kolbe−Schmitt synthesis of 2,4-dihydroxybenzoic acid from resorcinol was conducted under superheated conditions in a microcapillary reactor-heat exchanger operated with microwave energy [220]. The best yield of the microwave flow experiments was higher than conventionally heated synthesis, 52% at 90 s and 47% at 390 s, respectively, at reduced reaction time. The microwave flow productivity was up to 67 g/h, in the same range as the productivity of the conventional approach from 25 g/h (39%, 43 s) to 86 g/h (34%, 11 s). Using a CO_2-donating ionic liquid, ethyl methyl imidazolium hydrogen carbonate, instead of the conventional agent sodium hydrogen carbonate, raised the yield to 58% at a productivity of 25 g/h.

Scale-up and commercial manufacturing. Microwave operation can utilise the large reactivity of flow catalysis to reach the productivity of speciality chemical synthesis of 1 kg/day, as demonstrated for 1,3-diphenyl-2-propynyl piperidine, when reacting piperidine, benzaldehyde, and phenylacetylene [220]. A yield of 93% and a production rate of 333 kg product/(kg catalyst x·hour) was achieved at 373 K and a 6 ML/hour flow rate. 350 nm Cu films were coated on the channels of a counter-current multitubular millireactor/heat exchanger that allowed near-isothermal operation.

(d) Opportunities in ultrasound flow activation. Ultrasound processing overcomes the limits of microreactors in processing solids, particularly when formed under reaction conditions or for crystallization. The dimensions of the so-called "acoustophoretic microreactors" [221] match well with the size of the bubbles, and other characteristic phenomena, affected by ultrasound [222]; see Fig. 10.

The average particle size and the particle size distribution of precipitated products are reduced. Acoustophoretic processing, besides process intensification, can reduce fouling on the channel walls and clogging. The mechanism proceeds via cavitation bubbles for intense, vigorous translational motion, surface oscillation, and transient collapse. The energy efficiency of this intensified mixing is comparable to other microreactors. Residence time distribution is improved by axial dispersion [223]. Ultrasonic flow chemistry is effective beyond particle-generating processes (e.g. calcium carbonate and barium sulfate) and can promote biological, pharmaceutical and chemical processes. In particular, ultrasound can enhance multiphase chemical processing by enhanced mass transfer from liquid to catalyst [222].

The challenge is positioning the standing wave to the microchannel centre; a layered resonator has been proposed [224].

4. Modulation of the catalytic performances by application of an electrical field

4.1. Background

The effect of an electrical field on catalytic behaviour has been shown in some publications, although limited, over the last few years. They showed that some supported catalysts enhance their catalytic activity in some reactions, mainly those involving hydrogen-containing reactants, by applying a DC electric field to generate a current and a

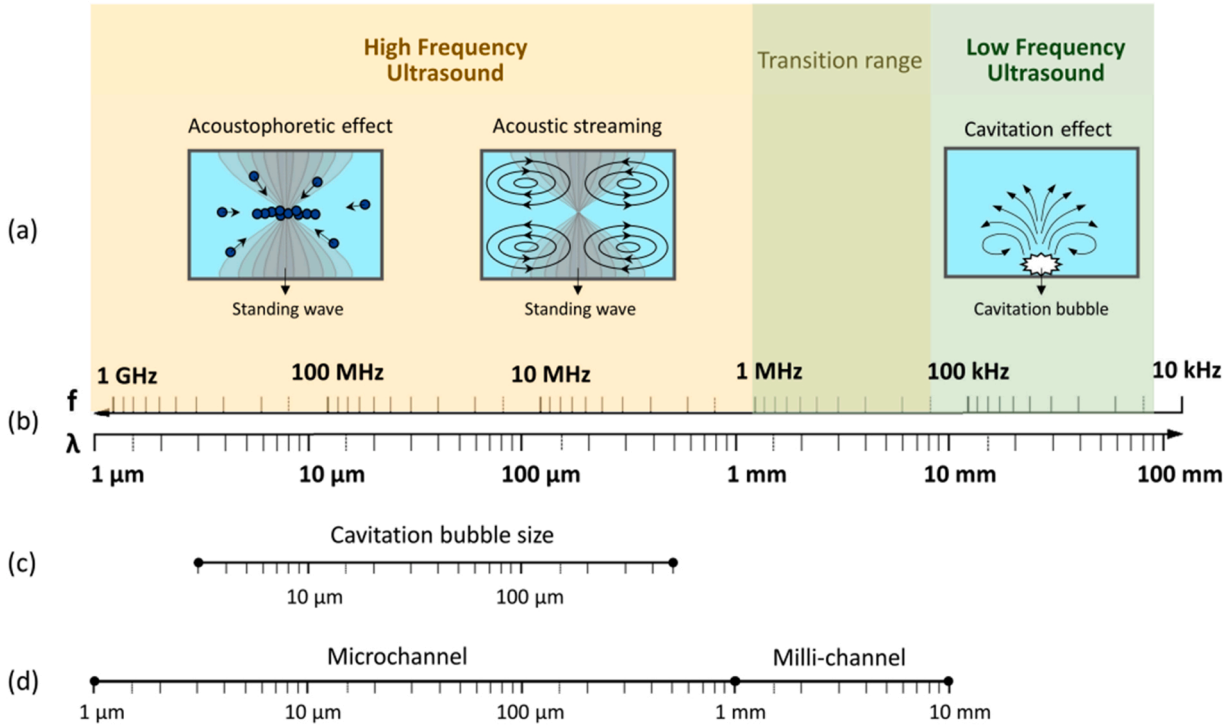

Fig. 10. Ultrasonic small scale flow reactors. (a) phenomena induced by high and low frequency ultrasound; (b) ultrasonic frequency (*f*) and wavelength (λ) in water; (c) cavitation bubble resonance size; (d) Match to the typical size of micro and milli-reactor channels.
Reproduced with permission from [222]. Copyright MDPI, 2020.

surface charge over a bed/layer. This effect was attributed to surface protonic conductivity on the porous ceramic support with a relatively high bandgap (semiconductors), high surface protonic conductivity and negligible bulk electrical conductivity (such as ZrO_2, CeO_2, $SrZrO_3$) [225].

Active metals are loaded on the support for preparing active catalysts, usually by an impregnation method. Various computational models describe the interaction between the protonic current, the metal catalyst nanoparticle and adsorbed reactants (such as NH_3 and CH_4). Several studies also demonstrated experimental evidence for the effect of a strong electric field and surface charge.

We mainly focus on non-equilibrium electrocatalytic processes. They include non-faradaic electrochemical modification of catalytic activity (NEMCA), plasmas, and electrical discharge reactions. This section is well complementary with that presented in the following section. NEMCA requires rather high reaction temperatures to promote the oxygen anion migration in the oxide support by applying an electric field. Plasma-assisted catalytic reactions require a rather high electrical energy input, and it is not easy to maintain high catalyst stability in plasma. Compared to these processes, the external electric field may be applied, increasing yields and selectivity of various chemical reactions at rather low temperatures. The effect originates from the proton migration on the support surface and their interaction with N_2, CO_2, and CH_4 at the metal-support interface [226]. It was also found that the apparent activation energy of the reaction is significantly reduced.

Physical principles of electric fields found in biocatalysis can be extended to non-biological systems. Biocatalysts operate at rather low temperatures, and their electrostatic fields can enhance their catalytic activity. The natural enzyme ketosteroid isomerase (KSI) catalyzes the isomerization of a wide variety of steroids to their conjugated isomers and exhibits a Michaelis–Menten catalytic efficiency. This makes KSI an ideal test system to quantify the effect of the electric field. The relative importance of the chemical positioning of the substrate in the active site of KSI to electrostatic preorganization was measured by vibrational Stark spectroscopy [227]. It was shown that the KSI environment created a strong electric field of 144 MV cm^{-1} in the enzyme's active site. Using the assumption that the electric field in the active site of KSI was the same in the reactant and the transition state, the authors estimated that electrostatic interactions contributed 30 kJ mol^{-1} to the reduction of KSI's activation energy.

The enclosing microstructure of the reactive site within a porous structure can alter the reactivity of guest molecules. These structures mimic the active site of enzymes and protect the guest substrate from undesired reactions in solution. Although structurally, they are very different from enzymes, the same interplay between electric fields and nanopore structure applies to zeolite catalysts [228]. Electrostatic interactions were observed to have a more significant impact than dispersive interactions on the geometries of ion-pair transition states and adsorbed species. The electric field stabilizes the transition state relative to the reactant species.

4.2. State of the art

A conventional fixed-bed flow structure consists of a reactor in a furnace and two electrodes made of Au plates or other materials for applying an electric field of about 10^7 V•cm^{-1} on the catalyst. A small current (a few mA) is applied to the catalyst bed while the voltage is maintained at 100–800 V. The catalyst layer acts as a solid electrolyte in fuel cells. The current and voltage are measured with an oscilloscope. This electric field is higher than used in NEMCA (10^5 V•cm^{-1}) but considerably lower than in plasma (> 10^9 V•cm^{-1}) [229]. At the DC field, the current may induce Joule heating. However, the induced heat of an order of a few Watts was estimated to increase by 10–30 K in catalyst bed temperature, which can be corrected using the Arrhenius plot [230]. Joule heating comes from the proton transport on the support surface since this is the dominating conduction mechanism in the support. The protons are produced from dissociated water and/or hydrogen on the catalyst surface.

4.3. Challenges

Effect of high-curvature regions. One of the most studied examples is the electrocatalytic reduction of CO_2 (CO_2RR) on metal surfaces to renewable fuels or for energy storage [231]. Field effects on adsorption energies were extensively studied in the literature to explain alkali promotion in heterogeneous catalysis [232] and as a basis for understanding surface electrochemistry. High-curvature regions have the potential to create an ideal microenvironment beneficial for the overall catalytic reaction, providing a basis for fundamentally new strategies to improve chemical activity. This way, nanostructured electrodes with high curvature at the tip produce high electric fields concentrating alkali cations near the interface [233]. This suggests that locally concentrating cations at reactive sites enhances CO_2 electroreduction.

Tip-enhanced field. Tip-enhanced field intensification at the nanometer-scale and related cation concentration was confirmed by finite-element modelling. In this study, cones with rounded tips were used to represent sharp electrode tips immersed in an electrolyte, with their tip-concentrated electron density (Fig. 11a). The locally enhanced electrostatic field was generated by the locally concentrated free electron density on the surface of the electrodes. It originated from the migration of free electrons to the regions of the sharpest curvature on a charged metallic electrode, a consequence of electrostatic repulsion. Tip sharpening from a radius of 140–5 nm enhanced electrostatic field intensity at the electrode tip by one order of magnitude (Fig. 11b). It was confirmed that CO_2RR mainly occurs at the electrode tips (Fig. 11c), with the reduction current increasing by two orders of magnitude compared to the flat electrode.

However, without alkali cations, the current density and selectivity decreased substantially. The tip-enhanced field phenomenon can be extended to other reactions to concentrate the reagents locally in a broader electrochemistry context. This suggests a novel principle for the design of efficient electrodes for electrocatalysis.

Combination of electrical and thermal fields. Like the electric field, the thermal field can promote the reaction rate by facilitating kinetics [234]. Therefore, introducing a combination of electric and thermal fields effectively improves the selectivity and reaction rate. This approach was studied in CO_2RR over a Cu nanoneedle catalyst [235]. A 5 nm polytetrafluoroethylene (PTFE) coating enhanced the electric field by seven times at the tips of nanoneedles and improved the coverage with CO intermediates. This, in turn, facilitated C–C coupling compared with bare copper nanoneedles. The reaction was performed in a conventional cell with a CO_2-saturated 0.1 M $KHCO_3$ electrolyte (pH 6.8) under a potential of − 1.5 V vs RHE. A very high TOF of 11.5 s^{-1} was reported. The catalyst had high stability in the flow cell with a total current density of 300 mA•cm^{-2} for over 25 h.

DFT calculations confirmed that the activation energy of *CO dimerization decreased with the electric field increasing, suggesting that the electric field is favourable for C_2 formation. Infrared imaging showed that the temperature on a Cu needle electrode was much higher near the tip, indicating that the sharp tip can produce a local thermal field due to electron collision. These results demonstrated that the electric–thermal field at the tip could be improved by tuning the PTFE coverage. The nanoneedle showed a 4-fold higher temperature increment than a planar Cu NP. Increasing the electrolyte temperature also increased the CO_2RR rate but shifted the selectivity towards methane and hydrogen formation.

4.4. How to overcome the challenges and create new opportunities

The strategy of tuning the local electric–thermal field on the catalyst surface was generalized to promote other electrocatalytic and plasma chemical reactions. In this way, the Ag nanoneedle array structure induced a strong electric field at the tips, which reduced the activation barrier for CO_2RR [236]. The high-curvature catalyst exhibited a local electric field strength of 5.92•10^7 V•m^{-1}, which is 3.7 times higher than the low-curvature sample (1.57•10^7 V•m^{-1}). DFT calculations confirmed that the strong local electric field on the surface of Ag reduced the thermodynamic reaction energy barrier of the CO_2 reduction reaction and increased the energy barrier of hydrogen evolution reactions (HER). The high-curvature Ag nanoneedle surface explained the latter demonstrated hydrophobic properties during the electrocatalytic process. The CO_2 reduction rate was higher in the ordered Cu nanoneedles arrays than in disordered randomly arranged Cu nanoneedles [237]. The periodic array exhibited a stronger tip local electric field than the randomly distributed nanoneedles. The stronger electric field leads to localized K^+ accumulation, which results in stronger *CO adsorption, thus reducing the C–C coupling energy barrier.

Periodic nanoneedles. It was reported that periodic nanoneedles also improved the chlorine evolution reaction (CER) rate over a Ti/RuO_2

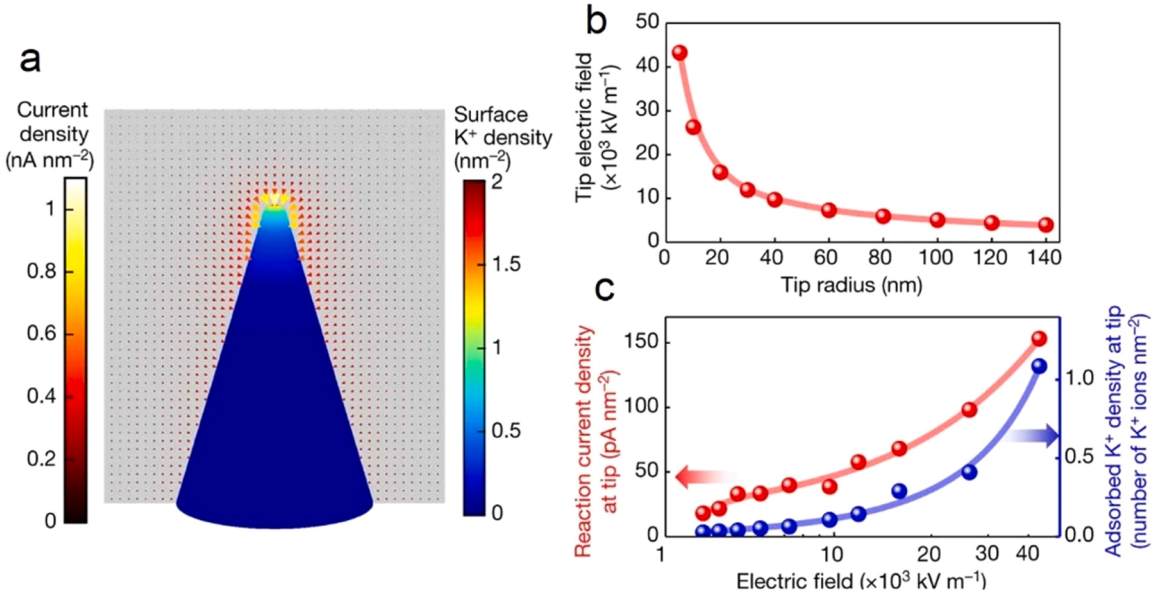

Fig. 11. (a) Electrostatic field intensity at the electrode tip increases as the tip radius decreases, (b) adsorbed K^+ and reaction current density as functions of the electric field intensity at the tip (c) surface K^+ density and current density distributions on the surface of Au needles. The tip radius is 5 nm. Reproduced from [233] with permission. Copyright Springer, 2016.

catalyst. The Cl^- consumption rate was 1.3 times higher than that of the flat electrode [238]. This work constructed a combined optical imaging and electrochemical reaction setup to experimentally demonstrate electrochemical reaction enhancement near the electrode's tip region. The preparation of electrodes with a well-controlled morphology was composed of steps of electrochemical anodization of Ti foil, magnetron sputtering of nanosized Ru, followed by calcination of the electrode under an air atmosphere [239]. The submicrometric resolved fluorescence microscopy images enabled to quantitative monitor the transport of Cl^- ions from the bulk of the solution to the Ti/RuO_2 electrode surface under working conditions.

Microstructured DBD. A similar enhancement in the reaction rate was observed in a microstructured dielectric barrier discharge (DBD) reactor operated in the pulse mode [240]. The plasma was formed between two electrodes (Fig. 12). The top electrode has a dielectric layer of 0.5 mm, while the bottom electrode is engraved to a periodic cone-shaped sharp array, and the cone tips were positioned at a distance of 0.5 mm from the top electrode. The cones formed a 2D periodic array with a pitch of 1.0 mm between the centres of two adjacent cones. A 40 ns pulse of − 1.6 kV was added to a DC bias of 400 V with a repetition rate of 10 kHz. In this reactor, the intensity of the electric field and the electron temperature were the highest in the cone tip region.

In contrast, the densities of electrons and ions get their maximum value near the dielectric layer surface. The location of the maximum electron density is positioned further away from the dielectric layer due to surface charge accumulation on the dielectric layer surface. The conversion of methane to ethylene strongly depended on the input pulse shape [241]. The electrons responded very quickly to voltage change, while heavy species like ions needed more time to update themself with the new electric field. A slight pulse duration increase increased neutral species' production rate.

Under optimised conditions, the selectivity towards C_2H_4 was 1.4 times higher than that of C_2H_6. This demonstrates the control of the reaction pathways of plasma methane, and thus the selectivity, by tailoring the pulse shape.

Microkinetic modelling. To better understand the role of surface chemistry in product yield distribution, a microkinetic surface model was developed for the non-oxidative coupling of methane over a Cu catalytic film [242]. In the presence of a catalyst, acetylene was the main product with a selectivity of 49% at a methane conversion of 47% with a discharge power of 70 W. Increase in power increased the methane conversion in agreement with other plasma studies in non-oxidative and dry reforming of methane [243].

The electric field brought a difference in the reaction pathway and facilitated methylcyclohexane dehydrogenation even at low temperatures over a 3 wt% Pt/TiO_2 catalyst. The DC field creates a 5 mA DC over the catalyst. At a temperature of 448 K, the conversion was increased from 3% to 37%, much higher than the equilibrium level (12%). The result was explained by irreversible pathways due to surface protons, as described elsewhere in the literature [244,245]. Hopping protons over an electric-field-imposed catalyst layer plays an important role, and hydrogen can be obtained even at low temperatures by proton hopping [244]. The apparent activation energy was 22.8 $kJ•mol^{-1}$ in the electric field and 47.9 $kJ•mol^{-1}$ without it. The conversion decreased after the pre-reduction treatment due to the change of oxygen stoichiometry by the pre-reduction. At the same time, the electron bulk conductivity was improved comparing the proton surface conductivity.

In reaction under an electric field, the value is calculated based on the number of metal atoms on the periphery of the metal particles (TOF-p). In conventional catalysis, the TOF is divided by the number of surface sites of the nanoparticles (TOF-s). It was shown that TOF divided by the perimeter area (TOF-p) takes a constant value in reactions with the addition of an electric field, confirming that the active, reactive centres are located at the metal-support interface around the metal nanoparticle [246].

(a) Opportunities for NH_3 synthesis. Applying an electric field on heterogeneous catalysts enhanced the rate of ammonia synthesis from nitrogen and hydrogen [247]. Manabe et al. [247] demonstrated a novel process using an electric field with high ammonia synthesis rates at low temperatures. This process had a higher energy efficiency than the plasma-based processes. With electric field and current enhancement, a reaction rate of 30 mmol $gcat^{-1}•h^{-1}$ was observed over a $Ru/SrZrO_3$ catalyst at a pressure of 0.9 MPa at a temperature of 453 K. Application of the electric field resulted in a drastic decrease in the apparent activation energy from 121 to 37 $kJ•mol^{-1}$. In-situ IR measurements and theoretical calculations revealed that N_2 dissociation is strongly promoted by proton hopping over the catalyst in the strong electric field.

It was shown that the N_2 dissociation proceeds through N_2H as an intermediate in the electric field, which is different from the conventional activation route via dissociative mechanism over Ru-supported catalysts [248]. By contrast, in the associative mechanism, the N_2 cleavage is determined by the potential energy of the adsorbed N_2H or NH. Therefore, the catalytic activity depends on different factors from conventional heterogeneous catalysts. The rate did not exhibit the volcano-shaped relation by applying the electric field, and the N_2H formation energy determined it at the metal-support interface. Fe- and Ni-supported catalysts under an electric field showed higher TOF than Ru catalysts.

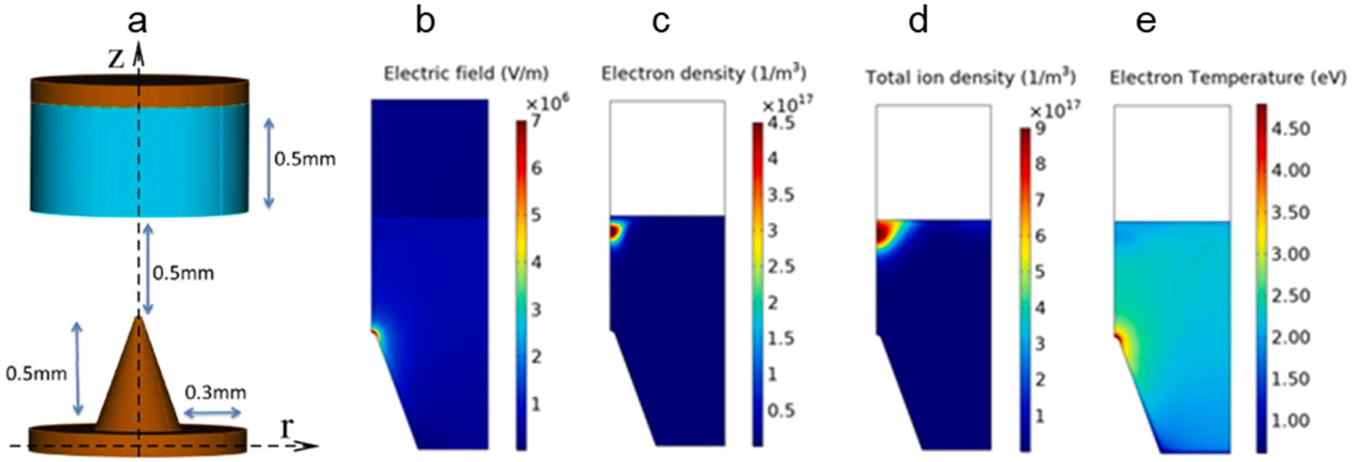

Fig. 12. (a) 3D unit cell of the reactor, electrostatic field intensity and the spatial distributions for (b) electric field, (c) time-averaged electron density, (d) total ion density, (e) electron temperature.
Reproduced from [240] with permission. Copyright AIP, 2021.

Electride. Low work-function materials (electrides) were indicated to replace alkali metal dopants in conventional K-doped iron catalysts [249]. An electride is an ionic compound composed of cations and electrons instead of anions, and it was first synthesized as Cs^+(18-crown-6)$2e^-$ where Cs^+ cations were sandwiched between crown ethers and electrons [250]. $C_{12}A_7$:e^- is a stable solid electride with strong electron-donating capability derived from $12CaO{\cdot}7Al_2O_3$. The unit cell of $C_{12}A_7$:O^{2-} is expressed as $[Ca_{24}Al_{28}O_{64}]^{4+}(O^{2-})_2$, where O^{2-} anions are accommodated in nanocages composed of Ca, Al and O. Ammonia synthesis over Ru nanoparticles-loaded $C_{12}A_7$:e– (Ru/$C_{12}A_7$:O^{2-}) is a distinct catalyst from other conventional catalysts in both mechanism and properties.

Ru/$C_{12}A_7$:e^- exhibits a reaction order of + 1 to H_2, which indicates that this catalyst is not subject to hydrogen poisoning. Hydrogen surface atoms on Ru readily spill over onto the $C_{12}A_7$:O^{2-} support and are incorporated into the positively charged nanocages as H^- ions by the reaction of $H + e^- \rightarrow H^-$, which prevents hydrogen adatoms from occupying the metal surface, which is the main problem over conventional catalysts. When H atoms are released from the cages, the electrons remain in the cages through the reaction: $H^- \rightarrow H + e^-$ [251].

The exceptional nature of the $C_{12}A7$:e^- support comes from the reversible exchange between an electron with a low work function and a hydride at the interface region of Ru. A few percent of the cage electrons were observed to be replaced with H^- ions at the early stage of the reaction (<20 h). This exchange level remained constant after long reaction times.

Alternatively, it was shown that nitrides containing surface nitrogen vacancies could activate N_2 molecules [252]. It was reported that much cheaper Ni-loaded lanthanum nitride (Ni/LaN) enables stable and highly efficient ammonia synthesis [253]. Other nitrides, such as cobalt molybdenum nitrides (Co_3Mo_3N), were also studied. In these catalysts, nitrogen-vacancy (V_N) sites surrounded by Mo are effective for the N_2 adsorption and activation through a Mars–van Krevelen mechanism to produce NH_3.

(b) Opportunities for steam and dry reforming of CH_4. 1 wt% Pd/CeO_2 catalyst promotes steam reforming of methane (SRM) in a DC electric field at 473 K [254]. The process was referred to as electroreforming (ER). Kinetic analysis demonstrated the synergetic effect between the catalyst and electric field, demonstrating a strong water pressure dependence on the reaction rate under the electric field. When an electric field was applied, the methane reaction order decreased from 0.9 to 0.25, and the water reaction order increased from 0.1 to 0.79. The apparent activation energy was significantly reduced from 54.4 to 14.3 kJ mol^{-1} under an electric field. ER proceeds through a different reaction pathway from steam reforming at temperatures below 623 K. DRIFTS measurements confirmed proton conduction via adsorbed water on the catalyst surface under an electric field.

SRM in an electric field proceeds at a relatively low temperature of 423 K. The conventional thermal reaction requires a much higher temperature to achieve the same reaction rate over Ni, Pt, Pd, and Rd catalysts supported on semiconductor oxides such as CeO_2 or $Ce_xZr_{1-x}O_2$ [255].

Fig. 13 compares activity and Arrhenius plots in SRM without an external electric field (SR) and in an electric field (ER). It can be seen that CH_4 conversion increased significantly with an electric field, especially at lower temperatures. In addition, CH_4 conversion at lower temperatures in the electric field exceeded thermodynamic equilibrium. That result indicates that the reaction mechanism in ER includes some irreversible steps [35].

A similar trend was observed in DRM over a 1 wt% Ni/10 mol% La–ZrO_2 catalyst at 473 K under an electric field. The apparent activation energy for CO_2 decreased from 62.3 to 12.1 kJ mol^{-1}, while that for CH4 decreased from 66.1 to 8.2 kJ mol^{-1} [246]. This indicates that DRM under the electric field proceeded via a different reaction mechanism from that observed in a conventional catalytic reaction. Due to surface adsorbed species such as H_2O and OH^- groups, the enhanced electrical conductivity was responsible for low temperatures' enhanced reaction rate [256]. The surface proton conduction was confirmed by the rotation of adsorbed water at 850 cm^{-1} in DRIFT spectra at 573 K under an electric field. Protons move through the rotating surface of adsorbed water with a weak electric current in this mechanism. They thus accelerate the surface catalytic reaction. Thus, surface protons efficiently promote SRM and DRM at low temperatures by applying the DC electric field.

(c) Opportunities for water gas shift reaction. The CO conversion over a Pt/La-ZrO_2 catalyst increased from 0% to 47.1% under DC electric field (3 mA, 2.9 W) at 423 K [255]. The apparent activation energy reduced from 98.3 to 50.9 kJ·mol^{-1} under an external electric field. At the same time, the reaction order in CO changed from − 0.28–0.33 and that of H_2O from 0.49 to 0.57. These changes in reactant reaction orders

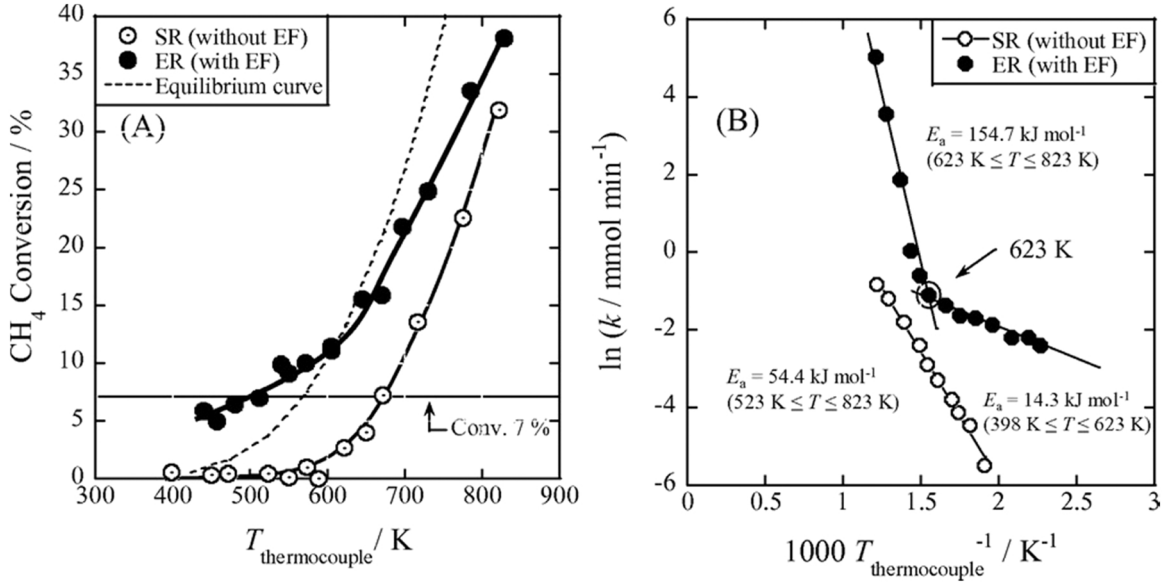

Fig. 13. Comparison of (a) activity and (b) Arrhenius plots between catalytic steam reforming of methane by heat (SR) and by an electric field (ER) over a 1.0 wt% Pd/CeO_2. catalyst. Concentrations: CH_4 12 vol%, H_2O = 24 vol%, Ar = 12 vol%, He -balance. Current: 0 or 5 mA.
Reproduced from [254] with permission. Copyright Springer, 2016.

indicate that the electric field accelerates the reaction at low temperatures. The primary isotope effect was confirmed, with the same r_D/r_H ratio of 0.317 in the presence and absence of an electric field. It was concluded that H_2O is activated on the support rather than the Pt metal and that O–H dissociation is not the rate-determining step in both cases. A surface redox mechanism using surface-lattice oxygen and H_2O (Mars–van Krevelen) was proposed to describe the transient and steady-state kinetic data under an electric field.

The frequency factor was negligible in all cases considered above because the apparent activation energy was significantly reduced under an electric field. The reaction mechanism changed from a reaction on the metal surface to a reaction at the metal and substrate interface. There were three common features under the electric field: (i) surface species showed proton hopping on the catalyst support, (ii) surface protons with high kinetic energy collided with reactants and accelerated the rate-determining step, and (iii) surface ionic conduction occurred on the catalyst support at lower temperatures.

Explaining the irreversibility requires further studies focused on the "dynamics" of the processes, such as based on ab initio molecular dynamics simulations. They will provide valuable insights into the collision frequency of protons. They will allow determining the fraction of the kinetic energy used to form an intermediate in the transition state. It is also essential to design new catalysts that can improve the efficiency of this step.

(d) Electrochemical promotion of catalysis (EPOC): Effect of surface charge. The EPOC effect (also called NEMCA) was used to promote the catalytic properties of catalytic coatings simultaneously acting as electrodes. They are deposited on solid electrolyte support. In this way, catalytic activity and/or selectivity of conductive catalysts deposited on solid electrolytes were altered in a very pronounced, reversible and, to some extent, predictably by applying electrical currents or potentials (typically up to ± 2 V) between the catalyst and a counter electrode deposited on solid electrolyte [257].

The supports used were either ionic conductors, such as yttria-stabilized-zirconia (YSZ, an O^{2-} conductor), Na-β″-Al_2O_3, (a Na^+ conductor) or K-β″-Al_2O_3, (a K^+ conductor) or mixed ionic-electronic conductors, such as titania or ceria. The EPOC effect originates due to an electrochemically controlled migration (backspillover) of promoting ionic species (e.g. O^{2-} in the case of YSZ) from the support to the gas-exposed catalyst surface through the catalyst/gas/electrolyte three-phase boundary. The catalyst potential (U_{WR}) is measured between the working and reference electrodes. The applied current flows between the catalyst and a counter electrode. Then the promotional rules were reported in [258].

$$\left(\frac{\partial r}{\partial U_{WR}}\right)\left(\frac{\partial r}{\partial p_D}\right) >; \left(\frac{\partial r}{\partial U_{WR}}\right)\left(\frac{\partial r}{\partial p_A}\right) < 0$$

where p_D and p_A stand for the electron donor and electron acceptor reactant. The adsorption of an electron donor/acceptor causes a decrease/increase in work function and, thus, the potential U_{WR}.

The electrochemical promotion of CO_2 hydrogenation to CH_4 and CO was compared for Ru catalyst films deposited on Na^+, K^+, H^+ and O^{2-} conducting solid electrolyte supports [259]. Positive potential enhanced the selectivity of CH_4 on all supports studied. Over K^+-promoted supports, CH_4 selectivity varied in the range of 0–98%, depending on the applied catalyst potential.

The performance of protonic ceramic electrolysis cells (PCEC, Fig. 14) cell stacks were evaluated in electro- and thermochemical routes to demonstrate the EPOC effect [260]. The gap between the fuel electrode and the endplate was 2.5 mm. The current collection was achieved via silver wires and paste. During electrochemical CO_2/H_2O co-conversion, the air electrode was supplied with synthetic air containing 20 vol% steam, and the fuel electrode was fed with a mixture of 4 vol% CO_2 in N_2. Peak power densities were reported to be 0.22, 0.15, 0.10 and 0.05 W cm^{-2} at 550, 500, 450 and 400 °C, respectively.

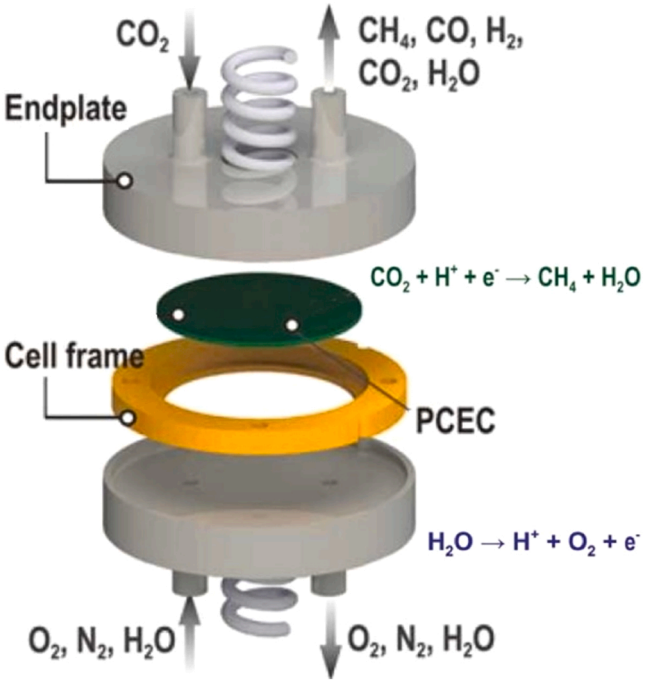

Fig. 14. Unit-cell stack assembly of the PCEC. The cell is bonded into a ceramic frame and sandwiched by two ferritic-steel endplates.
Reproduced from [260] with permission. Copyright Elsevier, 2022.

Electrochemical synthesis resulted in higher overall CH_4 yields than chemical synthesis at temperatures above 450 °C due to the electrochemical formation of hydrogen [261]. This increased methane yield, demonstrating a possible EPOC effect using the protonic ceramic electrolysis cell.

5. Nanoscale electrical fields induced by plasmonic catalysis

5.1. Background

TiO_2 has robustness, non-toxicity and efficiency characteristics, making it still the most used photocatalytic material [262–264]. The severe limit is the activity only with ultraviolet light. Many studies have been made either in modifying TiO_2 by different mechanisms (doping, band gap engineering, formation of heterojunctions, nanocomposites with other semiconductors, etc.) to increase visible-light activity [265–269] or developing alternative semiconductors with a wider band gap [270–273]. Still, progress has been limited in achieving high-performance and robust alternative photocatalytic materials. Therefore, significant interest has been given to enhancing the visible light absorption of TiO_a by plasmonic effect [274–277].

5.2. State of the art

Surface plasmons are collective coherent (in phase) oscillations of delocalised electrons in a metal particle excited by the electromagnetic field of incident light at a metal-dielectric interface. The effect relates to an ordered array of metal nanoparticles (NPs) on a dielectric material such as TiO_2. However, the plasmonic resonances occur in the visible region with few types of metal NPs such as Au, Ag and Cu. Note that the absorption band is unrelated to a direct charge separation as occurs for frequencies above the band gap. The metal nanostructures serve as antennas to convert light to a localised electrical field. This effect enhances the local field by several orders of magnitude and depends strongly on the arrangement of the metal NPs, besides their shape and dimensions. Fig. 15 presents the concept of surface plasmon resonance (SPR), the

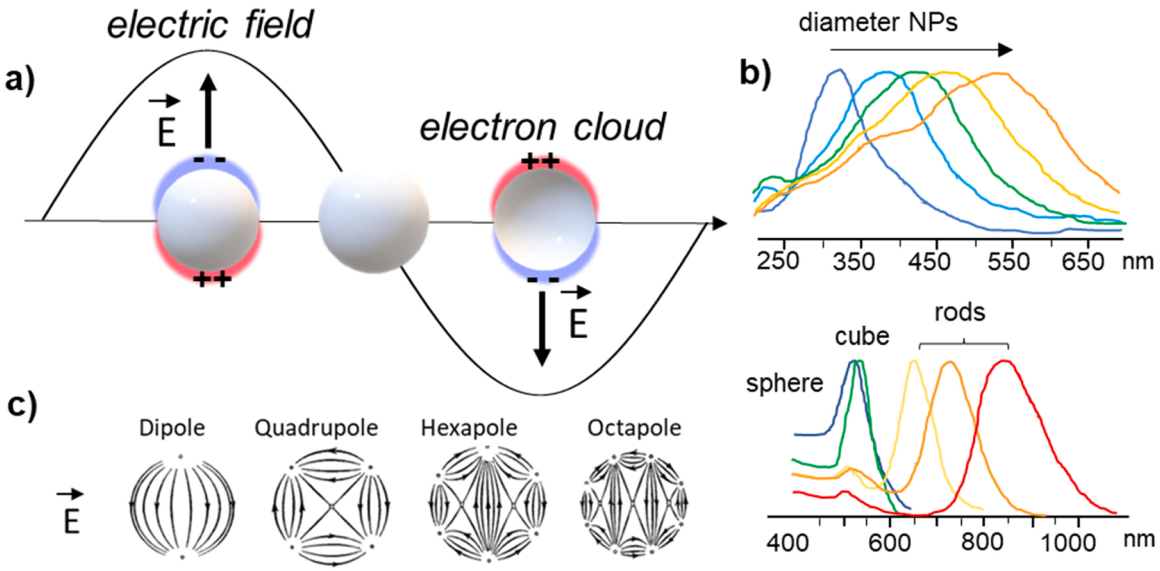

Fig. 15. (a) Concept of surface plasmon resonance, (b)the dependence of the absorption spectrum from metal NPs characteristics and (c) examples of how the local field depends on the arrangement of the metal NPs.

dependence of the absorption spectrum from metal nanoparticle characteristics and an indication of how the local field depends on the arrangement of the metal NPs. Note that the nanostructure of the dielectric material is typically not considered and analysed, but is expected to also play a relevant role based on the above indications.

Localised SPRs are created when the metal nanostructure is much smaller than the electron means free path and the wavelength of incoming light. The electron clouds in the conduction band of the metal oscillate collectively due to the electric fields induced by incident light. The relevance of this effect for the (photo)catalytic behaviour is related to the effects and paths associated with the resonant oscillation decays via non-radiative and radiative pathways. Two main decay mechanisms are present: (a) photothermal localised heating and (b) activation of molecules at the (photo)catalyst surface by resonant-generated charge carriers via direct and indirect pathways. After the local electric fields are generated around the NPs, energetic (hot) charge carriers are produced. These evolve by electron-electron scattering and electron-phonon scattering, the latter heating the catalyst NPs. The indirect transfer can occur if the excited electrons have enough energy to reach the adsorbate's unoccupied energy levels. An alternative mechanism consists of the excitation of charge carriers from the metal NP to the empty orbitals of the adsorbate.

Non-radiative damping (Landau damping) creates a non-thermal distribution of hot carriers. This distribution can scatter charge carriers of appropriate energy in the indirect pathway through the adsorbate states, generating a non-thermal vibrational excitation of a bond in the adsorbate. In the direct transfer pathway, a localised SPR-induced electron excitation from occupied to unoccupied orbitals of the metal–molecule or metal–adsorbate complex occurs. Localised SPR excited charge carriers can participate via vibrational or electronic activation of adsorbed molecules at the surface. The possibility of using this effect for coupling with vibrational-excited states of reactants created by non-thermal plasma, as discussed in the section on plasma-assisted catalysis, emerges. However, essentially no studies in this direction are present in the literature.

5.3. Challenges

The effect of plasmonic resonance is well studied, as indicated in selected reviews [8, 278–283] from a vast literature on the topic. Still, the great effort led to limited enhancement of the performances in TiO_2-based photocatalysts. However, great potential exists when turning the current approach. There are intrinsic mechanistic differences with those usually applied to promote (photo)catalysts, while indicating a link with the previous section on the modulation of the catalytic performances by applying an electrical field. The plasmonic effect could generate a strong electrical field at the catalyst surface. Still, the rational use for designing advanced catalysts of this and related effects associated with plasmonic resonance is limited. Mainly the plasmonic catalysis was associated with the hot carriers generated, and thus to photocatalysis. Instead, the strong generated local electrical field is the critical element, and its use is beyond photocatalysis.

Mechanisms of plasmonic-mediated activation. The mechanisms of plasmon-mediated bond activation occur through the photogeneration of an excited potential energy surface, on which the adsorbate moves to gain kinetic energy and react in the excited state. Otherwise, it decays to the ground-state potential energy surface in a vibrationally excited state lowering the barrier for dissociation. Vibrational-excited states in non-thermal plasma significantly modify the transformation paths, creating unexplored potential synergies. However, other possibilities are i) coupling with plasmons to generate specific energy transfer and ii) exploiting hot carriers directly in redox processes to overcome band gap limits. An overview of the different decay pathways after local SPR activation with an indication of the critical factors related to (photo)catalytic activation is presented in Fig. 16 [284].

Role of heterojunctions. Heterojunctions are generated in TiO_2-based plasmonic photocatalysts in addition to the plasmonic mechanisms described above. When plasmonic metal NPs such as Ag, Au, Cu, or alloys come in contact with the semiconductor (TiO_2), two types of heterojunctions are formed: (a) Schottky junction, where metal NPs possess a larger work function than that of the semiconductor, and (b) Ohmic junction, where metal NPs possess a smaller work function than semiconducting materials. These junctions determine the interfacial charge transfer between TiO_2 and the metal NPs, impacting the local electric field. It strongly depends on TiO_2 characteristics [285], thus demonstrating the previous comment on the impact of the titania substrate nanostructure, even if not systematically investigated. The enhancement in the local electric field is over 400 in comparing a TiO_2/Au/TiO_2 nanostructure prepared using a microorganism (Escherichia coli) as a template with a conventional Au/TiO_2 photocatalyst [285].

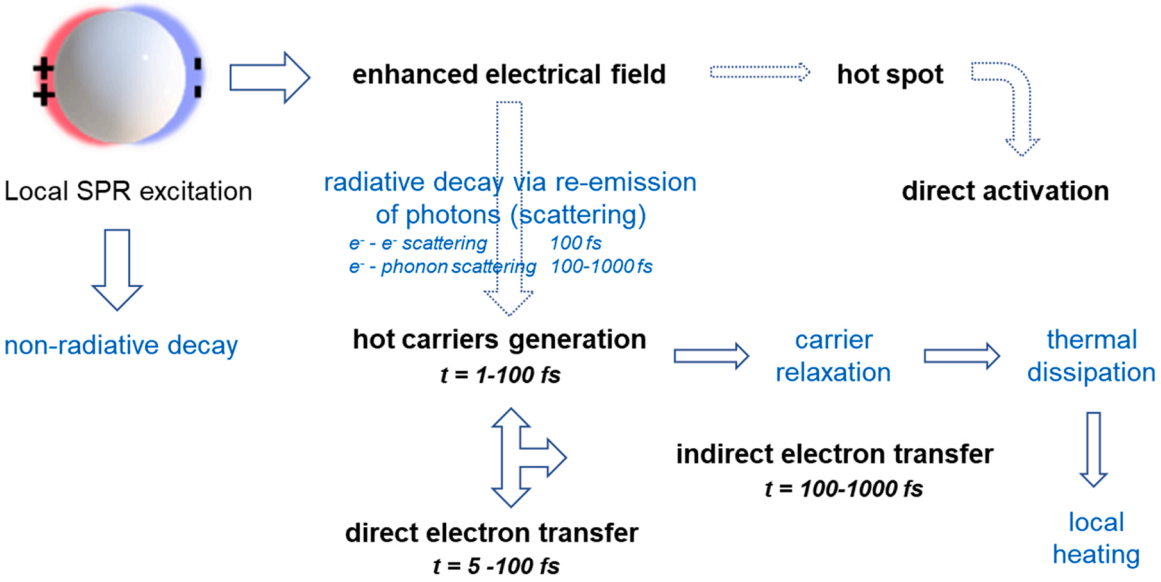

Fig. 16. Decay pathways after local SPR activation with an indication of the key factors related to (photo)catalytic activation and their characteristic time scale. Adapted with permission from Zhao et al. [284]. Copyright Elsevier, 2022.

Preparation of the plasmonic catalysts. Several different nanostructured TiO_2-based plasmonic photocatalysts have been prepared in the literature. Kumar et al. [274] reviewed them by lumping them into nine classes: (1) Janus plasmonic NPs and TiO_2 nanostructures; (2) TiO_2 capped plasmonic nanostars; (3) TiO_2 capped plasmonic nanorods; (4) plasmonic metal@TiO_2 yolk-shell systems; (5) plasmonic NPs decorated TiO_2 nanosheets; (6) core-shell plasmonic metal@TiO_2; (7) TiO_2 NPs nanoarrays decorated with plasmonic NPs; (8) TiO_2 NPs decorated with plasmonic NPs; and (9) plasmonic NPs decorated TiO_2 nanotubes. Thus, methods for precise control of the characteristics of both the TiO_2 support and metal NPs are available. Even if several of them were investigated as plasmon-mediated TiO_2-based photocatalysts, although often using sacrificial agents, their effective practical implementation and widespread use require a step forward in using the mechanistic understanding for a rational design, especially to investigate new potential areas and uses [274].

5.4. How to overcome the challenges and create new opportunities

We can identify a main limitation of the current approach in plasmonic catalysis, e.g., that it is mainly a way to increase the visible-light activity of photocatalysis. The essence of the plasmonic effect is to generate a very strong and localised electrical field at the catalyst's surface and interface with the fluid reactants. This electrical field modifies i) the catalyst surface itself, ii) the mobility and stability of the adsorbed species, iii) the energy of excited and transition states, and iv) the vibro-rotational modes or molecules in the fluid at the interface with the catalyst. Even if very limited studies exist on these aspects, and they are thus, in part, speculative, their possibility of control and tuning can significantly enhance the catalytic performances beyond photocatalysis.

Beyond photocatalysis. In electrocatalysis, a crucial factor determining the electron transfer rate is the solvation shell's rearrangement and solvent polarisation, which are drastically influenced by a strong localised electrical field. Depending on the strength of the electrical field, ionisation of the fluid may also occur. The strong electrical field around the particles depends on their nanostructure, which is also somewhat connected to the absorption in the visible region related to the plasmonic effect. Thus, strict relations exist between plasmonic absorption, catalyst NPs shape/size and local electrical field. This effect is visually presented in Fig. 17, reporting the results of Montaño-Priede and Pal [286] on near-electric field estimations of polyhedral gold

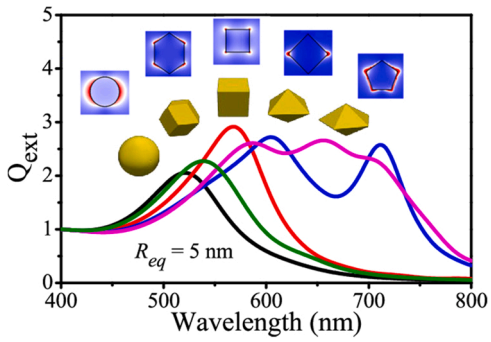

Fig. 17. Extinction efficiency factors of 5 nm gold nanoparticles of different shapes. At the top the calculated spatial distribution maps of a near electric field.
Adapted with permission from Montaño-Priede and Pal [286]. Copyright ACS, 2019.

nanoparticles. They showed that the octahedral NP presents the greater enhancement of the near electric field (40 times), followed by the cube (30 times), pentagonal bipyramid (20 times), the rhombic dodecahedron (15 times), and the sphere (6 times).

While these calculations refer to the plasmonic effect, they can be reasonably translated to charge accumulation associated with applying a potential, thus electrocatalysis. Surprisingly, little research has been performed in the literature on this crucial aspect and the interaction between the plasmonic effect and electrocatalysis. The literature on the size- and NPs morphology-dependence of the electrocatalytic performances is abundant, for example [287–292]. The interpretation of the effect was associated with the exposure of different facets or low-index planes, the creation of undercoordinated surface atoms, and similar effects related to essentially the crystal nanostructure of shape-controlled nanoparticles.

Role of nanoshape. The nanoshape strongly influences the local electrical field and potential distribution at the NP and, in turn, the characteristics of the electrified solid-liquid interfaces and electrocatalytic properties. Thus, several of the interpretation in electrocatalysis should be reconsidered from the perspective of how the NPs shape and size determines a distribution of the local electrical fields and potential and how this effect, rather than others, is associated with the

change in the electrocatalytic properties. The directional micro-electric field explains some effects, such as the role of ordered nanostructure in enhancing electrocatalytic performance [240]. In contrast, they cannot be explained by effects related to crystal nanostructure. These results indirectly proved the role of local electrical fields and shape-dependent potential distribution in NPs electrocatalysts. Huang et al. [293] presented the concept of the electrostatic field around electrocatalyst NPs, evidencing how it influences the double layer and the electrocatalytic behaviour. They used to explain the effect of particle "proximity", but the indications are well in line with the abovementioned aspects.

Field-induced reagent concentration. Li et al. [294] estimated the dependence on the field-induced reagent concentration from morphology characteristics of the NPs, in particular, effects such as the confinement of reaction intermediates in a nanocavity (an area in which research on electrocatalysis focus recently, but again based on different mechanistic interpretations [20, 295–298]) and high-curvature nanoscale features. See also the previous section. These authors propose theoretical protocols for the simulation of the electrochemical properties of these effects, which cannot be addressed by approaches such as DFT. These calculations include the local electric field, the electrode's current density, and the adjacent electrolyte. The Stern layer, the interface layer between the electrocatalyst and the electrolyte, is strongly influenced by the local field and, consequently, the electron transfer and reactant transport. These indications demonstrate well that without accounting specifically for the nanostructure and its effect on creating a local change in the electrical field and potential, the interpretation of the electrocatalytic results may not be correct. Similarly, it may be expected that a strong localized electrical field at catalysts NPs would also influence the way of adsorption and interaction with plasma-generated (gas-phase) species. However, these aspects are typically not considered, and literature studies are lacking.

(a) Opportunities for plasmonic-enhanced electrocatalysis. Above comments open exciting perspectives about the possibility of plasmonic-enhanced electrocatalysis. There are some studies and reviews as well, even though the interpretation is that localized surface plasmon resonance (LSPR) induces the generation of hot electrons and holes, catalyst heating, and resonant energy transfer as the primary factors to boost the electrocatalytic performances [299,300]. In other words, the "classical" effects of plasmonic resonance. We instead suggest that electromagnetic field enhancement is the dominant effect. Zhao et al. [299] and Choi et al. [300] provide examples of electrocatalytic reactions showing plasmonic-enhanced performances. They demonstrate that this effect can promote not only the performances but also the selectivity. Thus, while the interpretation of the effect, and therefore the design criteria could be a matter of discussion, there is enough convincing evidence that plasmonic-enhanced electrocatalysis, not only photo-catalysis or photoelectrocatalysis [301], is a relevant scientific area on which one should focus attention also from the application perspective. However, in some cases, it can be just a thermal effect induced by the plasmonic effect [302,303]. This is always possible, but we suggest that this is an exception rather than the normal situation and related to the fact that the systems were not adequately designed to maximize the true plasmonic effect commented before.

Antenna-reactor integrated design. It is necessary to realize an antenna-reactor integrated design to synergetically couple the strong, localized near field of the plasmonic metal nanoparticle to the catalytic properties of a nonplasmonic metal nanoparticle [304]. This concept is presented in Fig. 18. The strong localised electrical field generated on the core plasmonic particles influences the catalytic behaviour of near-lying nanoparticles, physically separated (through a thin layer) from the plasmonic nanoparticles. Combining plasmonic and catalytic metal nanoparticles in close proximity makes it possible to form an antenna–reactor complex, in which the plasmonic nanoparticle is the antenna, and the catalytic particle is the reactor. This opens a whole new field for catalysis, largely unexplored.

Li et al. [304] used core@shell/satellite (Ag@SiO_2/Pt) systems for plasmonic-enhanced catalytic CO oxidation. They observed plasmon-enhanced photocatalysis only for antenna–reactor complexes with plasmonic and catalytic NPs of specific size. They explained the effect as due to a balance between different aspects: (i) maximize the local field intensification at the catalytically active Pt surface, (ii) minimize the collective scattering of photons, and (iii) optimize the light absorption in the Ag nanoparticle antenna. Thus, plasmonic-enhanced electro- or photo-catalysis requires optimizing all these aspects. Otherwise, just side aspects could dominate the performances.

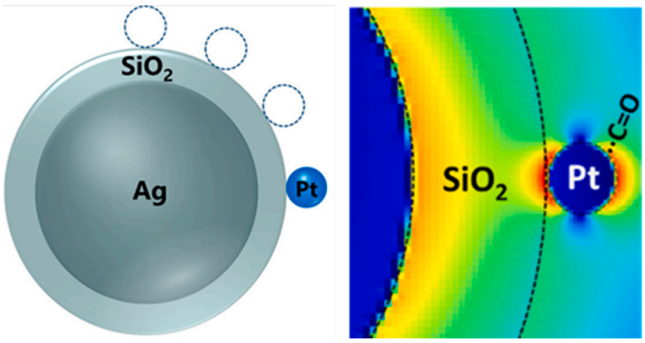

Fig. 18. Model for Ag@SiO_2 @Pt nanoparticles and of the electromagnetic field distributions at Pt surfaces created by the plasmonic effect of the Ag nanoparticle separated by a silica layer from the Pt nanoparticle.
Adapted with permission from Li et al. [304]. Copyright ACS, 2017.

Improve understanding. Advanced characterization would be thus necessary to understand these aspects better. Among them may be cited optically coupled transmission electron microscopy (OTEM) [305]. This technique allows imaging and control of light-induced chemical transformations at the nanoscale. One of the examples discussed by Swearer et al. [305] regards plasmonic photocatalysts formed by a gold nanoparticle "antenna" and Pd NPs as the active catalytic component. With OTEM, they showed the dynamic reconstruction by forming an α-phase in regions close to electromagnetic "hot spots". There are thus likely in-situ dynamic reconstructions during plasmonic-enhanced catalysis, although studies are still limited. Applying a potential and/or a strong electrical field causing charge separation is expected to create a possible dynamic reconstruction to minimize the surface energy of NPs. However, specific studies are still limited [44,306]. Using a theoretical approach, Núñez et al. [307] indicate that higher reactive reconstructed nanoparticles could form due to this in-situ reconstruction, even though the scope of the work was different. Bi et al. [308] showed that plasmonic AgPt bimetallic hollow NPs with an ultra-thin shell are subjected to a dynamic reconstruction leading to a surface charge heterogeneity due to irradiation, which induces a change in their reactivity. Swearer et al. [305] showed that plasmon-derived hot carriers change the PdH_x phase and selectivity behaviour under illumination. However, clear literature evidence about a link between surface reconstruction, plasmonic effect and changes induced in the reactivity is essentially missing.

(b) Exploiting the hot carriers generated by the plasmonic effect. Plasmon-generated hot carriers are well established [166, 256–262], as commented before. The physics of the process occurring is quite complex, although significant progress has been made in their understanding. Although more explored, this area still presents a series of novel possibilities to boost the catalytic properties by plasmonic effect. However, we do not enter here in the discussion of these processes. We only remark that these processes are typically faster than those occurring at the surface of nanoparticles to use the charges generated in these processes.

When a semiconductor absorbs photons with energy above the bandgap, hot carriers (HCs) are generated but lose their excess energy through fast thermalization and cooling processes leading to thermodynamic equilibrium towards the edge values of valence and conduction bands. Thus, only electrons/holes with energy corresponding to their

band edges are actually used in redox processes or to generate a photocurrent. Thus, there is a maximum theoretical solar-to-charge carrier efficiency of 33%, according to Shockley–Queisser (SQ) limit. This gives an upper limit in solar-to-fuel (STF) efficiencies. If the HC can be directly used before thermalization, breaking the SQ limits and radically increasing STF and the rate of the chemical reactions with the "hot" charges is possible. Quantum confined systems, including two-dimensional (2D) materials [10,309] and plasmonic nanoparticles, are among the promising candidates for HC generation/collection because of their low electron-phonon coupling, strong Coulomb interaction and relaxation of some energy-momentum conservation requirements. These and other approaches thus pave the way for a new hot-electron–mediated catalytic reactivity [310].

Nano-heterointerfaces. Another promising research direction is exploring different nano-heterointerfaces through which energetic holes can be localized to the catalytic sites [311]. By using advanced theoretical methods such as time-dependent density-functional theory (TDDFT), it is possible to show the presence of direct hot-electron transfer from the occupied states of plasmonic NPs (Ag) to the unoccupied molecular orbitals of the reactant (CO) [312]. With advanced imaging methods, it is also possible to monitor directly plasmonic hot-carrier reactions at the single particle level [313].

Plasmonic generation of hot charges and how to use them would require a more extended discussion on their mechanisms of generation and transformation. It is known that these processes depend on particle size and shape. Lower-coordinated surface sites such as corners, edges, and facets show an increased presence of hot electrons [314]. Thus, there are links with the previously commented aspects related to the nanomorphology of NPs.

In conclusion, we showed here that in this area of hot carriers generated by the plasmonic effect, significant further progress could derive from a better understanding of the physicochemical and catalytic phenomena occurring and how to use them more creatively beyond the ways considered today. Still, the performances exhibited by plasmonic-enhanced photo- and electro-catalytic processes, especially in STF processes, are limited. However, we believe this is due to the narrow approach used in considering the possibilities given by plasmonic catalysis beyond photocatalysis. The examples discussed remark on a possible bright future using these concepts to improve heterogeneous, electro- and possibly plasma catalysis.

6. Conclusions

A central message from this review is the need to expand the approaches in catalysis and foster research in new directions in unconventional catalysis, where the term "conventional" indicates heterogeneous and homogeneous catalysts currently in use. They were the pillar of our modern society. Still, the challenge of accelerating a transition to a sustainable, carbon-neutral society requires us to go beyond the catalysis of today and develop new catalytic technologies using directly renewable energy rather than "thermal" energy associated with fossil fuels.

Even if considerable attention is given today to scientific areas such as photo- and electro-catalysis, they are still addressed from a narrow perspective. A broader approach exploiting different unconventional catalysis based on renewable energy sources offers many clues to accelerate progress. For this reason, this review discusses four areas of unconventional or less conventional catalysis. Although apparently

Table 1
Future needs and tools to reach them for the four technologies analyzed.

Technology	*Needs*	*Tools to reach them*
Plasma catalysis	- Multi-disciplinary research: chemical (catalytic) + physical + electrical effects of catalyst (or supports) on plasma behaviour - Optimal interaction of plasma species with catalyst, without quenching or back-reaction into reactants - Design catalysts tailored to the plasma environment - Design plasma reactors with optimal transport of plasma species to the catalyst surface - Tune plasma conditions for optimal synergy with the catalyst	Deeper insight into the underlying mechanisms -Catalyst screening + machine learning -In-situ surface characterization -Chemical kinetic modelling
Flow chemistry catalysis	- Improved placement of catalyst: coating and immobilization - Catalyst performance in highly accelerated reaction conditions - Revisit of electric and electromagnetic-induced catalysis, which matches miniaturised processing - Use the current transfer of fossil to renewable energies - Chase real-world applications - Consider process design that allows scale-out to industrial capability for real-world opportunities - Consider emerging trends for holistic opportunity	- Design principles: "old-school learning" on process design still helps cutting-edge innovation - Intensification: flow chemistry intrinsically intensifies. Chase the opportunities - Sustainability: all kinds of sustainability assessments can guide flow chemistry catalysis, including life cycle assessment, techno-economic analysis, and circularity economy indicators.
Catalysis with application of an external electrical field	- Enlarge the database of cases proving the enhancement of reactivity and possibility to control selectivity - Quantify the effects in relation to intensity of the electrical field - Understand and modelling the effect of high-curvature regions and nanostructure - Tip-enhanced field intensification at the nanometer-scale - Combination of electrical and thermal fields	- Develop novel tailored materials, such as periodic nanoneedles - Develop microstructured DBD - Microkinetic modelling - Quantify TOF enhancements - Deeper insight into the underlying mechanisms and the influence of an external electrical field
Nanoscale electrical fields induced by plasmonic catalysis	- In-situ methods to quantify the electrical fields at nanoscale generated by plasmonic effect - Understand the complex phenomena associated to plasmonic effect - Analyze the mechanisms of plasmonic-mediated activation - Create a database of examples of reactions and catalysts promoted by nanoscale electrical fields induced by plasmonic catalysis - Combine plasmonic effect with electro- and plasma catalysis	- Deeper insight into the underlying mechanisms - Develop operando methods for time-resolved analysis of plasmonic enhancement - Correlate the behavior with the nanoshape - Determine field-induced reagent concentration - Antenna-reactor integrated design - Exploiting the hot carriers

disjointed, they share the common characteristic of i) direct use of renewable energy sources and ii) opening (or reinforcing) new prospects to develop breakthrough intensified catalytic processes. The four macrotopics discussed were: (i) plasma catalysis, (ii) catalysis for flow chemistry and process intensification, (iii) application of electromagnetic (EM) fields to modulate catalytic activity and (iv) nanoscale generation at the catalyst interface of a strong local EM by plasmonic effect. Table 1 provides a unitary comparative overview of the aspects remarked in the four sections and evidence of the common aspects and peculiarities. .

CRediT authorship contribution statement

All the authors equally contributed in preparing and writing the manuscript. G. Centi coordinated the effort.

Declaration of Competing Interest

The authors declare the following financial interests/personal relationships which may be considered as potential competing interests:A Bogaerts, G Centi, V Hessel and E Rebrov report that financial support was provided by the EU ERC Synergy SCOPE project 810182 " Surface-COnfined fast-modulated Plasma for process and Energy intensification in small molecules conversion".

Data Availability

No data was used for the research described in the article.

Acknowledgements

The EU ERC Synergy SCOPE project supported this work (project ID 810182) " Surface-COnfined fast-modulated Plasma for process and Energy intensification in small molecules conversion". This review thus aims to stimulate the reader to make new, creative catalysis to address the challenges of reaching a carbon-neutral world.

References

[1] E. Lucke, E.A. Ronces, Leveraging Synergies Between Refining and Petrochemical Processes, CRC Press, 2021.
[2] I. Fechete, Y. Wang, J.C. Védrine, The past, present and future of heterogeneous catalysis, Catal. Today 189 (2012) 2–27.
[3] F. Cavani, G. Centi, S. Perathoner, F. Trifiro, Sustainable Industrial Chemistry, Wiley-VCH, 2009.
[4] D. Uner, Advances in Refining. Catalysis, CRC Press, 2019.
[5] J. Ross, Contemporary. Catalysis, Fundamentals and Current Applications, Elsevier, 2018.
[6] B. Peng, H. Liu, Z. Liu, X. Duan, Y. Huang, Toward rational design of single-atom catalysts, J. Phys. Chem. Lett. 12 (2021) 2837–2847.
[7] H. Xu, D. Cheng, D. Cao, X.C. Zeng, A universal principle for a rational design of single-atom electrocatalysts, Nat. Catal. 1 (2018) 339–348.
[8] Z. Wang, P. Hu, Towards rational catalyst design: a general optimization framework, Philos. Trans. R. Soc. A: Math. Phys. Eng. Sci. 374 (2016), 20150078.
[9] J.D. Rimer, Rational design of zeolite catalysts, Nat. Catal. 1 (2018) 488–489.
[10] G. Centi, J. Čejka, Needs and gaps for catalysis in addressing transitions in chemistry and energy from a sustainability perspective, ChemSusChem 12 (2019) 621–632.
[11] J. Čejka, P. Nachtigall, G. Centi, New catalytic materials for energy and chemistry in transition, Chem. Soc. Rev. 47 (2018) 8066–8071.
[12] M.A. Alabdullah, A.R. Gomez, J. Vittenet, A. Bendjeriou-Sedjerari, W. Xu, I. A. Abba, J. Gascon, A viewpoint on the refinery of the future: catalyst and process challenges, ACS Catal. 10 (2020) 8131–8140.
[13] G. Papanikolaou, G. Centi, S. Perathoner, P. Lanzafame, Catalysis for e-chemistry: need and gaps for a future De-fossilized chemical production, with focus on the role of complex (direct) syntheses by electrocatalysis, ACS Catal. 12 (2022) 2861–2876.
[14] G. Centi, S. Perathoner, Catalysis for an electrified chemical production, Catal. Today (2022).
[15] G. Centi, S. Perathoner, Status and gaps toward fossil-free sustainable chemical production, Green. Chem. 24 (2022) 7305–7331.
[16] G. Papanikolaou, G. Centi, S. Perathoner, P. Lanzafame, Transforming catalysis to produce e-fuels: Prospects and gaps, Chin. J. Catal. 43 (2022) 1194–1203.
[17] G. Centi, S. Perathoner, Nanocarbon for energy material applications: N_2 reduction reaction, Small 17 (2021), 2007055.
[18] S. Perathoner, G. Centi, Catalysis for solar-driven chemistry: the role of electrocatalysis, Catal. Today 330 (2019) 157–170.
[19] A. Navarrete, G. Centi, A. Bogaerts, Á. Martín, A. York, G.D. Stefanidis, Harvesting renewable energy for carbon dioxide catalysis, energy, Technology 5 (2017) 796–811.
[20] J. Wordsworth, T.M. Benedetti, S.V. Somerville, W. Schuhmann, R.D. Tilley, J. J. Gooding, The influence of nanoconfinement on electrocatalysis, Angew. Chem. Int. Ed. 61 (2022), e202200755.
[21] Y. Pei, H. Zhong, F. Jin, A brief review of electrocatalytic reduction of CO_2 - materials, reaction conditions, and devices, Energy Sci. Eng. 9 (2021) 1012–1032.
[22] A.P. O'Mullane, M. Escudero-Escribano, I.E.L. Stephens, K. Krischer, The role of electrocatalysis in a sustainable future: from renewable energy conversion and storage to emerging reactions, ChemPhysChem 20 (2019) 2900–2903.
[23] J. Zhang, Z. Xia, L. Dai, Carbon-based electrocatalysts for advanced energy conversion and storage, Sci. Adv. 1 (2015), e1500564.
[24] G. Centi, G. Iaquaniello, S. Perathoner, Chemical engineering role in the use of renewable energy and alternative carbon sources in chemical production, BMC, Chem. Eng. 1 (2019) 5.
[25] R. Zheng, Z. Liu, Y. Wang, Z. Xie, M. He, The future of green energy and chemicals: Rational design of catalysis routes, Joule 6 (2022) 1148–1159.
[26] H. Li, C. Guo, J. Long, X. Fu, J. Xiao, Theoretical understanding of electrocatalysis beyond thermodynamic analysis, Chin. J. Catal. 43 (2022) 2746–2756.
[27] T. Shen, S. Wang, T. Zhao, Y. Hu, D. Wang, Recent advances of single-atom-alloy for energy electrocatalysis, advanced energy, Materials 12 (2022), 2201823.
[28] J.H. Kim, Y.J. Sa, T. Lim, J. Woo, S.H. Joo, Steering catalytic selectivity with atomically dispersed metal electrocatalysts for renewable energy conversion and commodity chemical production, Acc. Chem. Res. 55 (2022) 2672–2684.
[29] X. Zhang, Y. Tian, L. Chen, X. Hu, Z. Zhou, Machine learning: a new paradigm in computational electrocatalysis, J. Phys. Chem. Lett. 13 (2022) 7920–7930.
[30] X. Sun, S. Jiang, H. Huang, H. Li, B. Jia, T. Ma, Solar energy catalysis, Angew. Chem. Int. Ed. 61 (2022), e202204880.
[31] Y. Li, D. Zhang, W. Qiao, H. Xiang, F. Besenbacher, Y. Li, R. Su, Nanostructured heterogeneous photocatalyst materials for green synthesis of valuable chemicals, Chem. Synth. 2 (2022) 9.
[32] S. Lin, X. Zhang, L. Chen, Q. Zhang, L. Ma, J. Liu, A review on catalysts for electrocatalytic and photocatalytic reduction of N_2 to ammonia, Green. Chem. 24 (2022) 9003–9026.
[33] L. Candish, K.D. Collins, G.C. Cook, J.J. Douglas, A. Gómez-Suárez, A. Jolit, S. Keess, Photocatalysis in the Life Science Industry, Chem. Rev. 122 (2022) 2907–2980.
[34] J. Xuan, W.-J. Xiao, Visible-light photoredox catalysis, Angew. Chem. Int. Ed. 51 (2012) 6828–6838.
[35] S.N. Habisreutinger, L. Schmidt-Mende, J.K. Stolarczyk, Photocatalytic reduction of CO_2 on TiO_2 and other semiconductors, Angew. Chem. Int. Ed. 52 (2013) 7372–7408.
[36] J.Z. Bloh, R. Marschall, Heterogeneous photoredox catalysis: reactions, materials, and reaction engineering, Eur. J. Org. Chem. 2017 (2017) 2085–2094.
[37] J.C. Whitehead, Plasma-catalysis: is it just a question of scale? Front. Chem. Sci. Eng. 13 (2019) 264–273.
[38] H. Puliyalil, D. Lašič Jurković, V.D.B.C. Dasireddy, B. Likozar, A review of plasma-assisted catalytic conversion of gaseous carbon dioxide and methane into value-added platform chemicals and fuels, RSC Adv. 8 (2018) 27481–27508.
[39] P. Hinde, V. Demidyuk, A. Gkelios, C. Tipton, Plasma catalysis: a review of the interdisciplinary challenges faced: realising the potential of plasma catalysis on a commercial scale, Johns. Matthey Technol. Rev. 64 (2020) 138–147.
[40] S. Liu, L.R. Winter, J.G. Chen, Review of Plasma-Assisted Catalysis for Selective Generation of Oxygenates from CO_2 and CH_4, ACS, Catalysis 10 (2020) 2855–2871.
[41] A. Bogaerts, X. Tu, J.C. Whitehead, G. Centi, L. Lefferts, O. Guaitella, F. Azzolina-Jury, H.-H. Kim, A.B. Murphy, W.F. Schneider, T. Nozaki, J.C. Hicks, A. Rousseau, F. Thevenet, A. Khacef, M. Carreon, The 2020 plasma catalysis roadmap, J. Phys. D: Appl. Phys. 53 (2020), 443001.
[42] R. Snoeckx, A. Bogaerts, Plasma technology – a novel solution for CO_2 conversion? Chem. Soc. Rev. 46 (2017) 5805–5863.
[43] E.C. Neyts, K. Ostrikov, M.K. Sunkara, A. Bogaerts, Plasma catalysis: synergistic effects at the nanoscale, Chem. Rev. 115 (2015) 13408–13446.
[44] C. Genovese, M.E. Schuster, E.K. Gibson, D. Gianolio, V. Posligua, R. Grau-Crespo, G. Cibin, P.P. Wells, D. Garai, V. Solokha, S. Krick Calderon, J.J. Velasco-Velez, C. Ampelli, S. Perathoner, G. Held, G. Centi, R. Arrigo, Operando spectroscopy study of the carbon dioxide electro-reduction by iron species on nitrogen-doped carbon, Nat. Commun. 9 (2018) 935.
[45] A.I. Stankiewicz, H. Nigar, Beyond electrolysis: old challenges and new concepts of electricity-driven chemical reactors, React. Chem. Eng. 5 (2020) 1005–1016.
[46] T. Van Gerven, A. Stankiewicz, Structure, energy, synergy, time—the fundamentals of process intensification, Ind. Eng. Chem. Res. 48 (2009) 2465–2474.
[47] A. Stankiewicz, J.A. Moulijn, Process intensification, Ind. Eng. Chem. Res. 41 (2002) 1920–1924.
[48] F.J. Keil, Process intensification, Rev. Chem. Eng. 34 (2018) 135–200.
[49] L. Baharudin, A.A. Indera L, M.J. Watson, A.C.K. Yip, Process intensification in multifunctional reactors: a review of multi-functionality by catalytic structures, internals, operating modes, and unit integrations, Chem. Eng. Process. - Process. Intensif. 168 (2021), 108561.
[50] S. Sitter, Q. Chen, I.E. Grossmann, An overview of process intensification methods, Curr. Opin. Chem. Eng. 25 (2019) 87–94.

[51] R. Lin, J. Guo, X. Li, P. Patel, A. Seifitokaldani, Electrochemical reactors for CO_2 conversion, Catalysts 10 (2020) 473.
[52] S.C. Perry, C. Ponce de León, F.C. Walsh, Review—the design, performance and continuing development of electrochemical reactors for clean electrosynthesis, J. Electrochem. Soc. 167 (2020), 155525.
[53] L. Fan, C. Xia, F. Yang, J. Wang, H. Wang, Y. Lu, Strategies in catalysts and electrolyzer design for electrochemical CO_2 reduction toward C2+ products, Sci. Adv. 6 (2020) eaay3111.
[54] F. Tavella, D. Giusi, C. Ampelli, Nitrogen reduction reaction to ammonia at ambient conditions: a short review analysis of the critical factors limiting electrocatalytic performance, Curr. Opin. Green Sustain. Chem. 35 (2022), 100604.
[55] A. Visan, J.R. van Ommen, M.T. Kreutzer, R.G.H. Lammertink, Photocatalytic reactor design: guidelines for kinetic investigation, Ind. Eng. Chem. Res. 58 (2019) 5349–5357.
[56] O. Ola, M.M. Maroto-Valer, Review of material design and reactor engineering on TiO_2 photocatalysis for CO_2 reduction, J. Photochem. Photobiol. C: Photochem. Rev. 24 (2015) 16–42.
[57] R. Binjhade, R. Mondal, S. Mondal, Continuous photocatalytic reactor: critical review on the design and performance, J. Environ. Chem. Eng. 10 (2022), 107746.
[58] T. Nitsche, C. Unger, E. Weidner, Plasma catalytical reactors for atmospheric gas conversions, Chem. Ing. Tech. 90 (2018) 1453–1464.
[59] A. Bogaerts, G. Centi, Plasma technology for CO_2 conversion: a personal perspective on prospects and gaps, Front. Energy Res. 8 (2020) 111.
[60] S. Abate, K. Barbera, G. Centi, P. Lanzafame, S. Perathoner, Disruptive catalysis by zeolites, Catal. Sci. Technol. 6 (2016) 2485–2501.
[61] V. Russo, S. Haase, P. Tolvanen, Process intensification in chemical reaction engineering, Processes 10 (2022) 1294.
[62] G. Centi, Smart catalytic materials for energy transition, SmartMat 1 (2020), e1005.
[63] X. Qi, T. Shinagawa, F. Kishimoto, K. Takanabe, Determination and perturbation of the electronic potentials of solid catalysts for innovative catalysis, Chem. Sci. 12 (2021) 540–545.
[64] T. Löffler, A. Savan, A. Garzón-Manjón, M. Meischein, C. Scheu, A. Ludwig, W. Schuhmann, Toward a paradigm shift in electrocatalysis using complex solid solution nanoparticles, ACS Energy Lett. 4 (2019) 1206–1214.
[65] P. Lanzafame, S. Abate, C. Ampelli, C. Genovese, R. Passalacqua, G. Centi, S. Perathoner, Beyond solar fuels: renewable energy-driven chemistry, ChemSusChem 10 (2017) 4409–4419.
[66] G. Centi, S. Perathoner, Redesign chemical processes to substitute the use of fossil fuels: a viewpoint of the implications on catalysis, Catal. Today 387 (2022) 216–223.
[67] M. Scapinello, E. Delikonstantis, G.D. Stefanidis, The panorama of plasma-assisted non-oxidative methane reforming, Chem. Eng. Process.: Process.Intensif. 117 (2017) 120–140.
[68] J. Hong, S. Prawer, A.B. Murphy, Plasma catalysis as an alternative route for ammonia production: status, mechanisms, and prospects for progress, ACS Sustain. Chem. Eng. 6 (2018) 15–31.
[69] K.H.R. Rouwenhorst, F. Jardali, A. Bogaerts, L. Lefferts, From the Birkeland–Eyde process towards energy-efficient plasma-based NO_x synthesis: a techno-economic analysis, Energy Environ. Sci. 14 (2021) 2520–2534.
[70] K.H.R. Rouwenhorst, Y. Engelmann, K. van 't Veer, R.S. Postma, A. Bogaerts, L. Lefferts, Plasma-driven catalysis: green ammonia synthesis with intermittent electricity, Green. Chem. 22 (2020) 6258–6287.
[71] A. Bogaerts, E.C. Neyts, Plasma technology: an emerging technology for energy storage, ACS Energy Lett. 3 (2018) 1013–1027.
[72] A.-J. Zhang, A.-M. Zhu, J. Guo, Y. Xu, C. Shi, Conversion of greenhouse gases into syngas via combined effects of discharge activation and catalysis, Chem. Eng. J. 156 (2010) 601–606.
[73] A. Bogaerts, E.C. Neyts, O. Guaitella, A.B. Murphy, Foundations of plasma catalysis for environmental applications, Plasma Sources Sci. Technol. 31 (2022), 053002.
[74] H.-H. Kim, Nonthermal plasma processing for air-pollution control: a historical review, current issues, and future prospects, Plasma Process. Polym. 1 (2004) 91–110.
[75] J. Van Durme, J. Dewulf, C. Leys, H. Van, Langenhove, Combining non-thermal plasma with heterogeneous catalysis in waste gas treatment: a review, Appl. Catal. B: Environ. 78 (2008) 324–333.
[76] H.L. Chen, H.M. Lee, S.H. Chen, M.B. Chang, S.J. Yu, S.N. Li, Removal of volatile organic compounds by single-stage and two-stage plasma catalysis systems: a review of the performance enhancement mechanisms, current status, and suitable applications, Environ. Sci. Technol. 43 (2009) 2216–2227.
[77] A.M. Vandenbroucke, R. Morent, N. De Geyter, C. Leys, Non-thermal plasmas for non-catalytic and catalytic VOC abatement, J. Hazard. Mater. 195 (2011) 30–54.
[78] X. Tu, J.C. Whitehead, T. Nozaki, Plasma. Catalysis: Fundamentals and Applications, Springer, Cham, Switzerland, 2019.
[79] E.C. Neyts, A. Bogaerts, Understanding plasma catalysis through modelling and simulation—a review, J. Phys. D: Appl. Phys. 47 (2014), 224010.
[80] J.C. Whitehead, Plasma–catalysis: the known knowns, the known unknowns and the unknown unknowns, J. Phys. D: Appl. Phys. 49 (2016), 243001.
[81] I. Michielsen, Y. Uytdenhouwen, J. Pype, B. Michielsen, J. Mertens, F. Reniers, V. Meynen, A. Bogaerts, CO_2 dissociation in a packed bed DBD reactor: First steps towards a better understanding of plasma catalysis, Chem. Eng. J. 326 (2017) 477–488.
[82] Y. Uytdenhouwen, S. Van Alphen, I. Michielsen, V. Meynen, P. Cool, A. Bogaerts, A packed-bed DBD micro plasma reactor for CO_2 dissociation: Does size matter? Chem. Eng. J. 348 (2018) 557–568.
[83] K. Van Laer, A. Bogaerts, How bead size and dielectric constant affect the plasma behaviour in a packed bed plasma reactor: a modelling study, Plasma Sources Sci. Technol. 26 (2017), 085007.
[84] K. Van Laer, A. Bogaerts, Fluid modelling of a packed bed dielectric barrier discharge plasma reactor, Plasma Sources Sci. Technol. 25 (2016), 015002.
[85] S. Zhu, A. Zhou, F. Yu, B. Dai, C. Ma, Enhanced CO_2 decomposition via metallic foamed electrode packed in self-cooling DBD plasma device, Plasma Sci. Technol. 21 (2019), 085504.
[86] L. Wang, Y. Yi, H. Guo, X. Tu, Atmospheric pressure and room temperature synthesis of methanol through plasma-catalytic hydrogenation of CO_2, ACS Catal. 8 (2018) 90–100.
[87] Y. Uytdenhouwen, K.M. Bal, E.C. Neyts, V. Meynen, P. Cool, A. Bogaerts, On the kinetics and equilibria of plasma-based dry reforming of methane, Chem. Eng. J. 405 (2021), 126630.
[88] Y.X. Zeng, L. Wang, C.F. Wu, J.Q. Wang, B.X. Shen, X. Tu, Low temperature reforming of biogas over K-, Mg- and Ce-promoted Ni/Al_2O_3 catalysts for the production of hydrogen rich syngas: understanding the plasma-catalytic synergy, Appl. Catal. B: Environ. 224 (2018) 469–478.
[89] L. Wang, Y. Yi, C. Wu, H. Guo, X. Tu, One-step reforming of CO_2 and CH_4 into high-value liquid chemicals and fuels at room temperature by plasma-driven catalysis, Angew. Chem. Int. Ed. 56 (2017) 13679–13683.
[90] A.N. Biswas, L.R. Winter, B. Loenders, Z. Xie, A. Bogaerts, J.G. Chen, Oxygenate production from plasma-activated reaction of CO_2 and ethane, ACS Energy Lett. 7 (2022) 236–241.
[91] Y. Yi, X. Wang, A. Jafarzadeh, L. Wang, P. Liu, B. He, J. Yan, R. Zhang, H. Zhang, X. Liu, H. Guo, E.C. Neyts, A. Bogaerts, Plasma-catalytic ammonia reforming of methane over cu-based catalysts for the production of hcn and H_2 at reduced temperature, ACS Catal. 11 (2021) 1765–1773.
[92] Y. Yi, S. Li, Z. Cui, Y. Hao, Y. Zhang, L. Wang, P. Liu, X. Tu, X. Xu, H. Guo, A. Bogaerts, Selective oxidation of CH_4 to CH_3OH through plasma catalysis: Insights from catalyst characterization and chemical kinetics modelling, Applied Catalysis B: Environmental 296 (2021), 120384.
[93] J. Kim, M.S. Abbott, D.B. Go, J.C. Hicks, Enhancing C–H bond activation of methane via temperature-controlled, catalyst–plasma interactions, ACS Energy Lett. 1 (2016) 94–99.
[94] P. Mehta, P. Barboun, D.B. Go, J.C. Hicks, W.F. Schneider, Catalysis enabled by plasma activation of strong chemical bonds: a review, ACS Energy Lett. 4 (2019) 1115–1133.
[95] J. Kim, D.B. Go, J.C. Hicks, Synergistic effects of plasma–catalyst interactions for CH_4 activation, Phys. Chem. Chem. Phys. 19 (2017) 13010–13021.
[96] Z. Sheng, Y. Watanabe, H.-H. Kim, S. Yao, T. Nozaki, Plasma-enabled mode-selective activation of CH_4 for dry reforming: first touch on the kinetic analysis, Chem. Eng. J. 399 (2020), 125751.
[97] A. Astafan, C. Batiot-Dupeyrat, L. Pinard, Mechanism and kinetic of coke oxidation by nonthermal plasma in fixed-bed dielectric barrier reactor, J. Phys. Chem. C. 123 (2019) 9168–9175.
[98] E. Delikonstantis, M. Scapinello, G.D. Stefanidis, Low energy cost conversion of methane to ethylene in a hybrid plasma-catalytic reactor system, Fuel Process. Technol. 176 (2018) 33–42.
[99] E. Delikonstantis, E. Igos, M. Augustinus, E. Benetto, G.D. Stefanidis, Life cycle assessment of plasma-assisted ethylene production from rich-in-methane gas streams, Sustain. Energy Fuels 4 (2020) 1351–1362.
[100] L. Hollevoet, F. Jardali, Y. Gorbanev, J. Creel, A. Bogaerts, J.A. Martens, Towards green ammonia synthesis through plasma-driven nitrogen oxidation and catalytic reduction, Angew. Chem. Int. Ed. 59 (2020) 23825–23829.
[101] G. Akay, K. Zhang, Process intensification in ammonia synthesis using novel coassembled supported microporous catalysts promoted by nonthermal plasma, Ind. Eng. Chem. Res. 56 (2017) 457–468.
[102] L. Hollevoet, E. Vervloessem, Y. Gorbanev, A. Nikiforov, N. De Geyter, A. Bogaerts, J.A. Martens, Energy-efficient small-scale ammonia synthesis process with plasma-enabled nitrogen oxidation and catalytic reduction of adsorbed NO_x, ChemSusChem 15 (2022), e202102526.
[103] F. Jardali, S. Van Alphen, J. Creel, H. Ahmadi Eshtehardi, M. Axelsson, R. Ingels, R. Snyders, A. Bogaerts, NO_x production in a rotating gliding arc plasma: potential avenue for sustainable nitrogen fixation, Green. Chem. 23 (2021) 1748–1757.
[104] S. Kelly, A. Bogaerts, Nitrogen fixation in an electrode-free microwave plasma, Joule 5 (2021) 3006–3030.
[105] E. Vervloessem, Y. Gorbanev, A. Nikiforov, N. De Geyter, A. Bogaerts, Sustainable NO_x production from air in pulsed plasma: elucidating the chemistry behind the low energy consumption, Green. Chem. 24 (2022) 916–929.
[106] J. Sun, D. Alam, R. Daiyan, H. Masood, T. Zhang, R. Zhou, P.J. Cullen, E.C. Lovell, A. Jalili, R. Amal, A hybrid plasma electrocatalytic process for sustainable ammonia production, Energy Environ. Sci. 14 (2021) 865–872.
[107] L. Li, C. Tang, X. Cui, Y. Zheng, X. Wang, H. Xu, S. Zhang, T. Shao, K. Davey, S.-Z. Qiao, Efficient nitrogen fixation to ammonia through integration of plasma oxidation with electrocatalytic reduction, Angew. Chem. Int. Ed. 60 (2021) 14131–14137.
[108] A. Wu, J. Yang, B. Xu, X.-Y. Wu, Y. Wang, X. Lv, Y. Ma, A. Xu, J. Zheng, Q. Tan, Y. Peng, Z. Qi, H. Qi, J. Li, Y. Wang, J. Harding, X. Tu, A. Wang, J. Yan, X. Li, Direct ammonia synthesis from the air via gliding arc plasma integrated with single atom electrocatalysis, Appl. Catal. B: Environ. 299 (2021), 120667.

[109] I. Muzammil, Y.-N. Kim, H. Kang, D.K. Dinh, S. Choi, C. Jung, Y.-H. Song, E. Kim, J.M. Kim, D.H. Lee, Plasma catalyst-integrated system for ammonia production from H_2O and N_2 at atmospheric pressure, ACS Energy Lett. 6 (2021) 3004–3010.
[110] R.K. Sharma, H. Patel, U. Mushtaq, V. Kyriakou, G. Zafeiropoulos, F. Peeters, S. Welzel, M.C.M. van de Sanden, M.N. Tsampas, Plasma activated electrochemical ammonia synthesis from nitrogen and water, ACS Energy Lett. 6 (2021) 313–319.
[111] Q.-Z. Zhang, A. Bogaerts, Propagation of a plasma streamer in catalyst pores, Plasma Sources Sci. Technol. 27 (2018), 035009.
[112] Q.-Z. Zhang, W.-Z. Wang, A. Bogaerts, Importance of surface charging during plasma streamer propagation in catalyst pores, Plasma Sources Sci. Technol. 27 (2018), 065009.
[113] J.R. Kitchin, Machine learning in catalysis, Nat. Catal. 1 (2018) 230–232.
[114] N.A.S.Amin Istadi, Hybrid artificial neural network−genetic algorithm technique for modeling and optimization of plasma reactor, Ind. Eng. Chem. Res. 45 (2006) 6655–6664.
[115] P.A. Gorry, J.C. Whitehead, J. Wu, Adaptive control for NO_x removal in non-thermal plasma processing, Plasma Process. Polym. 4 (2007) 556–562.
[116] X. Zhu, S. Liu, Y. Cai, X. Gao, J. Zhou, C. Zheng, X. Tu, Post-plasma catalytic removal of methanol over Mn–Ce catalysts in an atmospheric dielectric barrier discharge, Appl. Catal. B: Environ. 183 (2016) 124–132.
[117] Y. Wang, Y. Chen, J. Harding, H. He, A. Bogaerts, X. Tu, Catalyst-free single-step plasma reforming of CH_4 and CO_2 to higher value oxygenates under ambient conditions, Chem. Eng. J. 450 (2022), 137860.
[118] S. Xu, S. Chansai, S. Xu, C.E. Stere, Y. Jiao, S. Yang, C. Hardacre, X. Fan, CO poisoning of Ru catalysts in CO_2 hydrogenation under thermal and plasma conditions: a combined kinetic and diffuse reflectance infrared fourier transform spectroscopy–mass spectrometry study, ACS Catal. 10 (2020) 12828–12840.
[119] A. Rodrigues, J.-M. Tatibouët, E. Fourré, Operando DRIFT spectroscopy characterization of intermediate species on catalysts surface in VOC removal from air by non-thermal plasma assisted catalysis, Plasma Chem. Plasma Process. 36 (2016) 901–915.
[120] C. Stere, S. Chansai, R. Gholami, K. Wangkawong, A. Singhania, A. Goguet, B. Inceesungvorn, C. Hardacre, A design of a fixed bed plasma DRIFTS cell for studying the NTP-assisted heterogeneously catalysed reactions, Catal. Sci. Technol. 10 (2020) 1458–1466.
[121] R. Vakili, R. Gholami, C.E. Stere, S. Chansai, H. Chen, S.M. Holmes, Y. Jiao, C. Hardacre, X. Fan, Plasma-assisted catalytic dry reforming of methane (DRM) over metal-organic frameworks (MOFs)-based catalysts, Appl. Catal. B: Environ. 260 (2020), 118195.
[122] A. Parastaev, N. Kosinov, E.J.M. Hensen, Mechanistic study of catalytic CO_2 hydrogenation in a plasma by operando DRIFT spectroscopy, J. Phys. D: Appl. Phys. 54 (2021), 264004.
[123] H. Li, M. Rivallan, F. Thibault-Starzyk, A. Travert, F.C. Meunier, Effective bulk and surface temperatures of the catalyst bed of FT-IR cells used for in situ and operando studies, Phys. Chem. Chem. Phys. 15 (2013) 7321–7327.
[124] F. Azzolina-Jury, F. Thibault-Starzyk, Mechanism of low pressure plasma-assisted CO_2 hydrogenation over Ni-USY by microsecond time-resolved FTIR spectroscopy, Top. Catal. 60 (2017) 1709–1721.
[125] Y. Sun, J. Wu, Y. Wang, J. Li, N. Wang, J. Harding, S. Mo, L. Chen, P. Chen, M. Fu, D. Ye, J. Huang, X. Tu, Plasma-catalytic CO_2 hydrogenation over a Pd/ZnO catalyst: in situ probing of gas-phase and surface reactions, JACS Au 2 (2022) 1800–1810.
[126] J. Van Turnhout, D. Aceto, A. Travert, P. Bazin, F. Thibault-Starzyk, A. Bogaerts, F. Azzolina-Jury, Observation of surface species in plasma-catalytic dry reforming of methane in a novel atmospheric pressure dielectric barrier discharge in situ IR cell, Catal. Sci. Technol. 12 (2022) 6676–6686.
[127] C.E. Stere, W. Adress, R. Burch, S. Chansai, A. Goguet, W.G. Graham, C. Hardacre, Probing a non-thermal plasma activated heterogeneously catalyzed reaction using in situ DRIFTS-MS, ACS Catal. 5 (2015) 956–964.
[128] A. Parastaev, W.F.L.M. Hoeben, B.E.J.M. van Heesch, N. Kosinov, E.J.M. Hensen, Temperature-programmed plasma surface reaction: an approach to determine plasma-catalytic performance, Appl. Catal. B: Environ. 239 (2018) 168–177.
[129] P. Navascués, J.M. Obrero-Pérez, J. Cotrino, A.R. González-Elipe, A. Gómez-Ramírez, Isotope labelling for reaction mechanism analysis in DBD plasma processes, Catalysts 9 (2019) 45.
[130] E.K. Gibson, C.E. Stere, B. Curran-McAteer, W. Jones, G. Cibin, D. Gianolio, A. Goguet, P.P. Wells, C.R.A. Catlow, P. Collier, P. Hinde, C. Hardacre, Probing the role of a non-thermal plasma (NTP) in the Hybrid NTP catalytic oxidation of methane, Angew. Chem. Int. Ed. 56 (2017) 9351–9355.
[131] K. van 't Veer, Y. Engelmann, F. Reniers, A. Bogaerts, Plasma-catalytic ammonia synthesis in a DBD plasma: role of microdischarges and their afterglows, J. Phys. Chem. C. 124 (2020) 22871–22883.
[132] K.H.R. Rouwenhorst, S. Mani, L. Lefferts, Improving the energy yield of plasma-based ammonia synthesis with in situ adsorption, ACS Sustain. Chem. Eng. 10 (2022) 1994–2000.
[133] Y. Wang, W. Yang, S. Xu, S. Zhao, G. Chen, A. Weidenkaff, C. Hardacre, X. Fan, J. Huang, X. Tu, Shielding protection by mesoporous catalysts for improving plasma-catalytic ambient ammonia synthesis, J. Am. Chem. Soc. 144 (2022) 12020–12031.
[134] Q.-Z. Zhang, A. Bogaerts, Plasma streamer propagation in structured catalysts, Plasma Sources Sci. Technol. 27 (2018), 105013.
[135] S. Li, F. Gallucci, CO_2 capture and activation with a plasma-sorbent system, Chem. Eng. J. 430 (2022), 132979.
[136] S. Li, M. Ongis, G. Manzolini, F. Gallucci, Non-thermal plasma-assisted capture and conversion of CO_2, Chem. Eng. J. 410 (2021), 128335.
[137] P. Mehta, P. Barboun, F.A. Herrera, J. Kim, P. Rumbach, D.B. Go, J.C. Hicks, W. F. Schneider, Overcoming ammonia synthesis scaling relations with plasma-enabled catalysis, Nat. Catal. 1 (2018) 269–275.
[138] P. Mehta, P.M. Barboun, Y. Engelmann, D.B. Go, A. Bogaerts, W.F. Schneider, J. C. Hicks, Plasma-catalytic ammonia synthesis beyond the equilibrium limit, ACS Catal. 10 (2020) 6726–6734.
[139] P. Barboun, P. Mehta, F.A. Herrera, D.B. Go, W.F. Schneider, J.C. Hicks, Distinguishing plasma contributions to catalyst performance in plasma-assisted ammonia synthesis, ACS Sustain. Chem. Eng. 7 (2019) 8621–8630.
[140] Y. Engelmann, K. van 't Veer, Y. Gorbanev, E.C. Neyts, W.F. Schneider, A. Bogaerts, Plasma catalysis for ammonia synthesis: a microkinetic modeling study on the contributions of eley–rideal reaction, ACS Sustain. Chem. Eng. 9 (2021) 13151–13163.
[141] Y. Gorbanev, Y. Engelmann, K. van't Veer, E. Vlasov, C. Ndayirinde, Y. Yi, S. Bals, Al_2O_3-supported transition metals for plasma-catalytic NH_3 synthesis in a DBD plasma: metal activity and insights into mechanisms, Catalysts (2021).
[142] C. Ndayirinde, Y. Gorbanev, R.-G. Ciocarlan, A. Smets, E. Vlasov, R. De Meyer, S. Bals, P. Cool, A. Bogaerts, Plasma-catalytic ammonia synthesis: packed catalysts act as plasma modifiers, Catalysis Today 419 (2023) 114156.
[143] K.H.R. Rouwenhorst, H.-H. Kim, L. Lefferts, Vibrationally excited activation of N_2 in Plasma-enhanced catalytic ammonia synthesis: a kinetic analysis, ACS Sustain. Chem. Eng. 7 (2019) 17515–17522.
[144] Y. Engelmann, P. Mehta, E.C. Neyts, W.F. Schneider, A. Bogaerts, Predicted influence of plasma activation on nonoxidative coupling of methane on transition metal catalysts, ACS Sustain. Chem. Eng. 8 (2020) 6043–6054.
[145] R. Michiels, Y. Engelmann, A. Bogaerts, Plasma catalysis for CO_2 hydrogenation: unlocking new pathways toward CH_3OH, J. Phys. Chem. C. 124 (2020) 25859–25872.
[146] B. Loenders, Y. Engelmann, A. Bogaerts, Plasma-catalytic partial oxidation of methane on Pt(111): a microkinetic study on the role of different plasma species, J. Phys. Chem. C. 125 (2021) 2966–2983.
[147] V. Vermeiren, A. Bogaerts, Plasma-based CO_2 conversion: to quench or not to quench? J. Phys. Chem. C. 124 (2020) 18401–18415.
[148] D.C.M. van den Bekerom, J.M.P. Linares, T. Verreycken, E.M. van Veldhuizen, S. Nijdam, G. Berden, W.A. Bongers, M.C.M. van de Sanden, G.J. van Rooij, The importance of thermal dissociation in CO_2 microwave discharges investigated by power pulsing and rotational Raman scattering, Plasma Sources Sci. Technol. 28 (2019), 055015.
[149] S. Van Alphen, H. Ahmadi Eshtehardi, C. O'Modhrain, J. Bogaerts, H. Van Poyer, J. Creel, M.-P. Delplancke, R. Snyders, A. Bogaerts, Effusion nozzle for energy-efficient NOx production in a rotating gliding arc plasma reactor, Chem. Eng. J. 443 (2022), 136529.
[150] A. Hecimovic, F.A. D'Isa, E. Carbone, U. Fantz, Enhancement of CO_2 conversion in microwave plasmas using a nozzle in the effluent, J. CO_2 Util. 57 (2022), 101870.
[151] E.R. Mercer, S. Van Alphen, C.F.A.M. van Deursen, T.W.H. Righart, W.A. Bongers, R. Snyders, A. Bogaerts, M.C.M. van de Sanden, F.J.J. Peeters, Post-plasma quenching to improve conversion and energy efficiency in a CO_2 microwave plasma, Fuel 334 (2023), 126734.
[152] E. Delikonstantis, M. Scapinello, V. Singh, H. Poelman, C. Montesano, L. M. Martini, P. Tosi, G.B. Marin, K.M. Van Geem, V.V. Galvita, G.D. Stefanidis, Exceeding equilibrium CO_2 conversion by plasma-assisted chemical looping, ACS Energy Lett. 7 (2022) 1896–1902.
[153] H. Xu, M. Shaban, S. Wang, A. Alkayal, D. Liu, M.G. Kong, F. Plasser, B. R. Buckley, F. Iza, Oxygen harvesting from carbon dioxide: simultaneous epoxidation and CO formation, Chem. Sci. 12 (2021) 13373–13378.
[154] Z. Li, T. Yang, S. Yuan, Y. Yin, E.J. Devid, Q. Huang, D. Auerbach, A.W. Kleyn, Boudouard reaction driven by thermal plasma for efficient CO_2 conversion and energy storage, J. Energy Chem. 45 (2020) 128–134.
[155] J. Huang, H. Zhang, Q. Tan, L. Li, R. Xu, Z. Xu, X. Li, Enhanced conversion of CO_2 into O2-free fuel gas via the Boudouard reaction with biochar in an atmospheric plasmatron, J. CO_2 Util. 45 (2021), 101429.
[156] F. Girard-Sahun, O. Biondo, G. Trenchev, G. van Rooij, A. Bogaerts, Carbon bed post-plasma to enhance the CO_2 conversion and remove O_2 from the product stream, Chem. Eng. J. 442 (2022), 136268.
[157] R. Porta, M. Benaglia, A. Puglisi, Flow chemistry: recent developments in the synthesis of pharmaceutical products, Org. Process Res. Dev. 20 (2016) 2–25.
[158] M.B. Plutschack, B. Pieber, K. Gilmore, P.H. Seeberger, The Hitchhiker's guide to flow chemistry, Chem. Rev. 117 (2017) 11796–11893.
[159] N.J.W. Straathof, Y. Su, V. Hessel, T. Noël, Accelerated gas-liquid visible light photoredox catalysis with continuous-flow photochemical microreactors, Nat. Protoc. 11 (2016) 10–21.
[160] V. Hessel, H. Löwe, Microchemical engineering: components, plant concepts, user acceptance – part II, Chem. Eng. Technol. 26 (2003) 391–408.
[161] K. Jähnisch, V. Hessel, H. Löwe, M. Baerns, Chemistry in microstructured reactors, Angew. Chem. Int. Ed. 43 (2004) 406–446.
[162] W. Ehrfeld, V. Hessel, H. Möbius, T. Richter, K. Russow, Potentials and realization of microreactors, Dechema Monographien, Dechema (Frankfurt am Main, Germany), Germany (1995) 1–28.
[163] T. Tsubogo, H. Oyamada, S. Kobayashi, Multistep continuous-flow synthesis of (R)- and (S)-rolipram using heterogeneous catalysts, Nature 520 (2015) 329–332.
[164] S. Rossi, M. Benaglia, A. Puglisi, C. Filippo, M. Maggini, Continuous-flow stereoselective synthesis in microreactors: nucleophilic additions to nitrostyrenes organocatalyzed by a chiral bifunctional catalyst, J. Flow. Chem. 5 (2015) 17–21.
[165] R. Porta, M. Benaglia, F. Coccia, S. Rossi, A. Puglisi, Enantioselective organocatalysis in microreactors: continuous flow synthesis of a (S)-pregabalin precursor and (S)-warfarin, Symmetry (2015) 1395–1409.

[166] G. Kolb, V. Hessel, Micro-structured reactors for gas phase reactions, Chem. Eng. J. 98 (2004) 1–38.
[167] S. Kressirer, L.N. Protasova, M.H.J.M. de Croon, V. Hessel, D. Kralisch, Removal and renewal of catalytic coatings from lab- and pilot-scale microreactors, accompanied by life cycle assessment and cost analysis, Green. Chem. 14 (2012) 3034–3046.
[168] S. Kobayashi, Flow Fine, Synthesis: high yielding and selective organic synthesis by flow methods, Chem. – Asian J. 11 (2016) 425–436.
[169] D. Zhao, K. Ding, Recent advances in asymmetric catalysis in flow, ACS Catal. 3 (2013) 928–944.
[170] T. Noël, S.L. Buchwald, Cross-coupling in flow, Chem. Soc. Rev. 40 (2011) 5010–5029.
[171] A. Gimbernat, M. Guehl, N. Lopes Ferreira, E. Heuson, P. Dhulster, M. Capron, F. Dumeignil, D. Delcroix, J.-S. Girardon, R. Froidevaux, From a sequential chemo-enzymatic approach to a continuous process for HMF production from glucose, Catalysts 8 (2018) 335.
[172] V. Hessel, D. Kralisch, N. Kockmann, T. Noël, Q. Wang, Novel process windows for enabling, accelerating, and uplifting flow chemistry, ChemSusChem 6 (2013) 746–789.
[173] V.K. Hessel, Dana Kockmann, Norbert Novel Process Windows: Innovative Gates to Intensified and Sustainable Chemical Processes, Wiley-VCH, Germany, 2014.
[174] V. Hessel, B. Cortese, M.H.J.M. de Croon, Novel process windows – concept, proposition and evaluation methodology, and intensified superheated processing, Chem. Eng. Sci. 66 (2011) 1426–1448.
[175] V. Hessel, Novel Process, Windows – gate to maximizing process intensification via flow chemistry, Chem. Eng. Technol. 32 (2009) 1655–1681.
[176] D. Cambié, C. Bottecchia, N.J.W. Straathof, V. Hessel, T. Noël, Applications of continuous-flow photochemistry in organic synthesis, material science, and water treatment, Chem. Rev. 116 (2016) 10276–10341.
[177] C. Sambiagio, T. Noël, Flow photochemistry: shine some light on those tubes!, Trends Chem. 2 (2020) 92–106.
[178] S.-H. Lau, A. Galván, R.R. Merchant, C. Battilocchio, J.A. Souto, M.B. Berry, S. V. Ley, Machines vs malaria: a flow-based preparation of the drug candidate OZ439, Org. Lett. 17 (2015) 3218–3221.
[179] T. Ouchi, C. Battilocchio, J.M. Hawkins, S.V. Ley, Process intensification for the continuous flow hydrogenation of ethyl nicotinate, Org. Process Res. Dev. 18 (2014) 1560–1566.
[180] C.Y. Stephenson, MacMillan Tehshik, W.C. David, Visible light photocatalysis in organic chemistry, Wiley-VCH, Weinheim, Germany, 2018.
[181] N.J.W. Straathof, T. Noël, Accelerating visible-light photoredox catalysis in continuous-flow reactors, Visible Light Photocatal. Org. Chem. (2018) 389–413.
[182] Z.J. Garlets, J.D. Nguyen, C.R.J. Stephenson, The development of visible-light photoredox catalysis in flow, Isr. J. Chem. 54 (2014) 351–360.
[183] P. Li, J.A. Terrett, J.R. Zbieg, Visible-light photocatalysis as an enabling technology for drug discovery: a paradigm shift for chemical reactivity, ACS Med. Chem. Lett. 11 (2020) 2120–2130.
[184] D. Aand, B. Mahajan, S. Pabbaraja, A.K. Singh, Integrated continuous flow/batch protocol for the photoreduction of ortho-methyl phenyl ketones using water as the hydrogen source, React. Chem. Eng. 4 (2019) 812–817.
[185] J. Hartwig, S. Ceylan, L. Kupracz, L. Coutable, A. Kirschning, Heating under high-frequency inductive conditions: application to the continuous synthesis of the neurolepticum olanzapine (Zyprexa), Angew. Chem. Int. Ed. 52 (2013) 9813–9817.
[186] A. Steiner, J.D. Williams, O. de Frutos, J.A. Rincón, C. Mateos, C.O. Kappe, Continuous photochemical benzylic bromination using in situ generated Br_2: process intensification towards optimal PMI and throughput, Green. Chem. 22 (2020) 448–454.
[187] K.L. Skubi, T.R. Blum, T.P. Yoon, Dual catalysis strategies in photochemical synthesis, Chem. Rev. 116 (2016) 10035–10074.
[188] C. Michelin, N. Hoffmann, Photosensitization and photocatalysis - perspectives in organic synthesis, ACS Catal. 8 (2018) 12046–12055.
[189] J.C. Tellis, C.B. Kelly, D.N. Primer, M. Jouffroy, N.R. Patel, G.A. Molander, Single-electron transmetalation via photoredox/nickel dual catalysis: unlocking a new paradigm for sp^3–sp^2 cross-coupling, Acc. Chem. Res. 49 (2016) 1429–1439.
[190] I.B. Perry, T.F. Brewer, P.J. Sarver, D.M. Schultz, D.A. DiRocco, D.W. C. MacMillan, Direct arylation of strong aliphatic C–H bonds, Nature 560 (2018) 70–75.
[191] X.-F. Tang, J.-N. Zhao, Y.-F. Wu, S.-H. Feng, F. Yang, Z.-Y. Yu, Q.-W. Meng, Visible-light-driven enantioselective aerobic oxidation of β-dicarbonyl compounds catalyzed by cinchona-derived phase transfer catalysts in batch and semi-flow, Adv. Synth. Catal. 361 (2019) 5245–5252.
[192] C.G.L. Thomson, A.-L. Vilela, F, Heterogeneous photocatalysis in flow chemical reactors, Beilstein J. Org. Chem. 16 (2020) 1495–1549.
[193] M. Colella, C. Carlucci, R. Luisi, Supported catalysts for continuous flow synthesis, Top. Curr. Chem. 376 (2018) 46.
[194] K. Masuda, T. Ichitsuka, N. Koumura, K. Sato, S. Kobayashi, Flow fine synthesis with heterogeneous catalysts, Tetrahedron 74 (2018) 1705–1730.
[195] F. Lévesque, P.H. Seeberger, Continuous-flow synthesis of the anti-malaria drug artemisinin, Angew. Chem. Int. Ed. 51 (2012) 1706–1709.
[196] D. Kopetzki, F. Lévesque, P.H. Seeberger, A. Continuous-Flow, Process for the synthesis of artemisinin, Chem. – A Eur. J. 19 (2013) 5450–5456.
[197] M. Peplow, Sanofi launches malaria drug production, ChemistryWorld, RCS (2013). https://www.chemistryworld.com/news/sanofi-launches-malaria-drug-production/6068.article.
[198] S. Triemer, K. Gilmore, G.T. Vu, P.H. Seeberger, A. Seidel-Morgenstern, Literally green chemical synthesis of artemisinin from plant extracts, Angew. Chem. Int. Ed. 57 (2018) 5525–5528.
[199] M. VanDeWalle, K. DeBruycker, T. Junkers, J.P. Blinco, C. Barner-Kowollik, Scalable synthesis of sequence-defined oligomers via photoflow chemistry, ChemPhotoChem 3 (2019) 225–228.
[200] T. Junkers, B. Wenn, Continuous photoflow synthesis of precision polymers, React. Chem. Eng. 1 (2016) 60–64.
[201] C. Len, R. Luisi, Catalytic methods in flow chemistry, Catalysts 9 (2019) 663.
[202] Y. Su, K. Kuijpers, V. Hessel, T. Noël, A convenient numbering-up strategy for the scale-up of gas–liquid photoredox catalysis in flow, React. Chem. Eng. 1 (2016) 73–81.
[203] L.D. Elliott, M. Berry, B. Harji, D. Klauber, J. Leonard, K.I. Booker-Milburn, A. Small-Footprint, High-capacity flow reactor for UV photochemical synthesis on the kilogram scale, Org. Process Res. Dev. 20 (2016) 1806–1811.
[204] C.J. Seel, A. Králík, M. Hacker, A. Frank, B. König, T. Gulder, Atom-economic electron donors for photobiocatalytic halogenations, ChemCatChem 10 (2018) 3960–3963.
[205] C.J. Seel, T. Gulder, Biocatalysis fueled by light: on the versatile combination of photocatalysis and enzymes, ChemBioChem 20 (2019) 1871–1897.
[206] D. Sorigué, B. Légeret, S. Cuiné, S. Blangy, S. Moulin, E. Billon, P. Richaud, S. Brugière, Y. Couté, D. Nurizzo, P. Müller, K. Brettel, D. Pignol, P. Arnoux, Y. Li-Beisson, G. Peltier, F. Beisson, An algal photoenzyme converts fatty acids to hydrocarbons, Science 357 (2017) 903–907.
[207] A. Ziogas, H. Löwe, M. Küpper, W. Ehrfeld, Electrochemical microreactors: a new approach for microreaction technology, in: W. Ehrfeld (Ed.), Microreaction Technology: Industrial Prospects, Springer Berlin Heidelberg, Berlin, Heidelberg, 2000, pp. 136–150.
[208] S. Zheng, J. Yan, K. Wang, Engineering research progress of electrochemical microreaction technology—a novel method for electrosynthesis of organic, in: Chemicals, Engineering, 7, 2021, pp. 22–32.
[209] G.S.J. Sturm, M.D. Verweij, A.I. Stankiewicz, G.D. Stefanidis, Microwaves and microreactors: design challenges and remedies, Chem. Eng. J. 243 (2014) 147–158.
[210] G. Laudadio, W. de Smet, L. Struik, Y. Cao, T. Noël, Design and application of a modular and scalable electrochemical flow microreactor, J. Flow. Chem. 8 (2018) 157–165.
[211] M.N. Pervez, A. Mahboubi, C. Uwineza, T. Zarra, V. Belgiorno, V. Naddeo, M. J. Taherzadeh, Factors influencing pressure-driven membrane-assisted volatile fatty acids recovery and purification-a review, Sci. Total Environ. 817 (2022), 152993.
[212] J.-i Yoshida, A. Shimizu, R. Hayashi, Electrogenerated cationic reactive intermediates: the pool method and further advances, Chem. Rev. 118 (2018) 4702–4730.
[213] T. Noël, Y. Cao, G. Laudadio, The fundamentals behind the use of flow reactors in electrochemistry, Acc. Chem. Res. 52 (2019) 2858–2869.
[214] R. D'Ambrosio, A. Cintio, A. Lazzeri, G. Annino, Design of an overmoded resonant cavity-based reactor for ceramic matrix composites production, Chem. Eng. J. 405 (2021), 126609.
[215] N.G. Patil, F. Benaskar, E.V. Rebrov, J. Meuldijk, L.A. Hulshof, V. Hessel, J. C. Schouten, Continuous multitubular millireactor with a Cu thin film for microwave-assisted fine-chemical synthesis, Ind. Eng. Chem. Res. 51 (2012) 14344–14354.
[216] E.V. Rebrov, Microwave-assisted organic synthesis in microstructured reactors, Russ. J. Gen. Chem. 82 (2012) 2060–2069.
[217] F. Benaskar, N.G. Patil, V. Engels, E.V. Rebrov, J. Meuldijk, L.A. Hulshof, V. Hessel, A.E.H. Wheatley, J.C. Schouten, Microwave-assisted Cu-catalyzed Ullmann ether synthesis in a continuous-flow milli-plant, Chem. Eng. J., 207- 208 (2012) 426–439.
[218] F. Benaskar, V. Engels, N. Patil, E.V. Rebrov, J. Meuldijk, V. Hessel, L.A. Hulshof, D.A. Jefferson, J.C. Schouten, A.E.H. Wheatley, Copper(0) in the Ullmann heterocycle-aryl ether synthesis of 4-phenoxypyridine using multimode microwave heating, Tetrahedron Lett. 51 (2010) 248–251.
[219] C. Wiles, P. Watts, Translation of microwave methodology to continuous flow for the efficient synthesis of diaryl ethers via a base-mediated SNAr reaction, Beilstein J. Org. Chem. 7 (2011) 1360–1371.
[220] F. Benaskar, V. Hessel, U. Krtschil, P. Löb, A. Stark, Intensification of the capillary-based kolbe−schmitt synthesis from resorcinol by reactive ionic liquids, microwave heating, or a combination thereof, Org. Process Res. Dev. 13 (2009) 970–982.
[221] V.V. Banakar, S.S. Sabnis, P.R. Gogate, A. Raha, Ultrasound assisted continuous processing in microreactors with focus on crystallization and chemical synthesis: a critical review, Chem. Eng. Res. Des. 182 (2022) 273–289.
[222] Z. Dong, C. Delacour, K. Mc Carogher, A.P. Udepurkar, S. Kuhn, Continuous ultrasonic reactors: design, mechanism and application, Materials 13 (2020) 344.
[223] Z. Dong, S. Zhao, Y. Zhang, C. Yao, Q. Yuan, G. Chen, Mixing and residence time distribution in ultrasonic microreactors, AIChE J. 63 (2017) 1404–1418.
[224] Z. Dong, D. Fernandez Rivas, S. Kuhn, Acoustophoretic focusing effects on particle synthesis and clogging in microreactors, Lab a Chip 19 (2019) 316–327.
[225] A. Gondo, R. Manabe, R. Sakai, K. Murakami, T. Yabe, S. Ogo, M. Ikeda, H. Tsuneki, Y. Sekine, Ammonia synthesis over Co catalyst in an electric field, Catal. Lett. 148 (2018) 1929–1938.
[226] Y. Hisai, Q. Ma, T. Qureishy, T. Watanabe, T. Higo, T. Norby, Y. Sekine, Enhanced activity of catalysts on substrates with surface protonic current in an electrical field – a review, Chem. Commun. 57 (2021) 5737–5749.

[227] S.D. Fried, S. Bagchi, S.G. Boxer, Extreme electric fields power catalysis in the active site of ketosteroid isomerase, Science 346 (2014) 1510–1514.
[228] E. Mansoor, J. Van der Mynsbrugge, M. Head-Gordon, A.T. Bell, Impact of long-range electrostatic and dispersive interactions on theoretical predictions of adsorption and catalysis in zeolites, Catal. Today 312 (2018) 51–65.
[229] Y. Sekine, K. Urasaki, S. Kado, M. Matsukata, E. Kikuchi, Nonequilibrium pulsed discharge: a novel method for steam reforming of hydrocarbons or alcohols, Energy Fuels 18 (2004) 455–459.
[230] M. Kosaka, T. Higo, S. Ogo, J.G. Seo, S. Kado, Low-temperature selective dehydrogenation of methylcyclohexane by surface protonics over Pt/anatase-TiO_2 catalyst, Int. J. Hydrog. Energy 45 (2020) 738–743.
[231] L.D. Chen, M. Urushihara, K. Chan, J.K. Nørskov, Electric field effects in electrochemical CO_2 reduction, ACS Catal. 6 (2016) 7133–7139.
[232] J.K. Nørskov, S. Holloway, N.D. Lang, Microscopic model for the poisoning and promotion of adsorption rates by electronegative and electropositive atoms, Surf. Sci. 137 (1984) 65–78.
[233] M. Liu, Y. Pang, B. Zhang, P. De Luna, O. Voznyy, J. Xu, X. Zheng, C.T. Dinh, F. Fan, C. Cao, F.P.G. de Arquer, T.S. Safaei, A. Mepham, A. Klinkova, E. Kumacheva, T. Filleter, D. Sinton, S.O. Kelley, E.H. Sargent, Enhanced electrocatalytic CO_2 reduction via field-induced reagent concentration, Nature 537 (2016) 382–386.
[234] H. Robatjazi, H. Zhao, D.F. Swearer, N.J. Hogan, L. Zhou, A. Alabastri, M. J. McClain, P. Nordlander, N.J. Halas, Plasmon-induced selective carbon dioxide conversion on earth-abundant aluminum-cuprous oxide antenna-reactor nanoparticles, Nature, Communications 8 (2017) 27.
[235] B. Yang, K. Liu, H. Li, C. Liu, J. Fu, H. Li, J.E. Huang, P. Ou, T. Alkayyali, C. Cai, Y. Duan, H. Liu, P. An, N. Zhang, W. Li, X. Qiu, C. Jia, J. Hu, L. Chai, Z. Lin, Y. Gao, M. Miyauchi, E. Cortés, S.A. Maier, M. Liu, Accelerating CO_2 electroreduction to multicarbon products via synergistic electric–thermal field on copper nanoneedles, J. Am. Chem. Soc. 144 (2022) 3039–3049.
[236] Q. Chen, K. Liu, Y. Zhou, X. Wang, K. Wu, H. Li, E. Pensa, J. Fu, M. Miyauchi, E. Cortés, M. Liu, Ordered Ag nanoneedle arrays with enhanced electrocatalytic CO_2 reduction via structure-induced inhibition of hydrogen evolution, Nano Lett. 22 (2022) 6276–6284.
[237] Y. Zhou, Y. Liang, J. Fu, K. Liu, Q. Chen, X. Wang, H. Li, L. Zhu, J. Hu, H. Pan, M. Miyauchi, L. Jiang, E. Cortés, M. Liu, Vertical Cu nanoneedle arrays enhance the local electric field promoting C2 hydrocarbons in the CO_2 electroreduction, Nano Lett. 22 (2022) 1963–1970.
[238] Y. Chen, G. Zhang, H. Liu, Y. Wang, Z. Chen, Q. Ji, H. Lan, R. Liu, J. Qu, Tip-intensified interfacial microenvironment reconstruction promotes an electrocatalytic chlorine evolution reaction, ACS Catal. 12 (2022) 14376–14386.
[239] S. Huang, C. Ning, W. Peng, H. Dong, Anodic formation of Ti nanorods with periodic length, Electrochem. Commun. 17 (2012) 14–17.
[240] N. Pourali, M.M. Sarafraz, V. Hessel, E.V. Rebrov, Simulation study of a pulsed DBD with an electrode containing charge injector parts, Phys. Plasmas 28 (2021), 013502.
[241] N. Pourali, V. Hessel, E.V. Rebrov, The effects of pulse shape on the selectivity and production rate in non-oxidative coupling of methane by a micro-DBD reactor, Plasma Chem. Plasma Process. 42 (2022) 619–640.
[242] N. Pourali, M. Vasilev, R. Abiev, E.V. Rebrov, Development of a microkinetic model for non-oxidative coupling of methane over a Cu catalyst in a non-thermal plasma reactor, J. Phys. D: Appl. Phys. 55 (2022), 395204.
[243] R.S. Abiev, D.A. Sladkovskiy, K.V. Semikin, D.Y. Murzin, E.V. Rebrov, Non-thermal plasma for process and energy intensification in dry reforming of methane, Catalysts 10 (2020) 1358.
[244] S. Okada, R. Manabe, R. Inagaki, S. Ogo, Y. Sekine, Methane dissociative adsorption in catalytic steam reforming of methane over Pd/CeO_2 in an electric field, Catal. Today 307 (2018) 272–276.
[245] K. Takise, A. Sato, K. Murakami, S. Ogo, J.G. Seo, S. K.-i. Imagawa, Y.Sekine Kado, Irreversible catalytic methylcyclohexane dehydrogenation by surface protonics at low temperature, RSC Adv. 9 (2019) 5918–5924.
[246] T. Yabe, K. Yamada, K. Murakami, K. Toko, K. Ito, T. Higo, S. Ogo, Y. Sekine, Role of electric field and surface protonics on low-temperature catalytic dry reforming of methane, ACS Sustain. Chem. Eng. 7 (2019) 5690–5697.
[247] R. Manabe, H. Nakatsubo, A. Gondo, K. Murakami, S. Ogo, H. Tsuneki, M. Ikeda, A. Ishikawa, H. Nakai, Y. Sekine, Electrocatalytic synthesis of ammonia by surface proton hopping, Chem. Sci. 8 (2017) 5434–5439.
[248] S. Dahl, A. Logadottir, C.J.H. Jacobsen, J.K. Nørskov, Electronic factors in catalysis: the volcano curve and the effect of promotion in catalytic ammonia synthesis, Appl. Catal. A: Gen. 222 (2001) 19–29.
[249] M. Hara, M. Kitano, H. Hosono, Ru-loaded $C_{12}A_7$:e^- electride as a catalyst for ammonia synthesis, ACS Catal. 7 (2017) 2313–2324.
[250] A. Ellaboudy, J.L. Dye, P.B. Smith, Cesium 18-crown-6 compounds. A crystalline ceside and a crystalline electride, J. Am. Chem. Soc. 105 (1983) 6490–6491.
[251] M. Kitano, Y. Inoue, Y. Yamazaki, F. Hayashi, S. Kanbara, S. Matsuishi, T. Yokoyama, S.-W. Kim, M. Hara, H. Hosono, Ammonia synthesis using a stable electride as an electron donor and reversible hydrogen store, Nat. Chem. 4 (2012) 934–940.
[252] S. Laassiri, C.D. Zeinalipour-Yazdi, C.R.A. Catlow, J.S.J. Hargreaves, The potential of manganese nitride based materials as nitrogen transfer reagents for nitrogen chemical looping, Appl. Catal. B: Environ. 223 (2018) 60–66.
[253] T.-N. Ye, S.-W. Park, Y. Lu, J. Li, M. Sasase, M. Kitano, T. Tada, H. Hosono, Vacancy-enabled N2 activation for ammonia synthesis on an Ni-loaded catalyst, Nature 583 (2020) 391–395.
[254] R. Manabe, S. Okada, R. Inagaki, K. Oshima, S. Ogo, Y. Sekine, Surface protonics promotes catalysis, Sci. Rep. 6 (2016) 38007.
[255] S. Ogo, Y. Sekine, Catalytic reaction assisted by plasma or electric field, Chem. Rec. 17 (2017) 726–738.
[256] B. Scherrer, M.V.F. Schlupp, D. Stender, J. Martynczuk, J.G. Grolig, H. Ma, P. Kocher, T. Lippert, M. Prestat, L.J. Gauckler, On proton conductivity in porous and dense yttria stabilized zirconia at low temperature, Adv. Funct. Mater. 23 (2013) 1957–1964.
[257] M. Stoukides, C.G. Vayenas, The effect of electrochemical oxygen pumping on the rate and selectivity of ethylene oxidation on polycrystalline silver, J. Catal. 70 (1981) 137–146.
[258] S. Brosda, C.G. Vayenas, J. Wei, Rules of chemical promotion, Appl. Catal. B: Environ. 68 (2006) 109–124.
[259] I. Kalaitzidou, M. Makri, D. Theleritis, A. Katsaounis, C.G. Vayenas, Comparative study of the electrochemical promotion of CO_2 hydrogenation on Ru using Na^+, K^+, H^+ and O_2^- conducting solid electrolytes, Surf. Sci. 646 (2016) 194–203.
[260] Z. Pan, C. Duan, T. Pritchard, A. Thatte, E. White, R. Braun, R. O'Hayre, N. P. Sullivan, High-yield electrochemical upgrading of CO_2 into CH_4 using large-area protonic ceramic electrolysis cells, Appl. Catal. B: Environ. 307 (2022), 121196.
[261] C. Duan, R.J. Kee, H. Zhu, C. Karakaya, Y. Chen, S. Ricote, A. Jarry, E.J. Crumlin, D. Hook, R. Braun, N.P. Sullivan, R. O'Hayre, Highly durable, coking and sulfur tolerant, fuel-flexible protonic ceramic fuel cells, Nature 557 (2018) 217–222.
[262] J. Wang, R.-t Guo, Z.-x Bi, X. Chen, X. Hu, W.-g Pan, A review on TiO_{2-x}-based materials for photocatalytic CO_2 reduction, Nanoscale 14 (2022) 11512–11528.
[263] J. Arun, S. Nachiappan, G. Rangarajan, R.P. Alagappan, K.P. Gopinath, E. Lichtfouse, Synthesis and application of titanium dioxide photocatalysis for energy, decontamination and viral disinfection: a review, Environ. Chem. Lett. 21 (2022) 339–362.
[264] W.-H. Chen, J.E. Lee, S.-H. Jang, S.-S. Lam, G.H. Rhee, K.-J. Jeon, M. Hussain, Y.-K. Park, A review on the visible light active modified photocatalysts for water splitting for hydrogen production, Int. J. Energy Res. 46 (2022) 5467–5477.
[265] Y.-Q. Cao, T.-Q. Zi, X.-R. Zhao, C. Liu, Q. Ren, J.-B. Fang, W.-M. Li, A.-D. Li, Enhanced visible light photocatalytic activity of Fe_2O_3 modified TiO_2 prepared by atomic layer deposition, Sci. Rep. 10 (2020) 13437.
[266] I. Arora, H. Chawla, A. Chandra, S. Sagadevan, S. Garg, Advances in the strategies for enhancing the photocatalytic activity of TiO_2: conversion from UV-light active to visible-light active photocatalyst, Inorg. Chem. Commun. 143 (2022), 109700.
[267] M. Humayun, F. Raziq, A. Khan, W. Luo, Modification strategies of TiO_2 for potential applications in photocatalysis: a critical review, Green. Chem. Lett. Rev. 11 (2018) 86–102.
[268] V. Etacheri, C. Di Valentin, J. Schneider, D. Bahnemann, S.C. Pillai, Visible-light activation of TiO_2 photocatalysts: advances in theory and experiments, J. Photochem. Photobiol. C: Photochem. Rev. 25 (2015) 1–29.
[269] R.V. Nair, V.S. Gummaluri, M.V. Matham, V. C, A review on optical bandgap engineering in TiO2 nanostructures via doping and intrinsic vacancy modulation towards visible light applications, J. Phys. D: Appl. Phys. 55 (2022), 313003.
[270] R. Woods-Robinson, Y. Han, H. Zhang, T. Ablekim, I. Khan, K.A. Persson, A. Zakutayev, Wide band gap chalcogenide semiconductors, Chem. Rev. 120 (2020) 4007–4055.
[271] H.L. Tan, F.F. Abdi, Y.H. Ng, Heterogeneous photocatalysts: an overview of classic and modern approaches for optical, electronic, and charge dynamics evaluation, Chem. Soc. Rev. 48 (2019) 1255–1271.
[272] F. Zhang, X. Wang, H. Liu, C. Liu, Y. Wan, Y. Long, Z. Cai, Recent advances and applications of semiconductor photocatalytictechnology, Appl. Sci. 9 (2019) 2489.
[273] W. Jiao, W. Shen, Z.U. Rahman, D. Wang, Recent progress in red semiconductor photocatalysts for solar energy conversion and utilization, 5 (2016) 135–145.
[274] A. Kumar, P. Choudhary, A. Kumar, P.H.C. Camargo, V. Krishnan, Recent advances in plasmonic photocatalysis based on TiO_2 and noble metal nanoparticles for energy conversion, Environ. Remediat. Organic Synth. Small 18 (2022), 2101638.
[275] L. Gomathi Devi, R. Kavitha, A review on plasmonic metal-TiO_2 composite for generation, trapping, storing and dynamic vectorial transfer of photogenerated electrons across the Schottky junction in a photocatalytic system, Appl. Surf. Sci. 360 (2016) 601–622.
[276] M. Thangamuthu, T.V. Raziman, O.J.F. Martin, J. Tang, Review - origin and promotional effects of plasmonics in photocatalysis, J. Electrochem. Soc. 169 (2022), 036512.
[277] M.I. Stockman, K. Kneipp, S.I. Bozhevolnyi, S. Saha, A. Dutta, J. Ndukaife, N. Kinsey, H. Reddy, U. Guler, V.M. Shalaev, A. Boltasseva, B. Gholipour, H.N. S. Krishnamoorthy, K.F. MacDonald, C. Soci, N.I. Zheludev, V. Savinov, R. Singh, P. Groß, C. Lienau, M. Vadai, M.L. Solomon, D.R. Barton, M. Lawrence, J. A. Dionne, S.V. Boriskina, R. Esteban, J. Aizpurua, X. Zhang, S. Yang, D. Wang, W. Wang, T.W. Odom, N. Accanto, P.M. de Roque, I.M. Hancu, L. Piatkowski, N. F. van Hulst, M.F. Kling, Roadmap on plasmonics, J. Opt. 20 (2018), 043001.
[278] T.P. Araujo, J. Quiroz, E.C.M. Barbosa, P.H.C. Camargo, Understanding plasmonic catalysis with controlled nanomaterials based on catalytic and plasmonic metals, Curr. Opin. Colloid Interface Sci. 39 (2019) 110–122.
[279] L. Du, A. Furube, K. Hara, R. Katoh, M. Tachiya, Ultrafast plasmon induced electron injection mechanism in gold–TiO_2 nanoparticle system, J. Photochem. Photobiol. C: Photochem. Rev. 15 (2013) 21–30.
[280] E. Cortés, L.V. Besteiro, A. Alabastri, A. Baldi, G. Tagliabue, A. Demetriadou, P. Narang, Challenges in plasmonic catalysis, ACS Nano 14 (2020) 16202–16219.
[281] X. Meng, L. Liu, S. Ouyang, H. Xu, D. Wang, N. Zhao, J. Ye, Nanometals for solar-to-chemical energy conversion: from semiconductor-based photocatalysis to plasmon-mediated photocatalysis and photo-thermocatalysis, Adv. Mater. 28 (2016) 6781–6803.

[282] A.G.M. da Silva, T.S. Rodrigues, J. Wang, P.H.C. Camargo, Plasmonic catalysis with designer nanoparticles, Chem. Commun. 58 (2022) 2055–2074.
[283] J. Becerra, V.N. Gopalakrishnan, T.-A. Quach, T.-O. Do, Plasmonic materials: opportunities and challenges on reticular chemistry for photocatalytic applications, ChemCatChem 13 (2021) 1059–1073.
[284] J. Zhao, J. Wang, A.J. Brock, H. Zhu, Plasmonic heterogeneous catalysis for organic transformations, J. Photochem. Photobiol. C: Photochem. Rev. 52 (2022), 100539.
[285] X. Yu, X. Jin, X. Chen, A. Wang, J. Zhang, J. Zhang, Z. Zhao, M. Gao, L. Razzari, H. Liu, A. Microorganism, Bred TiO_2/Au/TiO_2 heterostructure for whispering gallery mode resonance assisted plasmonic photocatalysis, ACS Nano 14 (2020) 13876–13885.
[286] J.L. Montaño-Priede, U. Pal, Estimating near electric field of polyhedral gold nanoparticles for plasmon-enhanced spectroscopies, J. Phys. Chem. C. 123 (2019) 11833–11839.
[287] B. Pramanick, T. Kumar, A. Halder, P.F. Siril, Engineering the morphology of palladium nanostructures to tune their electrocatalytic activity in formic acid oxidation reactions, Nanoscale Adv. 2 (2020) 5810–5820.
[288] H. Ou, D. Wang, Y. Li, How to select effective electrocatalysts: nano or single atom? Nano Sel. 2 (2021) 492–511.
[289] A. Loiudice, P. Lobaccaro, E.A. Kamali, T. Thao, B.H. Huang, J.W. Ager, R. Buonsanti, Tailoring copper nanocrystals towards C2 products in electrochemical CO_2 reduction, Angew. Chem. Int. Ed. 55 (2016) 5789–5792.
[290] L. García-Cruz, V. Montiel, J. Solla-Gullón, Shape-controlled metal nanoparticles for electrocatalytic applications, Phys Sci Rev 4 (2019) 201701244.
[291] P. Strasser, M. Gliech, S. Kuehl, T. Moeller, Electrochemical processes on solid shaped nanoparticles with defined facets, Chem. Soc. Rev. 47 (2018) 715–735.
[292] R. Rizo, B. Roldan Cuenya, Shape-controlled nanoparticles as anodic catalysts in low-temperature fuel cells, ACS Energy Lett. 4 (2019) 1484–1495.
[293] J. Huang, J. Zhang, M.H. Eikerling, Particle proximity effect in nanoparticle electrocatalysis: surface charging and electrostatic interactions, J. Phys. Chem. C. 121 (2017) 4806–4815.
[294] F. Li, C. Zhou, A. Klinkova, Simulating electric field and current density in nanostructured electrocatalysts, Phys. Chem. Chem. Phys. 24 (2022) 25695–25719.
[295] J. Wordsworth, T.M. Benedetti, A. Alinezhad, R.D. Tilley, M.A. Edwards, W. Schuhmann, J.J. Gooding, The importance of nanoscale confinement to electrocatalytic performance, Chem. Sci. 11 (2020) 1233–1240.
[296] S.V. Somerville, P.B. O'Mara, T.M. Benedetti, S. Cheong, W. Schuhmann, R. D. Tilley, J.J. Gooding, Nanoconfinement Allows a Less Active Cascade Catalyst to Produce More C2+ Products in Electrochemical CO_2 Reduction, J. Phys. Chem. C 127 (2023) 289–299.
[297] L.-H. Yang, R. Luo, X.-J. Wen, Z.-T. Liu, Z.-H. Fei, L. Hu, Nanoconfinement effects of Ni@CNT for efficient electrocatalytic oxygen reduction and evolution reaction, J. Alloy. Compd. 897 (2022), 163206.
[298] Y. Wu, S. Jamali, R.D. Tilley, J.J. Gooding, Spiers Memorial Lecture. Next generation nanoelectrochemistry: the fundamental advances needed for applications, Faraday Discuss. 233 (2022) 10–32.
[299] J. Zhao, S. Xue, R. Ji, B. Li, J. Li, Localized surface plasmon resonance for enhanced electrocatalysis, Chem. Soc. Rev. 50 (2021) 12070–12097.
[300] C.H. Choi, K. Chung, T.-T.H. Nguyen, D.H. Kim, Plasmon-mediated electrocatalysis for sustainable energy: from electrochemical conversion of different feedstocks to fuel cell reactions, ACS Energy Lett. 3 (2018) 1415–1433.
[301] H.M. Chen, C.K. Chen, C.J. Chen, L.C. Cheng, P.C. Wu, B.H. Cheng, Y.Z. Ho, M. L. Tseng, Y.Y. Hsu, T.S. Chan, J.F. Lee, R.S. Liu, D.P. Tsai, Plasmon inducing effects for enhanced photoelectrochemical water splitting: X-ray absorption approach to electronic structures, ACS Nano 6 (2012) 7362–7372.
[302] H. Wu, Z. Wu, B. Liu, X. Zhao, Can plasmonic effect cause an increase in the catalytic reduction of p-nitrophenol by sodium borohydride over Au nanorods? ACS Omega 5 (2020) 11998–12004.
[303] X. Zhang, X. Li, M.E. Reish, D. Zhang, N.Q. Su, Y. Gutiérrez, F. Moreno, W. Yang, H.O. Everitt, J. Liu, Plasmon-enhanced catalysis: distinguishing thermal and nonthermal effects, Nano Lett. 18 (2018) 1714–1723.
[304] K. Li, N.J. Hogan, M.J. Kale, N.J. Halas, P. Nordlander, P. Christopher, Balancing near-field enhancement, absorption, and scattering for effective antenna–reactor plasmonic photocatalysis, Nano Lett. 17 (2017) 3710–3717.
[305] D.F. Swearer, B.B. Bourgeois, D.K. Angell, J.A. Dionne, Advancing plasmon-induced selectivity in chemical transformations with optically coupled transmission electron microscopy, Acc. Chem. Res. 54 (2021) 3632–3642.
[306] S. Lee, K. Sim, S.Y. Moon, J. Choi, Y. Jeon, J.-M. Nam, S.-J. Park, Controlled assembly of plasmonic nanoparticles: from static to dynamic nanostructures, Adv. Mater. 33 (2021), 2007668.
[307] M. Núñez, J.L. Lansford, D.G. Vlachos, Optimization of the facet structure of transition-metal catalysts applied to the oxygen reduction reaction, Nat. Chem. 11 (2019) 449–456.
[308] J. Bi, H. Cai, B. Wang, C. Kong, S. Yang, Localized surface plasmon enhanced electrocatalytic methanol oxidation of AgPt bimetallic nanoparticles with an ultra-thin shell, Chem. Commun. 55 (2019) 3943–3946.
[309] C.J. Heard, J. Čejka, M. Opanasenko, P. Nachtigall, G. Centi, S. Perathoner, 2D oxide nanomaterials to address the energy transition and catalysis, Adv. Mater. 31 (2019), 1801712.
[310] L. Zhou, M. Lou, J.L. Bao, C. Zhang, J.G. Liu, J.M.P. Martirez, S. Tian, L. Yuan, D. F. Swearer, H. Robatjazi, E.A. Carter, P. Nordlander, N.J. Halas, Hot carrier multiplication in plasmonic photocatalysis, Proc. Natl. Acad. Sci. 118 (2021) e2022109118.
[311] M. Ahlawat, D. Mittal, V. Govind Rao, Plasmon-induced hot-hole generation and extraction at nano-heterointerfaces for photocatalysis, Communications, Materials 2 (2021) 114.
[312] P.V. Kumar, T.P. Rossi, M. Kuisma, P. Erhart, D.J. Norris, Direct hot-carrier transfer in plasmonic catalysis, Faraday Discuss. 214 (2019) 189–197.
[313] S. Simoncelli, E.L. Pensa, T. Brick, J. Gargiulo, A. Lauri, J. Cambiasso, Y. Li, S. A. Maier, E. Cortés, Monitoring plasmonic hot-carrier chemical reactions at the single particle level, Faraday Discuss. 214 (2019) 73–87.
[314] T.P. Rossi, P. Erhart, M. Kuisma, Hot-carrier generation in plasmonic nanoparticles: the importance of atomic structure, ACS Nano 14 (2020) 9963–9971.